Working session: Long-span roofs, underground and marine structures. Papers and posters

Working Session

Long-Span Roofs, Underground and Marine Structures

Papers and Poster

Leere Seite
Blank page
Page vide

Structural Design of the Osaka Dome

Katsumi HARA
Structural Eng.
Nikken Sekkei Ltd
Osaka, Japan

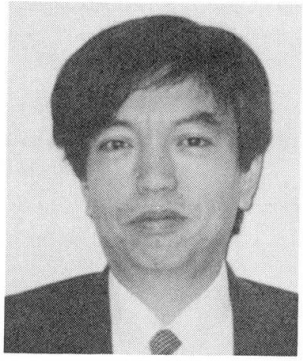

Katsumi Hara, born in 1948, obtained his master's degree at the Univ. of Waseda, Tokyo, Japan in 1974. For nineteen years he was involved in structural design of buildings. Katsumi Hara is now Senior Structural Eng. of Nikken Sekkei in Japan.

SUMMARY

The Osaka Dome, completed in 1997, is a large scale domed stadium intended for sports events such as baseball and football games and also for music concerts and big assemblies.
The Dome is composed of a doughnut-shaped stadium having an outside diameter of 200 m by a dome roof which measures 166 m in diameter.
This paper is intended to describe the design concepts and the structural features of the domed stadium and the dome construction procedure.

1. Outline of Osaka Dome

The Osaka Dome is planned as a multi-purpose dome with a seating capacity of 44,000 persons for sports events and a maximum seating capacity of 55,000 persons for other events. Visually, the dome's exterior features "Fiesta Mall", which created an image of a floating skyline suggestive of waves and clouds that surround the dome.

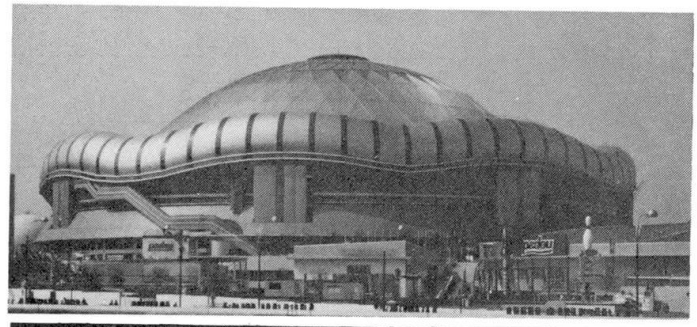

The Osaka Dome has two design concepts. One is to attract regularly many visitors so as to vitalize the entire local area. For this purpose, the dome has to have commercial and amusement facilities to attract many visitors even if there is no events held in the arena. To satisfy this requirement, the dome is designed to have two facilities, one is "Fiesta Mall" which is put round all the circumference of the dome of 600 at the 9th floor level, housing amusement facilities, and the other is commercial mall at the 2nd floor level.
The other design concept is that the arena should have volume-variable indoor space to create most suitable space for each of various events to be held in the arena.
The dome is provided with a mechanized system that can change the arena/seating space configurations to those most suitable

for the event taking place in the dome.

The ceiling shape is also variable, being composed of layers of ring-shaped elements (called "Super-rings") that can be raised and lowered as necessary to create the internal space configuration desired.

2. Outline of Structural Design

The Dome's roof consists of a 134 m diameter center dome portion and a 16 m wide perimeter portion which resembles a brim of a round hat in shape. This perimeter portion is more gently sloped than the central dome.

Construction Details

Owner:	*Osaka City Dome Co., Ltd.*
Design	*Nikken Sekkei Ltd*
constructionsupervision:	*Nikken Sekkei Ltd*
Cooperation in Design:	*Takenaka Corporation, Obayashi Corporation, Dentsu Inc.*
Construction:	*Osaka Dome Construction JV (Obayahsi Corporation, Takenaka Corporation and others)*
Design period:	*March 1993 to June 1994*
Construction period:	*July 1994 to February 1997*
Site area:	*34,617m²*
Building area:	*33,765m²*
Total floor area:	*156,408m²*
Roof:	
Top portion:	*Polycarbonate panel*
Other major portion:	*Stainless steel sheet (welding),dull finish*
Festa Mall:	*Stainless steel panel,dull finish*

Structurally, the roof framing of the central dome forms a uniform geometry of a steel lamella and perimeter is composed of uniform laid out 36 pairs of Y-shaped steel girders. The bases of these girders are located on the top of the grandstand.

As for the stresses developed by the dead loads, compressive stresses are caused in both the radial and the perimeter directions of the center dome portion while compressive and bending stresses are developed in the perimeter portion.

Intensive stresses developed at the borderline area between the center and the perimeter section are

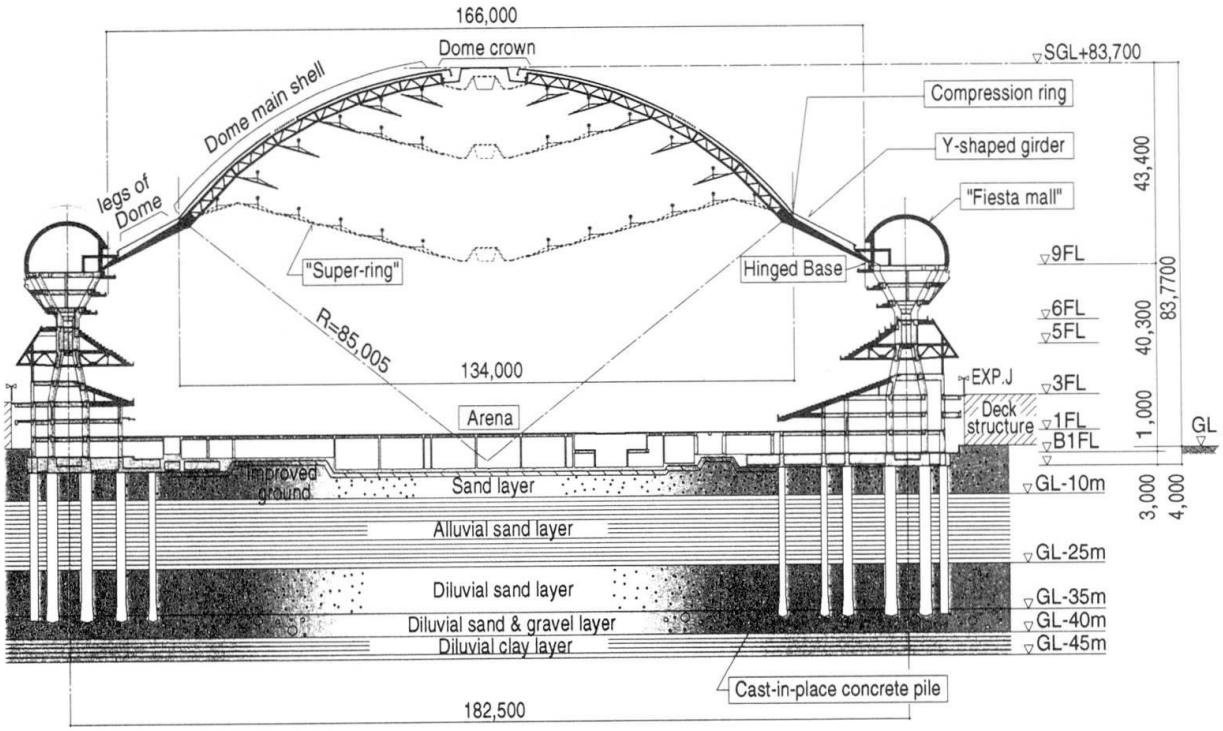

Fig.1 Outline of Structure

taken care of by the compression ring beam.

The dome's deadweight which is about 7,000 tons is carried to the substructure by way of the hinged dome bases. Since these hinged bases are interconnected by the tension ring beam and great lateral force is carried by tension hoops, almost no lateral force is transferred to the Grandstand structure below.

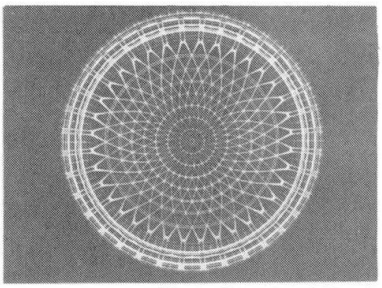

Fig.2 Structural Steel Members Arrangement

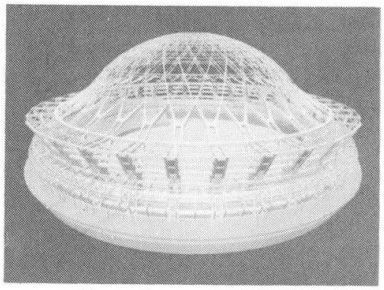

Fig.3 Structure in Perspective

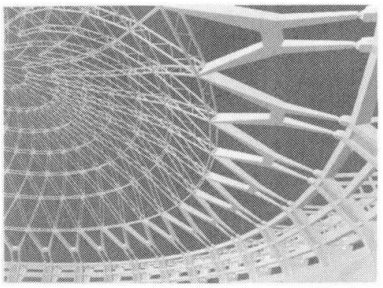

Fig.4 Y-shaped Girder

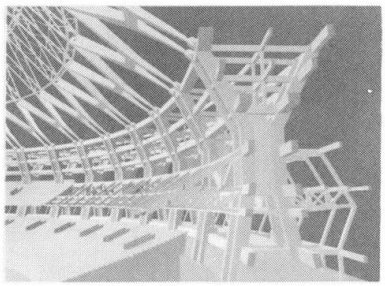

Fig.5 Grandstand Structure Supporting Dome

The grandstand structure under the domed roof is of steel framed reinforce concrete construction. From the view point of architectural planning as well as exterior design effects the structure in the radial direction consists of Y-shaped frames which have comparatively low rigidly. On the other hand, the frame in the circumferential direction is provided with shear walls to have high rigidity and strength. The frame in the radial direction and that in the circumferential direction are integrated into one by the floor slab that extends in the circumferential direction to form a rigid and strong structure which looks like a big doughnut.

2.1 Design of the Dome

Stresses and deflection induced in the dome by the deadweight is as shown in Fig. 6.
The spherical dome portion is subjectzed to compressive force both in the radial and the circumferential direction. Since Y-shaped girders are subjected to bending moments in addition to compressive forces, these girders are designed to have an H-shaped cross section which has high rigidity against bending (see Fig. 8). As the circumferential direction of the boundary portion formed by the Y-shaped girders and the spherical dome must carry large compressive force, a compression ring made up of highly rigid trusses are located at this portion (see Fig. 7).

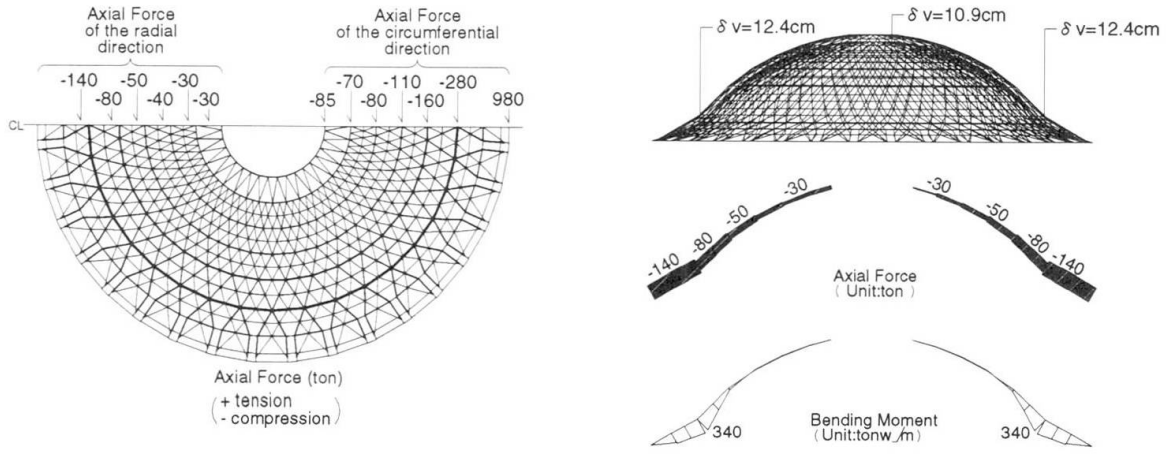

Fig.6 Stress and Deflection Induced by Dead Weight

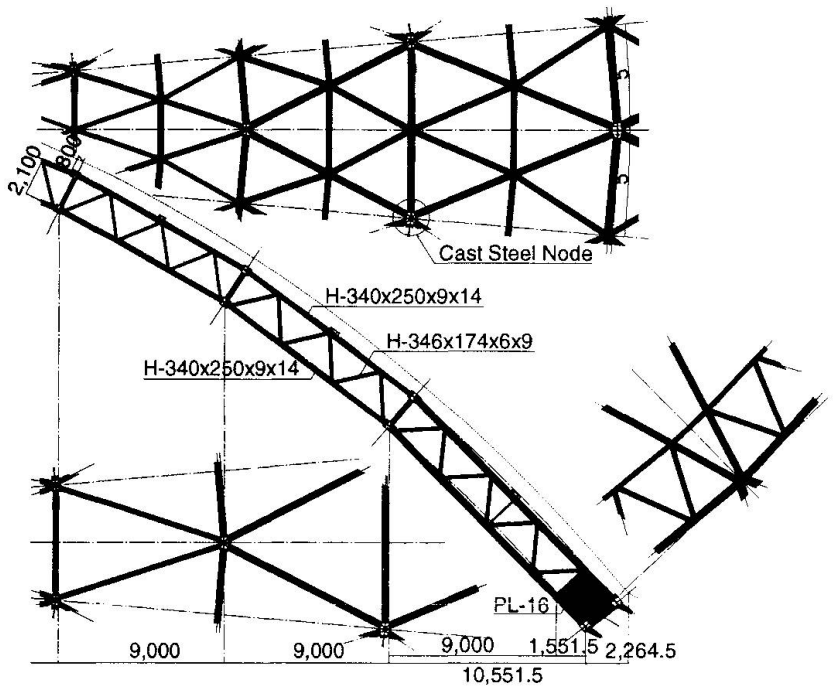

Fig.7 Lamella Dome

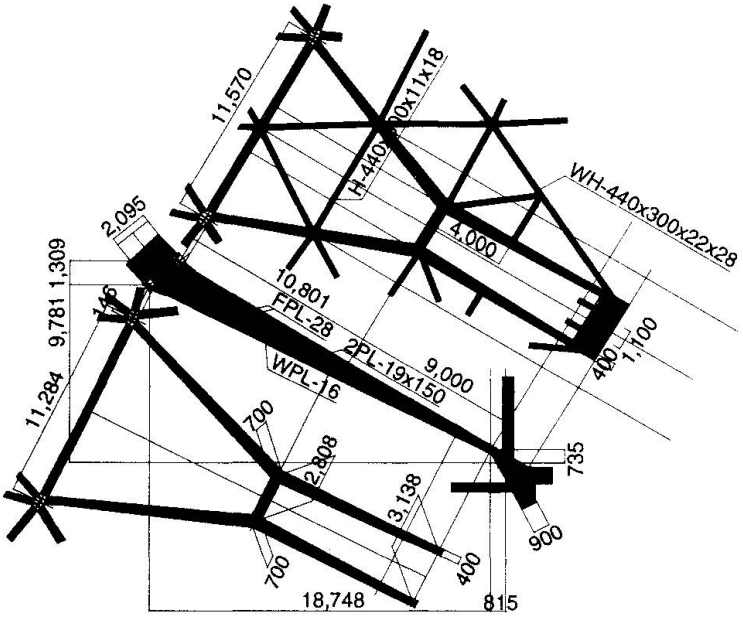

Fig.8 Y-shaped Girder

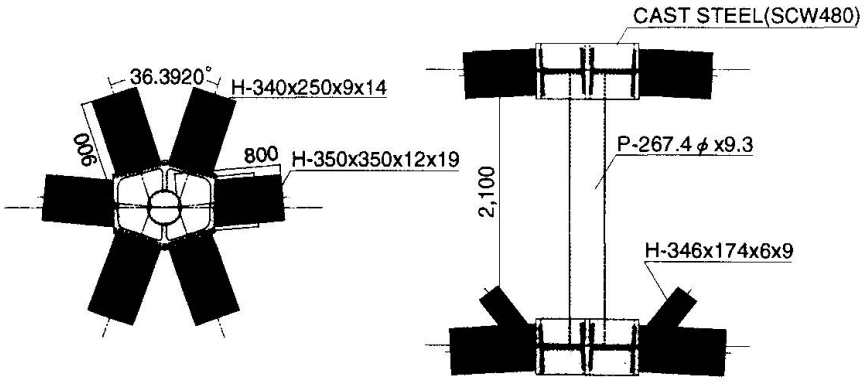

Fig.9 Cast Steel Node

3. Outline of Construction Work

3.1 Severe Conditions for Construction Work

There were very severe conditions for implementation of the construction work. Namely, the building structure occupies almost all the site area, which meant that the 16-m wide road surrounding the site was the only and sole circulation line and loading/unloading area for the work. Infrastructure including sewage lines runs under the road and aerial decks had to be constructed above the road. How to use this road was the key for smooth implementation of the construction work all the time from the very beginning of the work to the completion of the work. Therefore, the plan of using the road was carefully worked out but it should be reviewed with great effort on the day-by-day basis.

Another severe condition was the short construction term of two and a half years.

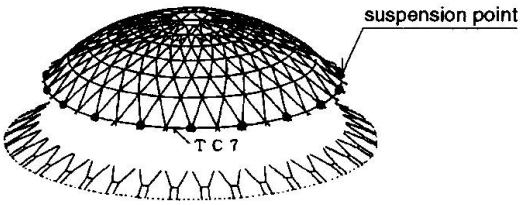

Fig.10 Lift-up Method Construction

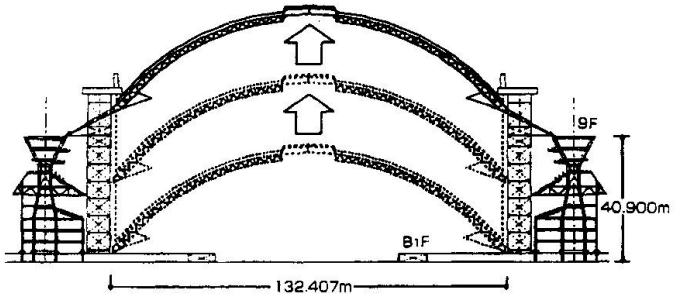

Fig.11 Lift-up Method Construction

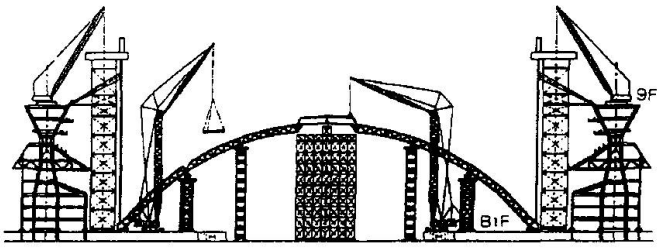

Fig.12 Steel Members Erection of the Dome

3.2 Erection of roof truss on the ground level

As a result of various study on construction sequence of the doom roof, lifting-up method was selected, in which the roof doom truss is erected on the ground and then lifted up to the required position. In the actual construction, the erection was done at the 1st basement level, and also finishing of ceiling and roofing and relevant building services work were conducted as much as possible to reduce such works after lifting up the doom truss structure. At the perimeter, construction of the stand structure were carried out simultaneously with construction of bent bases for the lifting-up operation and Y-shaped girders. Ninth floor-level structure should be a tension ring to receive deadweight of the dome roof structure at the time of jack-down operation when the lifted up dome roof structure was lowered to the final position and connected with Y-shaped girders, shifting supporting structure form the jack mechanism to the stand structure. Therefore, the construction of the stand structure had to be completed before the lifting-up operation.

3.3 Lifting-up Operation

Total deadweight of the dome roof as lifted up was about 5,500 ton. Lifting up was made by using 18 jacks, each with 600-ton capacity. Lifting up system was elaborated to automatically and precisely control the levels of each suspension points, keeping horizontal level difference among those points within 20 mm. The lifting-up volume was taken at 48.97 meters. The lifting up could be successfully done after 8 hours of careful operation. In the operation, real-time measurement of deformations of and stresses in the dome roof was carried out, which could confirm that deformations and stresses of the structure during the operation were within the range estimated by structural

analyses conducted in advance. They are shown in Fig.13.

3.4 Jack-down Operation

Jack-down operation is to shift the entire lifting-up load to th e stand structure by connecting the dome roof structure to Y-shaped girders after the lifting-up operation. The total jacking-down weight including those of Y-shaped girders was 6,700 tons. In the construction work, the compression ring (forming perimeter part of the dome structure itself) functioned as a tension ring to receive 610-ton tensile force during the lifting-up operation, and carries 240-ton compressive force after the jack-down operation.

The deformation and stresses during the jacking down work showed about 80% of those estimated by the analysis. (Fig. 14)

This means that the stand structure effectively functioned also in the construction procedures without any special reinforcement to the stand structure itself.

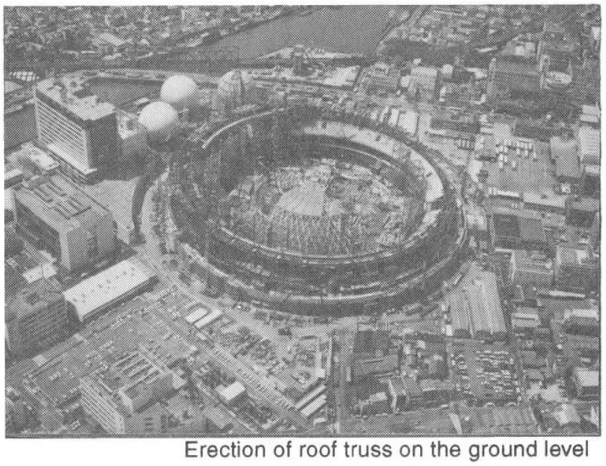

Erection of roof truss on the ground level

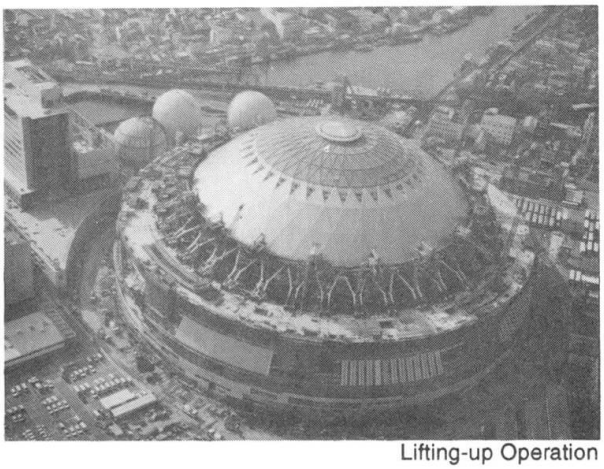

Lifting-up Operation

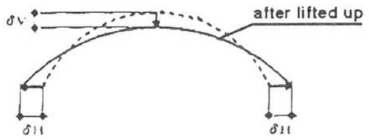

	Suspending point Measured vs Computed	Top of Dome Measured vs Computed
Horizontal disp. δ_H	28 mm vs 39 mm	—
Vertical disp. δ_V		38 mm vs 40 mm
C-Ring's Axial	430 ton vs 610 ton	—

Fig.13 Stresses and Deformations during Lifting-up Operation

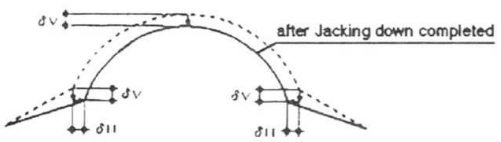

	Suspending point Measured vs Computed	Top of Dome Measured vs Computed
Horizontal disp. δ_H	-32 mm vs - 38 mm	—
Vertical disp. δ_V	65 mm vs 74 mm	29 mm vs 33 mm
C-Ring's Axial	-190 ton vs - 240 ton	—
Y-Girder's Axial	-100 ton vs - 160 ton	—

Fig.14 Stresses and Deformations during Jacking-down Operation

After completion of Dome's construction

Structural Design of Large-Span Single Layer Latticed Dome

N. SAHASHI
Dep. Senior Mgr
Takenaka Corp.
Nagoya, Japan

Y. HANGAI
Prof. Dr
Tokyo Univ.
Tokyo, Japan

T HISATOKU
Man. Dir.
Takenaka Corp.
Tokyo, Japan

M. YAMADA
Prof. Dr
Tohoku Univ.
Sendai, Japan

Summary

This report describes the types and effects of imperfections which will affect the strength of a large-scale steel single-layer latticed dome, by taking the case of designing and constructing a single-layer latticed dome as large as approx. 190 m in plane diameter.
We have conducted extensive analyses on the buckling strength, vibration characteristics, construction method and so on in consideration of imperfect loads and imperfections in order to realize a large-scale single-layer latticed dome which has been rarely built.
This report describes the following effects:
1) How imperfections affect the buckling strength and/or member stresses of a roof; and
2) The causes and amplitudes of the under-construction imperfections, and how they affect the roof stresses.

1. Outline of Roof Structure

The building dealt with in this report is "Nagoya Dome" constructed in Nagoya City, Japan. This building is a multi-purpose stadium with steel roof, mainly used for baseball games. The construction of the building was commenced in August, 1994 and completed in March, 1997. (Photo 1-1)
The roof, located at the height of approx. 36 m above the ground level, covers the ball park with the seating capacity of approx. 40 thousand. It is as large as approx. 29,000 m^2 in area and has an approx. 5,000 m^2 glass rooflight at the center.
The structural type of the roof is a steel single-layer latticed dome, 187.2 m in plane diameter and 32.95 m in height, which is one of the largest single-layer latticed dome structures in the world. (Fig. 1-1)
The under-roof structure is a steel framed reinforced concrete structure, which is 36 m high. The diameter on centers of columns along the outermost circumference is 229.6 m, and the diameter on column centers of the top floor is 187.2 m. The tension rings for the roof are located on the girders, each of which over-hangs 1.8 m inward from the center of column on the top floor of the under-roof structure because applied was the lift-up method in which the roof was built on the ground and hung up for the purpose of rationalizing the construction method. Therefore, the roof's plane diameter on centers of the tension ring members is 183.6 m, and the roof height on centers of the members is 32.95 m. Thus the rise-to-span ratio (H/L) is 0.179. (Fig. 1-2)
Each lattice component of the roof consists of 4 triangles approx. 10 m per side each, produced by splitting a triangular plane approx. 20 m per side. Those triangles are rigidly jointed to each other by welding them at the points of contact.
The lattice is made of steel pipes, 650 mm in diameter, the thickness of which is gradually increased from 19 mm at the roof center to 28 mm along the outer circumference. For the tension rings, steel pipes 950 mm in diameter and 50 mm in thickness are used. (Fig. 1-3)

2. How Geometrical Imperfections Affect Single-Layer Latticed Dome Strength

The typical structural type of the large-scale steel structure domes which have been constructed is multiple truss. Some of the reasons in designing them are as follows:

1) The out-of-plane stiffness of single-layer roofs is as small as 1/10 – 1/30 compared with that of multiple-layer roofs, and their buckling strength is likely to be largely affected by geometrical imperfections.
2) Though it is predicted that the imperfections affect others as well as the buckling strength of a single-layer latticed dome, their amplitudes and the degrees of their effects are unclear.
3) It is predicted that the geometrical imperfections occur under construction. Since the causes and amplitudes of imperfections are unclear, the effects of imperfections shall be conservatively evaluated in designing a real structure, which will require the assumption of larger geometrical imperfections and result in smaller design strength of a single-layer latticed roof.

This chapter describes the result of comparative study on how the amplitudes of geometrical imperfections affect the elastic limit strength and buckling strength of the steel single-layer lattices under the different load conditions. We evaluate buckling strengths and elastic-plastic strengths in consideration of various imperfections; The analysis model was a three-dimensional model with 577 nodal points and each nodal point was provided with 6 degrees of freedom. Non-linear incremental analysis was applied for any analyses by considering the characteristics of a single-layer latticed structure, exc[illegible] for seismic time history response analysis. The main frame under the roof was replaced by equivalent springs in the model. The analytical results are shown in Figs. 2-1 to 2-3.

The analytical results are summarized as follows:
1) The elastic limit loads were approx. 1/3 to 1/2 of the global buckling loads, and the ultimate loads were approx. 1/2. Therefore, the member yield precedes the global buckling on such a scale as the single-layer latticed dome used in analyses.
2) The effects that geometrical imperfections exercised on buckling loads were the largest during the full load application: the strength accounted for approx. 60 % at the imperfection $\xi \fallingdotseq 1.0$ and reduced to approx. 47% at the imperfection $\xi \fallingdotseq 2.0$.
3) The perfect system buckling load with the partial load considered at the center of the roof was the smallest: 76% of that during the full load application. The effects of the imperfections were relatively small. Near the imperfection $\xi \fallingdotseq 2.0$ in any load distribution, the buckling strength was approx. 1/2 of that during the full load application.
4) The effects that imperfections exercised on the ultimate strength were relatively small: approx. 92 % at the imperfection $\xi \fallingdotseq 1.0$.
5) The effects that imperfections exercised on the elastic limit strength at the imperfection $\xi \fallingdotseq 2.0$ varied to 85% $\sim$ 65% of the perfect system, which shows the result of the effects exercised by the combination of load distribution and imperfection distribution.

The above listed results show that the geometrical imperfections affect the member stresses and the member strength as well as the global buckling strength. They also shows that the effects greatly differ depending on the pattern of imperfection distribution.

To rationally realize a large-scale single-layer latticed dome, the amplitudes and distribution of the imperfections used for conservative evaluation shall be precisely defined. The next chapter describes the distribution and amplitudes of the imperfections which occur during the construction of a real structure as well as their effects.

3. Evaluation on Imperfections of Steel Single-Layer Latticed Dome

This chapter presents the types and amplitudes of the imperfections which occur at a steel single-layer latticed dome under construction, and the degrees of their effects, all of which are found in analyses.
The under-construction conditions taken into consideration were

1) (erection analysis) ・・・the assembling procedure / temporary structure support conditions, and the load conditions;
2) (temperature analysis) ・・・the local temperature variation under construction; and
3) (welding analysis)・・・the variation in the effects of the members' axial shrinkages caused by the assembly welding, during the period of assembling the steel lattice for the roof on the site.

The above listed analyses 1) to 3) were individually conducted, and their results were accumulated to define the effects.
Specifically, the typical under-construction configurations during the roof fabrication were set in the analytical models. The analysis in consideration of the above conditions 1) to 3) was conducted on each of the set models, the results of which were calculated in the addition, and thus the predicted effects of the construction were grasped.
The imperfections accompanying the construction are shown by the differences between the member stresses / contact deformations calculated in the above method and the results obtained in the method (perfect system analysis) where all the loads were applied together to the perfect system model usually used for the structural analysis. Photo 3-1 shows the construction in progress, and Fig. 3-1 shows the sketch of the analytical models.
The results of expressing the effects of the construction in the variation correlative distributions of the member stress ratios are shown in Figs. 3-2 to 3-5.
The abscissa indicates the perfect-system analytical results, and the ordinate indicates the under-construction imperfection analytical results.
Figs. 3-6 and 3-7 show the distributions of the vertical imperfections at the points of contact. Fig. 3-6 shows the plane distribution of geometrical imperfections, while Fig. 3-7 shows the imperfections graphed by nondimensionalizing the geometrical imperfections at the radius of gyration of the members and splitting them into 6 between the center and the outer circumference of the roof.

The summary of the results is as follows:

1) Most of the imperfections which occur under on-site erection are caused by welding.
2) The effects of the whole construction result in the member stress ratio of approx. ± 0.2.
3) The effects on the member stresses under the different analytical conditions vary from one another in amplitude and affected member. Therefore, the effects of the whole construction are smaller than the result of the simple accumulation of the analytical results.
4) The geometrical imperfections under construction are as small as approx. 0.15 i (i = radius of gyration of the member) in case of the nondimensionalized imperfections.

The effects that construction exercised on a single-layer latticed dome resulted in larger imperfections of member stresses and rather smaller geometrical imperfections. It is also concluded that the member stress imperfections were mainly caused by the bending moment variation.

The similar analyses were conducted on the various under-construction conditions which were changed from the original ones. The degree of effects increased by approx. 50 %, but there was no great difference in the tendency of effects.

4. Conclusion

The measurement of member stress variations started during the construction. The propriety of the analyses has been verified in comparison between the analytical results of under-construction imperfections and the actual measurements. The analytical results are in good agreement with the results of actual measurements, which means that the imperfections of a large-scale single-layer latticed dome can be grasped to some degree in analyses. Therefore, the conservative evaluation where the effects of imperfections are rationally considered is available in designing a large-scale single-layer latticed dome.

Lastly, here by taking this opportunity, I would like to express my gratitude to Professor Yamada of Tohoku University, Professor Hangai of Tokyo University, and many other people concerned for their kind cooperation and guidance in this research.

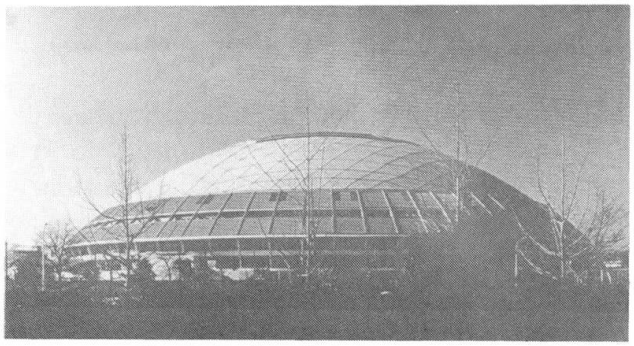

Panoramic view

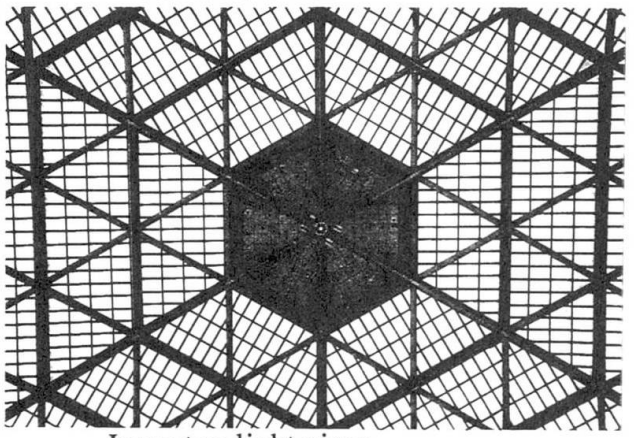

Inner top-light view

Photo 1-1 Panoramic view of Nagoya Dome

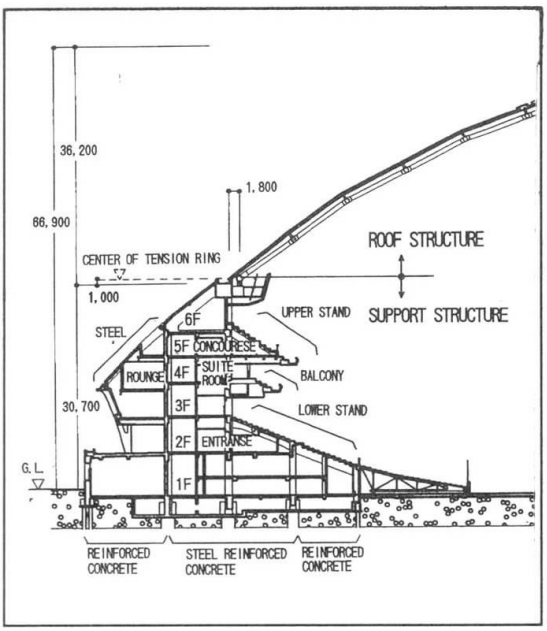

Fig. 1-1 Section of the building frame

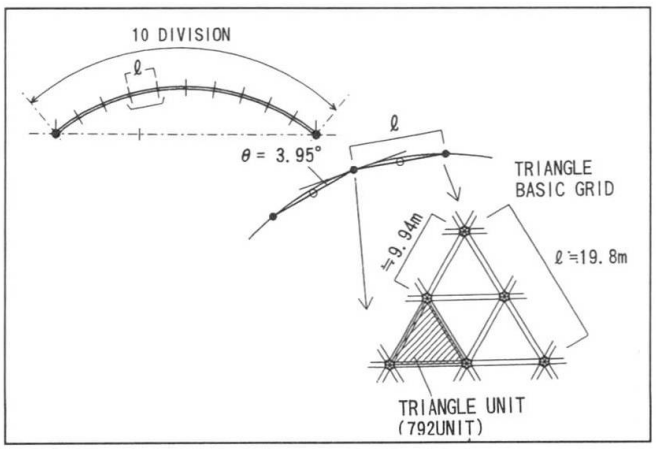

Fig. 1-2 The lattice division pattern

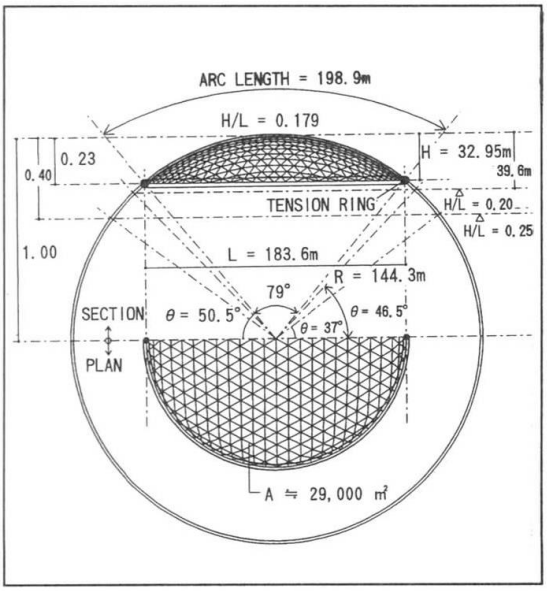

Fig 1-3 The roof Structure section

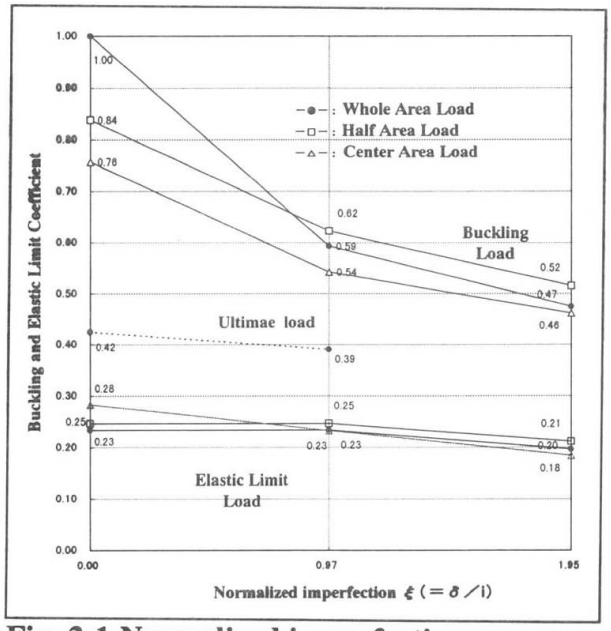

Fig. 2-1 Normalized imperfection amplitude and buckling coefficient

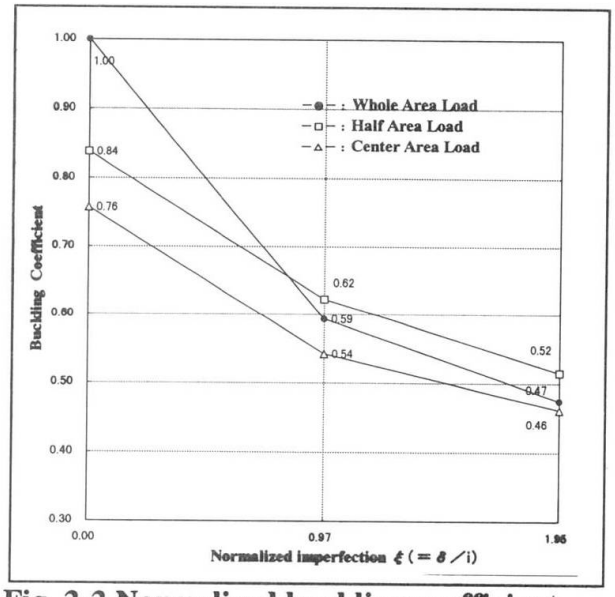

Fig. 2-2 Normalized buckling coefficient

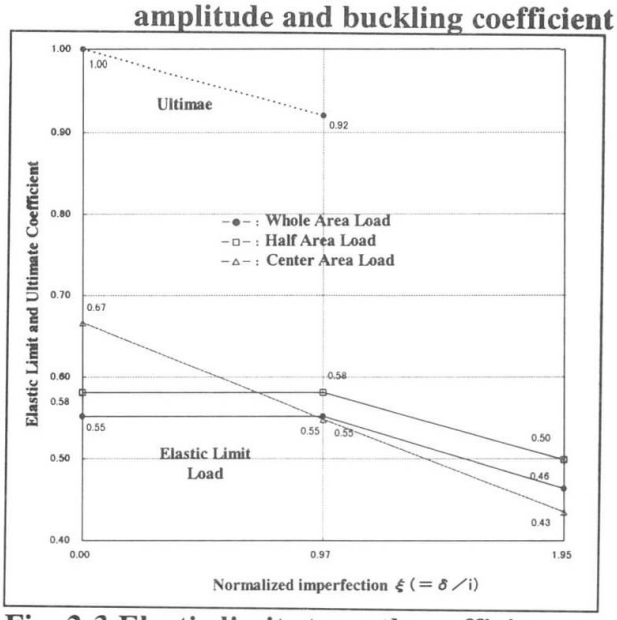

Fig. 2-3 Elastic limit strength coefficient

Photo. 3-1 Over view of construction state

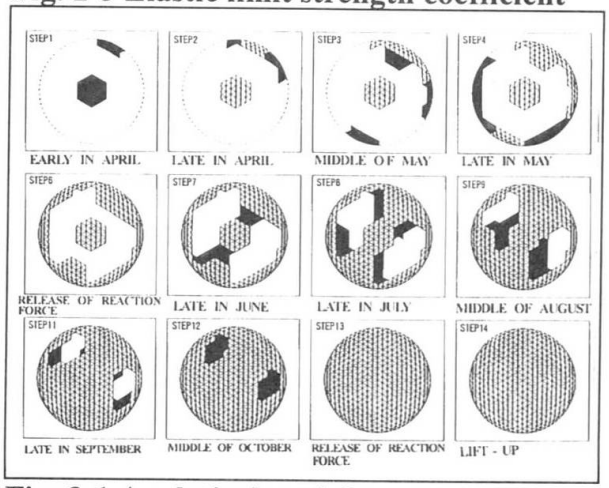

Fig. 3-1 Analytical models corresponding to construction steps

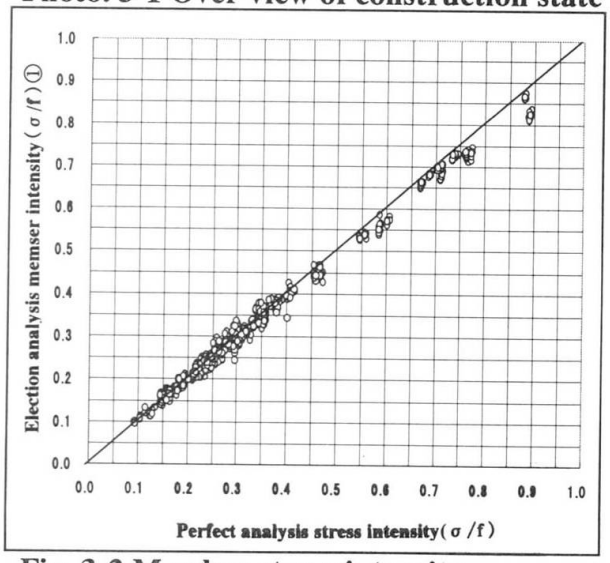

Fig. 3-2 Member stress intensity correlation (Erection analysis)

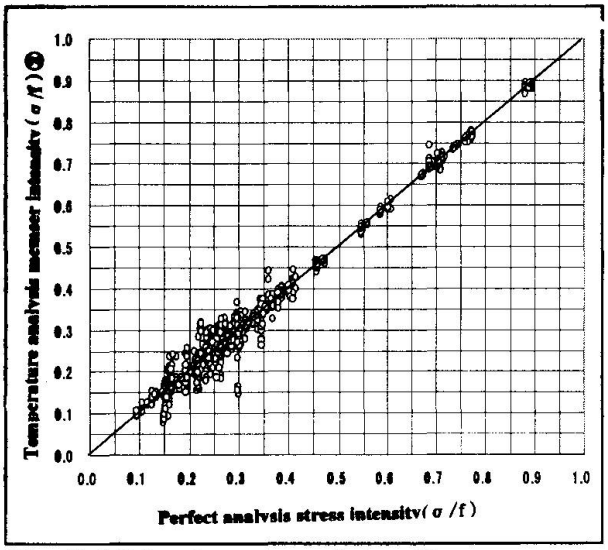

Fig. 3-3 Member stress intensity correlation (Temperature analysis)

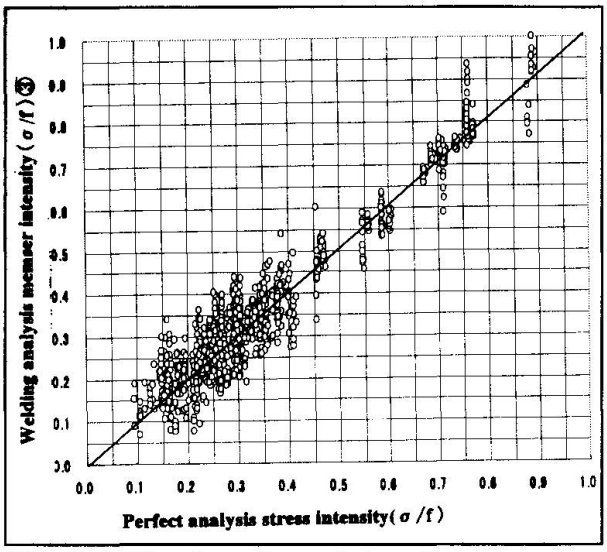

Fig. 3-4 Member stress intensity correlation (Welding analysis)

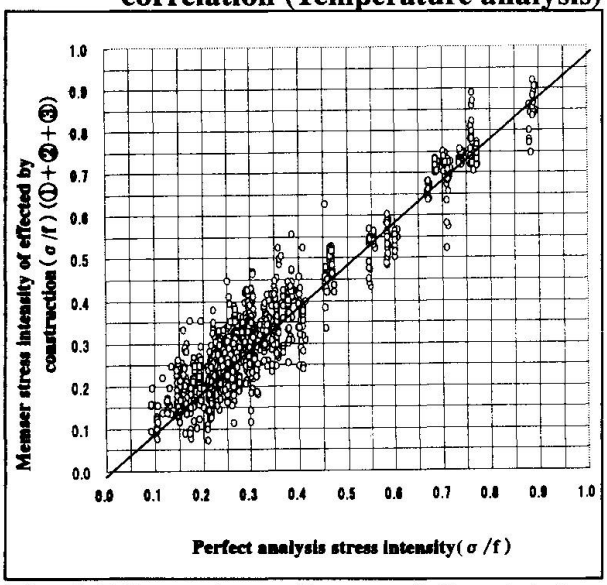

Fig. 3-5 Stress intensity correlation total (under-construction)

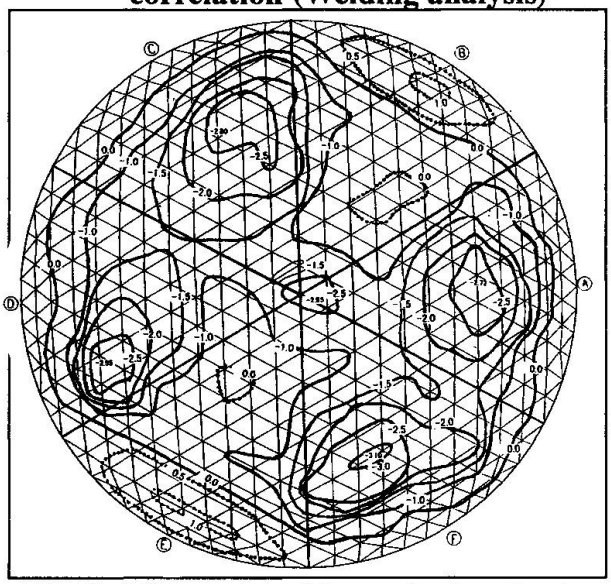

Fig. 3-6 Geometrical imperfections(cm) (plane distribution)

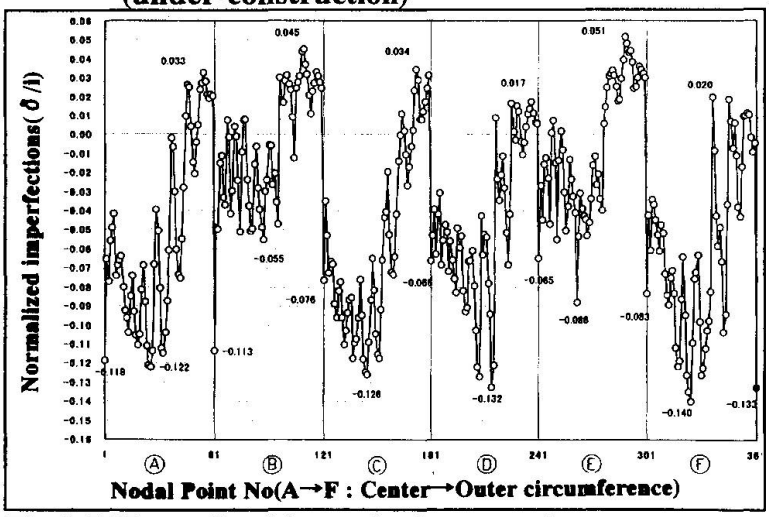

Fig.3-7 Normalized imperfections graph of each nodal point

reference
1)K.Heki,Y.Hangai,M.Yamada,S.Kato; Stability Analysis of Single Layer Latticed Dome; Architectural Institute of Japan
2)N.Sahashi,T.Hisatoku;etc.; Structural Design and Construction of Large-Scale Single-Layer Latticed Dome of Nagoya Dome; IASS Proceedings(1996)

Nagano Olympic Memorial Arena: Design and Construction

Shigeru BAN
Kajima Arch. and Eng.
Design
Tokyo, Japan

Arata YOSHIDA
Kajima Arch. and Eng.
Design
Tokyo, Japan

Shohei MOTOHASHI
Kajima Arch. and Eng.
Design
Tokyo, Japan

Haruji TSUBOTA
Kajima Techn. Research Inst.
Tokyo, Japan

Summary

The Nagano Olympic Memorial Arena, located in Nagano-City, Japan is where the 18th winter Olympic games will be held in February 1998. It is one of the world's largest speed skating arenas, covering an 80m x 216m free space containing a 400m speed skate oval and seating for about 10,000 spectators.
One of the main features of the structure is the 30cm thick, 80m long semi-rigid hybrid suspended roof. Each hanging member is composed of two glued laminated timbers (glulams) sandwiching a steel plate. Hanging structures generally incorporate bracing members to increase roof stability and to resist wind up-lift and lateral load. This structure instead utilizes the bending stiffness of glulams and the in-plane stiffness of plywood panels attached to roofing members.
This paper describes the structural system and design, and its construction method.

1. Structural concept

A new type of hanging roof structure covering an 80 m x 216 m free space has been developed, designed and constructed. As shown in Photo.1, it comprises a series of suspended roof elements inspired by the peaks of the Japan Alps. It creates a new and fresh impression, contrasting the more traditional round dome configuration. This shape also decreases the total volume of the inner space. The most distinctive characteristic of the structure is its semi-rigid hanging roof spanning 80m. It's thickness is only 30cm. The structure consists of fifteen hanging roof panels, each composed of composite hanging beams with plywood fixed to them. Each composite hanging beam is composed of two glulam beams sandwiching a steel plate.
In general , one way hanging roof structures deform easily under up-lift and lateral wind loads. Therefore, this kind of hanging structure is usually designed with bracing and/or suppressing members to resist up-lift and lateral movements. However, the semi-rigid hanging roof structure here was required by its architectural design to have no bracing and suppressing members. Instead, it utilizes the bending stiffness of the composite beams (glulams) resisting the up-lift load and the shearing stiffness of the plywood panels resisting the lateral load.

2. Outline of structural system and design

The structural system and design of this speed skate ovals is outlined in Fig.1. As shown, the overall structure consists of fifteen structural units. Each unit has two reinforced concrete counterweights, two leaning walls, and a hanging roof panel pin connected to the top edge of the leaning walls. The center roof unit is the highest , and roof unit height reduces in 3-meter gaps toward the outside units. The configuration of the hanging roof portion is the same for all units,

and is as follows: span, 80 meters; sag, 5 meters; and width, 18 meters.
According to the Japanese Building Code, snow load is assumed to be 160kg/m^2 and wind load is assumed to be 185kg/m^2. The up-lift wind load coefficient is assumed to be 0.7 according to the results of wind tunnel tests. The basic load bearing mechanism of each roof unit is shown in Fig.2. The details of each structural portion are summarized in follows.

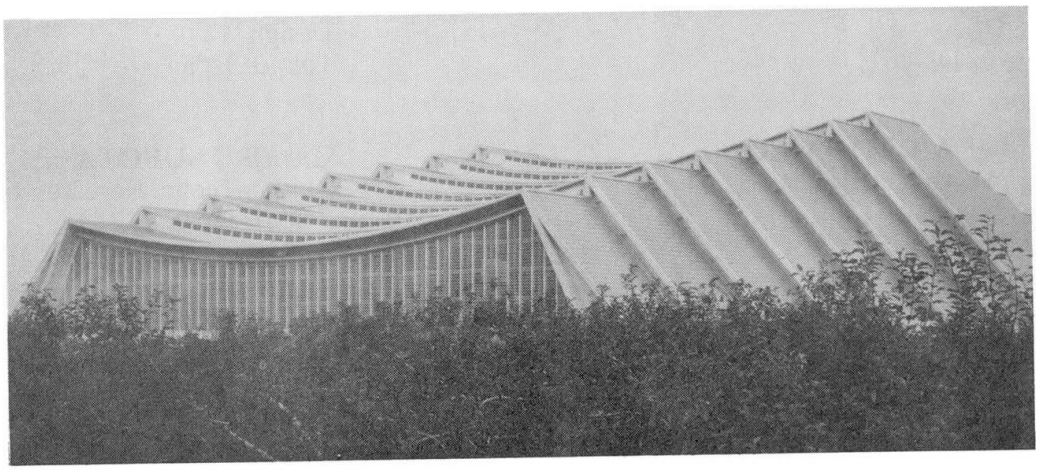

Photo. 1 General View

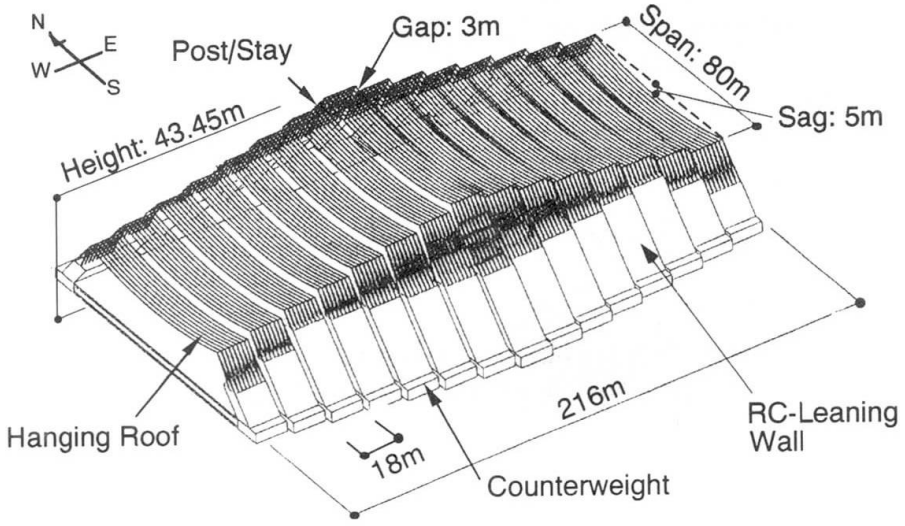

Fig.1 Outline of the Structure

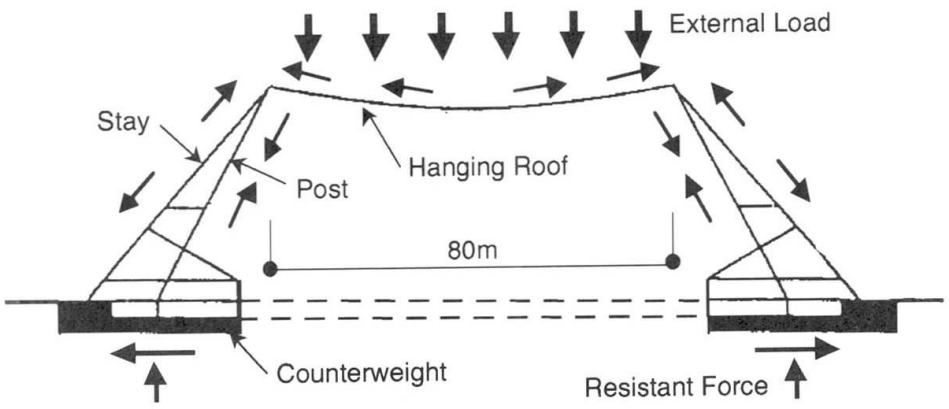

Fig.2 Basic Load Bearing Mechanism

2.1 Hanging roof

A section of the roof panel is shown in Fig.3. Each main beam is a composite member composed of glulams and a steel plate. Two glulam beams (300mm x 125mm x 2) sandwich a steel plate (200mm x 12mm) and they are connected to each other with steel bolts at 2m pitch. In the design of this composite member, the axial force and the bending moment are sustained by glulams and steel plate corresponding to their stiffness[*1]. Because of the feature of the structural system, the axial tensile force is dominant and the bending moment is rather small.
The most important thing in stabilizing this hanging roof under wind load is to maintain the tensile force in the composite member. This is assured by the three-dimensional wind-induced response analysis considering geometric non-linearity[*2]. Furthermore dynamic tests were conducted on a 1/4 scale hanging roof model[*3] and an actual hanging roof[*4] to confirm its dynamic characteristics.
The beams are spaced at 600mm. Thus, one roof panel consists of thirty main beams pin supported at the ends of the steel plate, and connected to each other at 10m intervals by steel tie plates.
Plywood panels 12mm thick are nailed to the top surface of the glulams. The panels work not only as sheeting roof boards, but also as structural members to increase the in-plane stiffness of the roof panels.

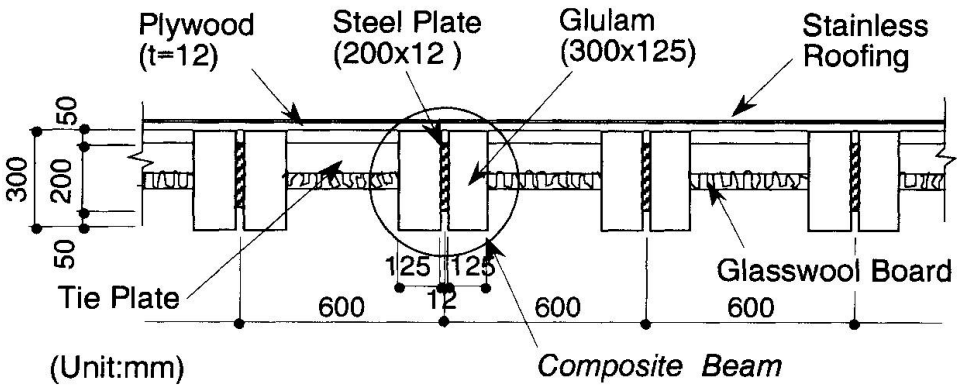

Fig.3 Section of Hanging Roof

2.2 Leaning wall

The leaning walls transmit loads from the hanging roofs to the foundation. Their upper portions are composed of steel posts and stays, forming a triangle. The posts resist compression and the stays resist tension. The lower portions of the walls are made of reinforced concrete. Pre-stressed steel rods are added to the outer portion of the wall to resist the tensile force, which is caused by the hanging roof, from steel stays. The center triangle is the highest, and the height reduces in 3-meter gaps toward the outer units.

2.3 Foundation

Reinforced concrete counterweights, which resist tensile forces from the hanging roofs, are located under the leaning walls. Pre-stressed steel rods are fixed into this counterweight. All of these structures are supported by pre-stressed concrete piles, 600mm in diameter and 10 - 12m long, founded on a sand gravel layer.

3. Construction

One of the most important problems was how to construct these flexible hanging roofs. Unlike conventional rigid roofs, the 80-m-span hanging roofs are stabilized by introducing the necessary tension into structural elements, even in the construction stage. Furthermore, there was no available construction record on such large flexible hanging roofs. Therefore, a rational and new construction method have to be developed. Various construction methods were proposed and investigated. Finally, a new lift-up construction method was devised and actually employed.

3.1 Construction Method

The newly developed construction method is illustrated in Fig.4. The outline of the construction sequence is summarized as follows.

First, six composite hanging members composed of glulams and a steel plate were assembled into one lift-up unit (80m long and 3.6m wide) on the ground level. Next, both ends of the lift-up unit were temporarily fixed to lift-up racks. At this point, the necessary tension was introduced into the lift-up unit. The lift-up racks were then raised gradually with winches along vertical guide frames by wires hanging at the four corners of the lift-up unit. Hydraulic jacks were installed on the lift-up racks. When the lift-up unit rose to the specified level, the hydraulic jacks were used to adjust its horizontal position for inserting pins into shoes of steel posts. At this stage, the lift-up unit is completely pin-connected to the steel post. Then, the lift-up racks were returned to ground level and moved horizontally along the rails. One hanging roof was completed by repeating this procedure five times.

With this method, the necessary tension was introduced into the flexible 80-m-span lift-up units, and were stable even under strong wind during construction. Furthermore, this method reduced the work load at high levels, maintained safety and shortened construction time.

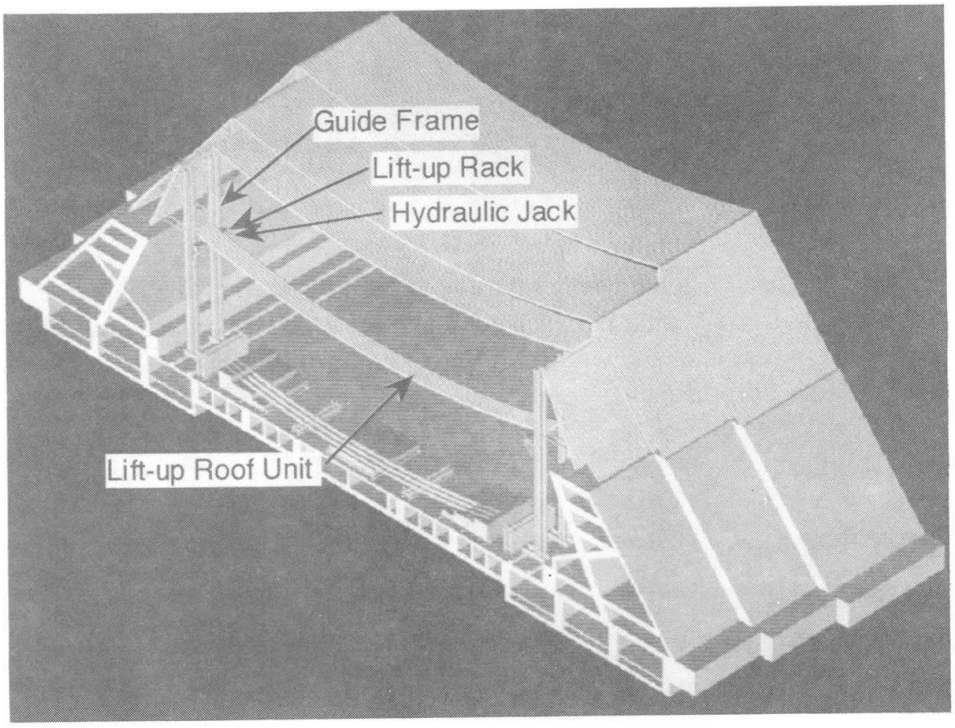

Fig. 4 Lift-Up Construction Method

3.2 Scale-model test for construction

Prior to actual construction, a scale-model test was carried out to confirm the feasibility, safety and workability of this lift-up method. The test specimen was a 1/4-scale hanging roof panel model, with 20m span and 4.5m width. As shown in Photo.2, the same equipment, i.e. a lift-up racks, wires, winches and hydraulic jacks were installed to this model, and one lift-up unit was raised. During the test, strains in the hanging members, tension in the hanging wires, forces in the hydraulic jacks, lift-up height and configuration of the model were measured. In the test, in addition to the normal lift-up procedure without error or accident, abnormal procedures which correspond to strong wind conditions and/or unbalanced lift-up state assumed in the actual construction were tested.

This scale-model test confirmed the feasibility of the proposed lift-up method. The measured stresses of the lift-up unit during the lift-up state were within the allowable range, and the structural safety during construction was confirmed. Furthermore, the stresses and configurations under the abnormal lift-up procedure were grasped, and the tolerance construction errors in the actual construction were quantitatively evaluated. Finally, these data obtained from the scale-model test were fed back to the actual construction .

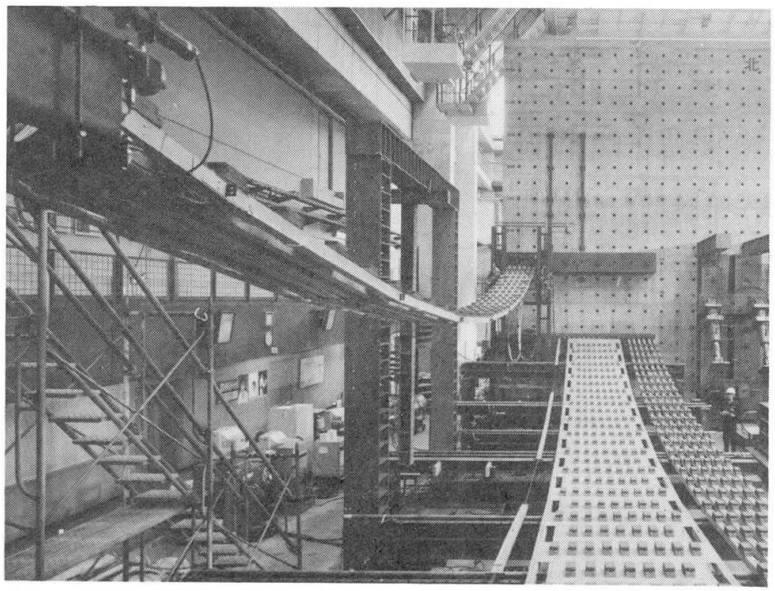

Photo. 2 Overview of the Scale-Model Test for Construction

3.3 Actual construction

The set of equipment consisting of lift-up racks, guide frames and hydraulic jacks, employed in the actual construction is shown in Photo.3 and Photo.4, and the actual lift-up state is shown in Photo.5. During the actual lift-up procedure, the stresses in the lift-up unit and supporting steel frames were measured to reconfirm the structural safety of the hanging roof panels during construction. Furthermore, its final configuration after raising procedure was also measured to examine the construction accuracy.

The measured stresses were within the allowable range predicted in the scale-model test, and its final configuration was almost same as that specified in the design. Therefore, these measurements confirmed that the proposed construction method was rational and safe.

In the actual construction, two of lift-up systems were employed, and three lift-up units were raised per two days. As a result, it took about two months to raise the all hanging roofs. This construction

period was very short compared with conventional erection methods, and the construction time was significantly reduced.

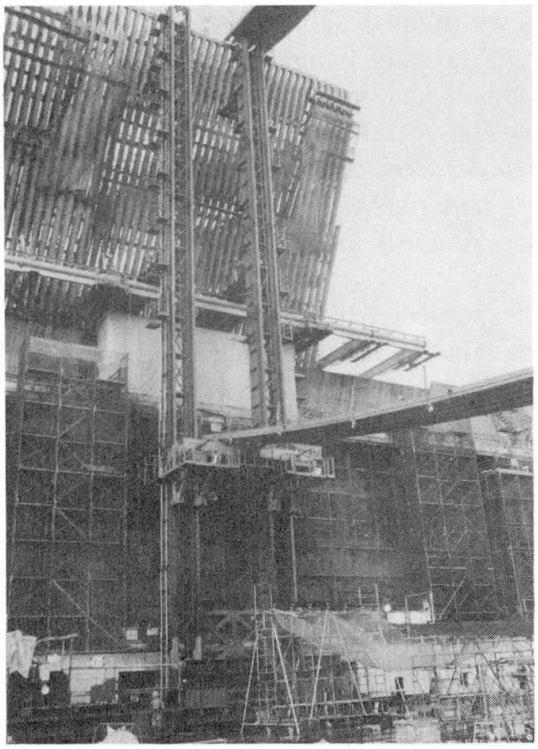

Photo. 3 Lift-Up Equipment (Start)

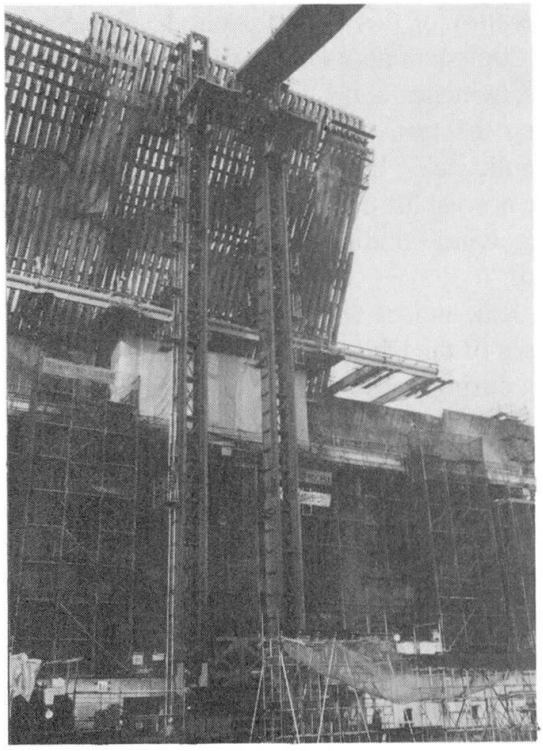

Photo. 4 Lift-Up Equipment (Top portion)

Photo. 5 Overview of the Actual Lift-Up State

References

*1 Tsubota et al, "Development of a Semi-Rigid Hanging Roof Structure Composed of Glulams and a Steel Plate, Part 1:Outline of the Structure and Structural Test on Composite Members", IASS International Symposium, 1995

*2 Hayami et al, "A Semi-Rigid Hanging Roof Structure Composed of Glulams and a Steel Plate, Part 4:Three-Dimensional Wind Induced Response Analysis", IASS Int. Symposium, 1996

*3 Motohashi et al, "A Semi-Rigid Hanging Roof Structure Composed of Glulams and a Steel Plate, Part 3:Dynamic and Static Model Test", IASS Int. Symposium, 1996

*4 Tsubota et al, "A Semi-Rigid Hanging Roof Structure Composed of Glulams and a Steel Plate, Part 5:Dynamic Tests on an Actual Roof Panel ", IASS Int. Symposium, 1997

Structural Design and Construction of the Wins Garden Plaza

Yuji SHIGEMATSU
Gen. Mgr
Tohata Arch. Eng.
Osaka, Japan

Masanori FUJITA
Mgr
Nippon Steel Corp.
Tokyo, Japan

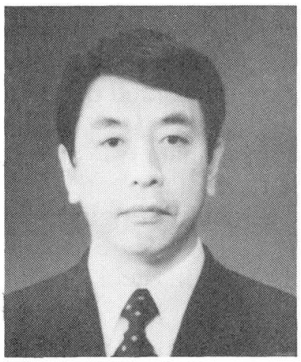

Mamoru IWATA
Dr Eng., Gen. Mgr
Nippon Steel Corp.
Tokyo, Japan

Summary

The Wins Garden Plaza represents a pioneer building in urban waterfront development in Kyushu. This facility is composed of the Wins building, which functions as a communitiy place and the garden plaza, which provides a place of interchange for citizens. The site is located on the Dokai Bay, and the plan was designed especially with the sea and waterfront in mind. The large roof of the Garden Plaza is intended to convey a feeling of lightness, and is shaped to somewhat resemble the wings of a seagull (Fig.1). The design of the Garden Plaza has a high decorativeness with the membranes and the structural members in harmony. This report describes the structural design and the construction of the suspension structure for the large roof of the Wins Garden Plaza.

1. Structural concept

The roof (88 m x 45 m) has a low-rise form (rise-span ratio: 0.08-0.13), and is composed of eight units 20 m x 20 m each with a column at the center. The center-to-center distance of each column is 20 m and the curvature is in two directions (Fig.2). The structure is composed of the three parts : membrame, columns and beams of nonuniform section and strings. These

Fig.1 Wins Garden Plaza

strings are composed of 64 upper strings (hereinafter referred to as "strings") for supporting dead load and 24 lower strings(hereinafter referred to as "stays") in the peripheral parts for suppressing the deformation under an upward wind load . Tensile forces are introduced in the strings and membrane so that they can resist thrust and wind load. The foundation is directly supported with reinforced concrete piles by the all-casing construction.

- Project :Wins Yahata
- Site: Kyushu,Japan
- Client :Class Media
- Construction schedule : June1996 to July 1997
- Architects, Structural Engineers:TOHATA ARCHITECTS ENGINEERS and Nippon Steel Corporation
- Contractor :Nippon Steel Corporation and Taisei Corporation J.V.

2. Structural plan

1)This is a rational structural system in which a reduction in weight is aimed at by adopting a single-layer structure and a suspension structure. The thrusts of the roof are suppressed by the girders and tensile forces applied to the membrame and strings.

2)The structure is composed of columns(C1-3), which are members of nonuniform section composed of square sections, girders (G) of nonuniform section, which are composed of square sections with a depth of 470 mm at the center and a depth of 740 mm at the ends, and peripheral girders of triangle section that function as tension rings,which are all rigidly jointed(Fig. 3).

3)For the roof supported with eight columns, strings are arranged on the diagonal lines to each corner where maximum displacement occurs under vertical load and stays are arranged at the peripheral girders (S2). In order to suppress displacement of strings under additional load, tensile forces of 98-108 KN and tensile forces of 19.6-58.8 KN are introduced in each strings and stays, respectively. In consideration of safety, two groups of strings or stays are used as one set.

2.1 Design Load

1)Dead load: DL = 1.47 KN / m^2
(membrane: 0.0147 KN / m^2, surrounding glass sash: 0.294 KN / m^2)
2) Temperature load: 15° C
3) Snow load: 0.65 KN / m^2
For the snow load, total load and half load were considered.
4) Wind load (Coefficient of wind load)

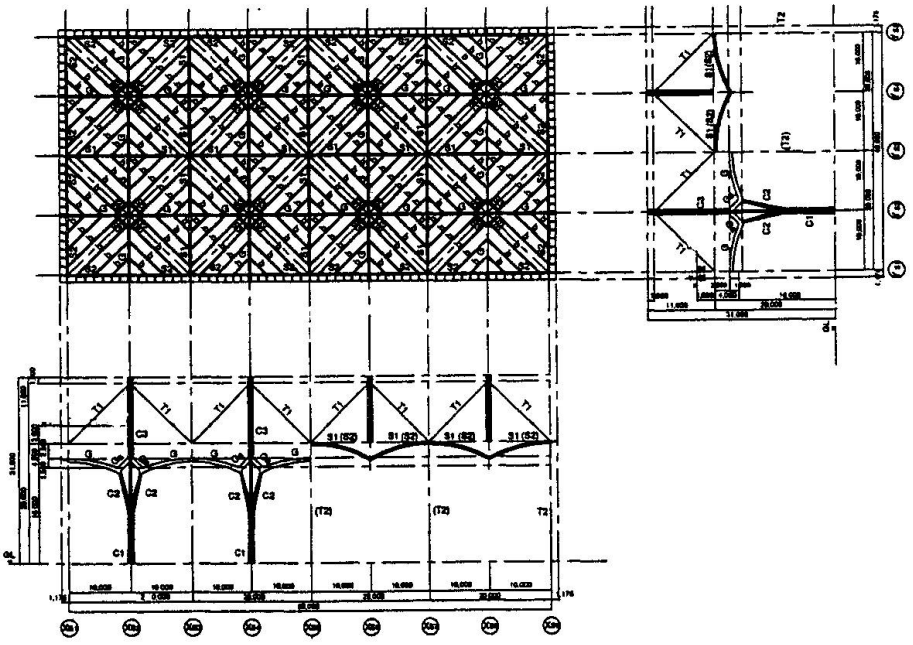

Fig.2 Plan and Section

- General part of the roof in X direction: -0.7
- Eaves part of the roof in X direction: +0.65, +0.6
- General part of the roof in Y direction: -0.7
- Eaves part of the roof in Y direction: -1.3, +0.6

Note (- : upward wind, + : downward wind)

5) Earthquake load

Lateral seismic coefficient k = 0.24 (C_0 = 0.3, regional coefficient = 0.8)

2.2 Structural Materials

1) Membrane: Glass fiber of ethylene tetrafluoride resin (Type A membrane)

2) String and stay

• Tie rod: 2 ϕ 38, SS490 • Pin: SS490

(Yield point: 275 N/mm^2 and more, tensile strength: 490-610 N/mm^2, elongation 21% and more)

• Turn buckle: S35C • Fork end: SN490B

3) Beam and column: SN490B (string-supporting plates are made of SN490C)

2.3 Strings with height difference

When a uniform load p is applied to a string with a height difference (supposed to be a parabola), the tensile force is affected by sag which is natural deflection by own weight(Fig. 4).

The relation between the sag and the tensile force of string is shown in Fig. 5. The analytical value of the tensile force is almost equal to the roughly-calculated value supposed to be a parabola. The tensile force increases abruptly with decreasing sag. This shows that it is very difficult to keep a string in a straight line condition, and that it is necessary to consider the effect of sag due to natural deflection.

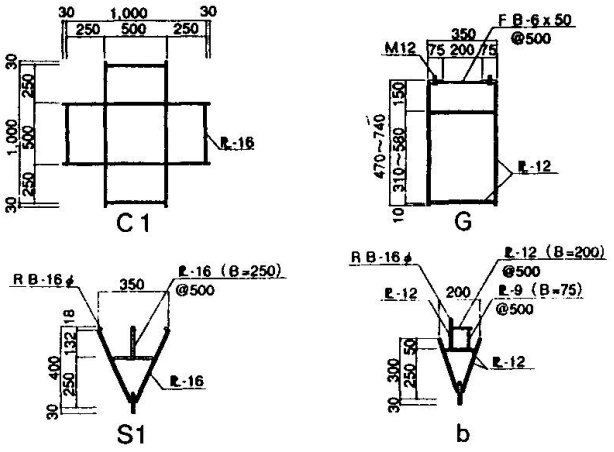

Fig.3 Section

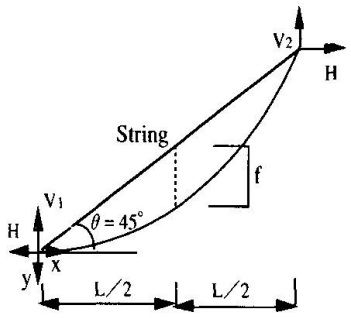

Fig.4 String with a height difference

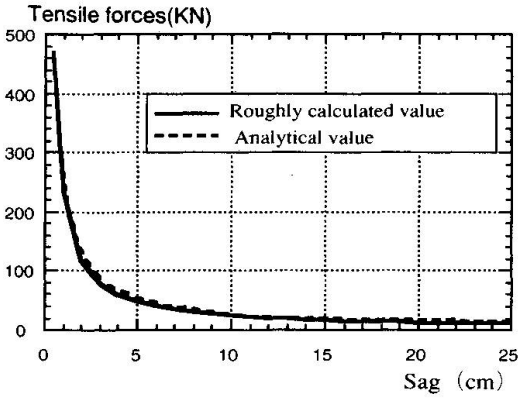

Fig.5 Tensile force and sag of string

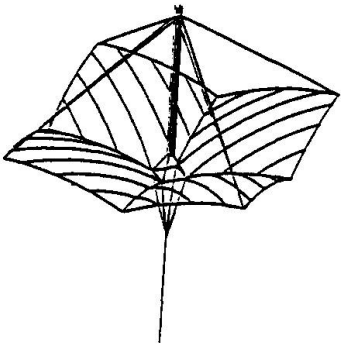

Fig.6 *Single model for preliminary analyses*

2.4 Structural Analysis and Member Design

Frames and membrane were separately analyzed by working the reaction force of the membrane to the frames as an external force. As preliminary analyses of a model 20 m x 20 m (Fig. 6), a geometric nonlinear analysis was first conducted using girders and columns as beam elements and strings and stays as cable elements. This analysis is based on the assumption that the cable elements are linear elastic members which only resist tensile forces and that the bending rigidity of strings and stays is neglected. As a result of this preliminary analysis, it was found that the ratio of tensile forces of string is about 30% of dead load. The tensile force working on strings, which shows nonlinear property, was set in consideration of the natural deflection due to the own weight of the string.
The tensile forces of strings and stays were set in truss elements in an overall model, owing to the limited calculation processing capacity and determined by repeated simulations so that the tensile forces of strings and stays and the rigidity of frames are well-balanced (tensile forces of strings: 98 -108 KN). The axial force and deformation under dead load are respectively shown in Fig.7 . The girder (G) at the center functions as a compression ring and the frames and strings of the roof acquire self-balance. In addition, owing to the tensile forces (19.6-58.8 KN) introduced in the stays, the tensile forces of strings finally does not disappear under wind load.

3. Behavior under construction

The construction site of this structure is near a wharf and has a marine transportation to the fabrication shop (Wakamatsu Fabrication Center of Nippon Steel Corporation), thus providing adequate conditions. Therefore, the large block construction was accomplished in the fabrication shop, lateral movement was accomplished using dollies which are used to move and install large structures,and marine transportation by barge, and jacking down were carried out by dollies (Fig.8). The adoption of these processes resulted in a shortened construction schedule, reduced site welding, minimized welding strain, etc. The behaviors of stress, displacement and reaction force during construction were examined by conducting analyses because the form of the structure changes from the fabrication stage to the construction stage.

3.1 Fabrication of large block

In the large block process, the structure is assembled in the fabrication stage, lifted with two 650-t crawler cranes, and then set on columns which are assembled beforehand. After that, the structure is welded at the junctions of girder and column. The structure was divided into two blocks, owing to the limited turning space of the dolly at the site. Each block was lifted at four points near the positions of the columns of each block.

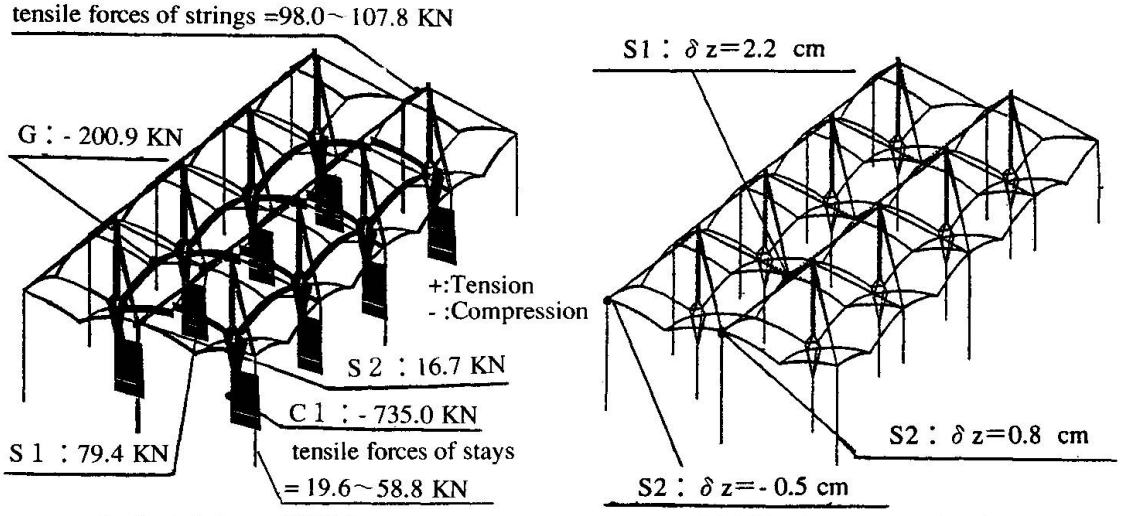

a) Axial force(KN) b) Displacement (cm)

Fig.7 Axial force and displacement under vertical load

3.2 Marine transportation by barge

In the marine transportation by barge, block 1 (2548 KN) and block 2 (2940 KN) are jacked up by dollies. These two blocks rolled on Wakamatsu Fabrication Center by barge, and rolled off Yahata higashida port (Fig. 9). To obtain the supporting points of each block to dollies and the required degree of fixing of base of column, temporary truss were installed around the column. Furthermore, wire ropes were installed on each column on the diagonal lines in order to prevent overturns, thus ensuring safety during fabrication and construction.

3.3 Jacking-down

After lateral moving by dollies on site, jacking-down was conducted using individual hydraulic jacks installed beforehand in the dollies at the supporting points (4 points) of temporary truss. Each block of structure was set so that the displacement of the bottom end of the column was 5 mm or less, because the supporting positions of temporary truss are away from the columns. After the completion of jacking-down, junction of each block of structure and the base of column installed beforehand are welded on site. After the concrete of the bases of the columns had obtained the prescribed strength, the temporary truss were then removed.

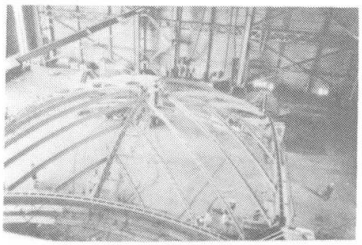

1)Fabrication on plant

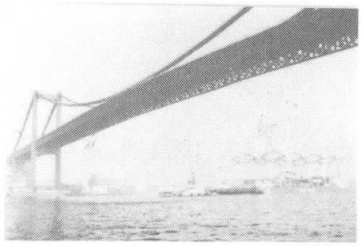

5) Marine transportation

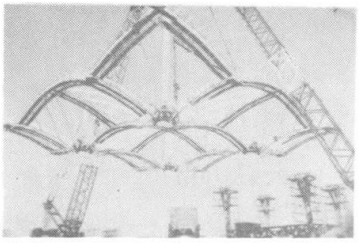

2)Large block fabrication

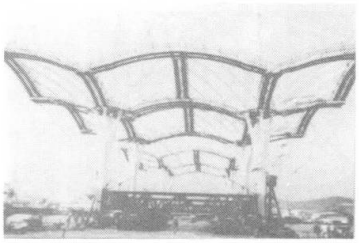

6)Lateral movement by dollies

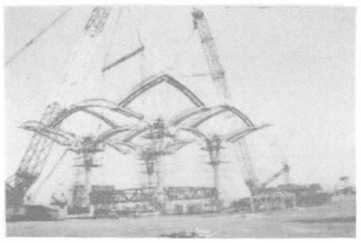

3)Setting structure on column

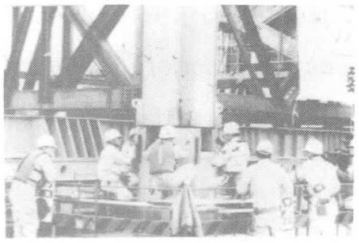

7)Jacking down by dollies

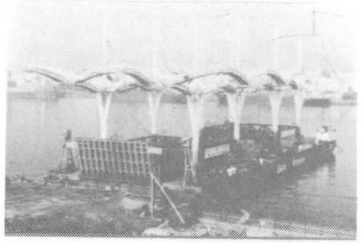

4)Rolling on by barge

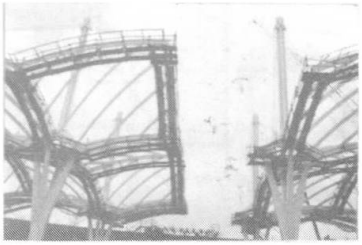

8)Junction of joint

Fig 8 Process of construction

3.4 Tensile Forces

In each unit, the strings in the diagonal direction with the column at the center and the structure are arranged in symmetry. Therefore, the structural property is close to self-balance. Because tensile forces of strings are introduced by the own weight of the structure (Fig.10). Because the strings attached to the peripheral girder (S2) (1, 3, 5, 7, 10 and 12 indicate the order of introduction of tensile force) are affected by loss of tensile forces of adjacent strings, the tensile forces of strings were introduced at the same time from the center

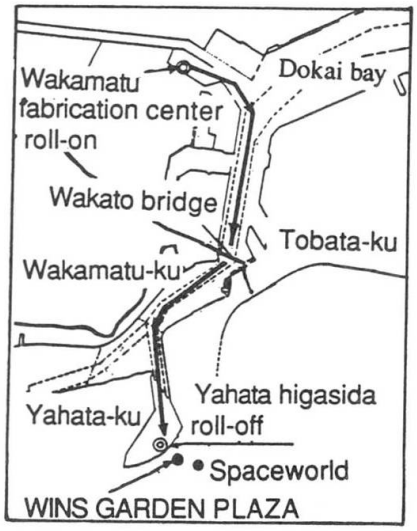

Fig 9 Marine transportation by barge

to the ends.The control of tensile forces of strings and stays was conducted using strain gauges. The tensile forces were set so that the maximum value is 1.3 relative to the design value and the minimum value is 0.9 relative to the design value. The measurements of tensile forces were carried out in six steps: before the jacking-down of each block (Step1), after jacking-down (Step 2: temporary truss exist), after the welding of the junctions (Step 3: after the removal of temporary truss), and 60%, 80% and 100% of design value (Steps 4 to 6) (Fig.11). For the tensile forces of strings and stays, however, the total of the measured values of two members was adopted. The tensile forces of strings and stays finally met the target values relative to the design values.The change of tensile forces of stays are little compared to that of temperature (Fig.12).

4. Conclusions

This paper described the design and construction of the suspension stucture applied in the large roof of the Wins Garden Plaza. In order to cope with the behavior in each form of this structure from the fabrication to the final stucture, examinations were conducted into the residual stresses due to welding strains, and fabrication procedure were also conducted so as to ensure initial form in addition to the above technical problems. The authors would like to extend their thanks to those persons concerned who gave their cooperation in constructing this structure.

References

Recommendations for Design of Cable Structures : A.I.J. ,1994, June

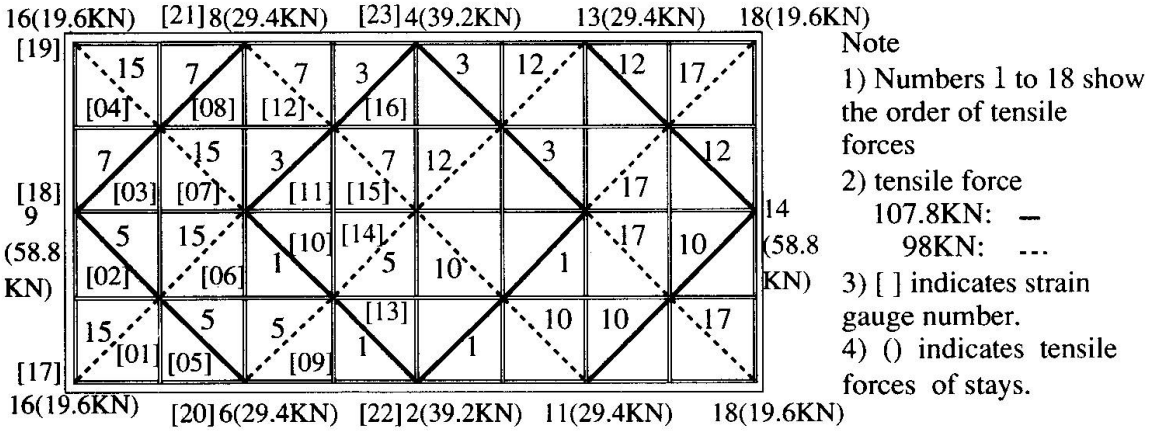

Fig.10 Tensile forces and order of introduction

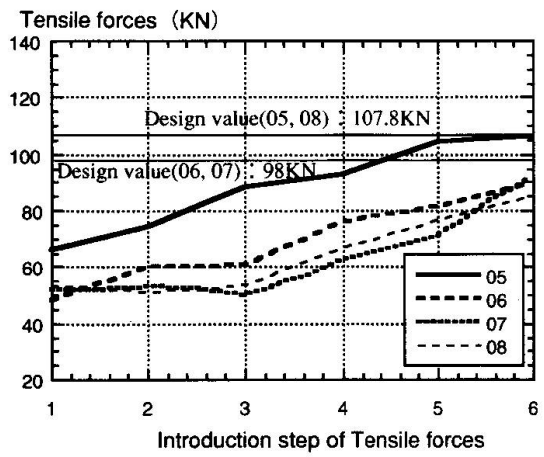

Fig.11 Transition of tensile forces of strings

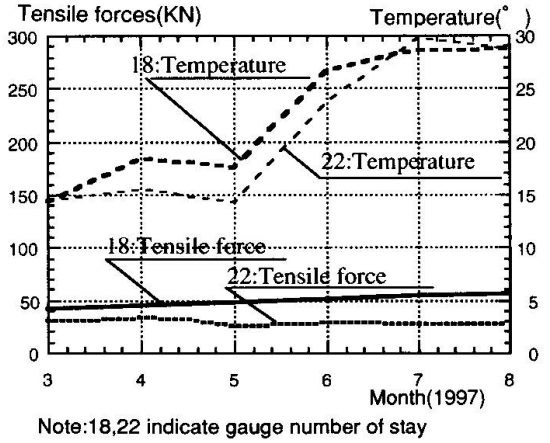

Fig.12 Transition of tensile forces and temperature of stays

Bangkok International Trade and Exhibition Center: Large-Scale Suspended Roof

Hiroaki KAMISAWA
Eng.
Thai Konoike Constr. Co. Ltd
Bangkok, Thailand

M. YAMAJI
Mgr
NKK Corp.
Yokohama, Japan

Kenichi KATAGIHARA
Dir
Konoike Constr. Co. Ltd
Osaka, Japan.

T. YAMASHITA
Eng.
Tomoe Corp.
Tokyo, Japan

Summary

This report shows the structural design and the construction process of large roof (about 35,000 m^2 area covered) which is suspended by masts and tie-rods system. BITEC (Bangkok International Trade & Exhibition Center) has a large scale exhibition hall which was built in Bangkok city and was completed in July 1997. In this building, we have employed the suspension structure for indoor exhibition hall to obtain no column space over 20,000m^2 . Suspended roof is composed of seven parallel frames which are laid side by side at the distance of 27m. Each frame has two main steel masts standing on the reinforced concrete columns, one main steel truss girder covering 100m span, reaction beam (36m long) at the outer sides of both columns and high-strength tie-rods for suspending girders and beams.

1. Introduction

In Bangkok, capital of Thailand, the BITEC (Bangkok International Trade and Exhibition Centre) was constructed as the international exhibition center capable of sending information to the world through all available media. The BITEC was built at a distance of about 8 km from the center of city, along highway stretched toward the east from Bangkok, ensuring easy access from Don Muan International Airport through highways and from hotels in the city.
BITEC is a large scale exhibition center which has 20,000 m^2 indoor exhibition hall, meeting facilities, restaurant, etc. So as to realize no-column space in the large scale indoor exhibition hall, the suspension structure was adopted. The steel frame truss type mast and tie rods are used to suspend a large roof (100 m in span direction, 200 m in beam direction).
Figure 1 shows the outline of plot plan having an area of about 240,000 m^2. One heliport, outdoor exhibition zone, outdoor park, pond, green space, etc. are located around the outdoor exhibition zone. Table 1 shows the outline of buildings. Photo 1 shows the whole view of buildings and Figure 2 shows cross-section. The 2nd and 1st basements are mainly used for machine room and indoor parking for about 1,500 cars. On the first floor, entrance, restaurant and loading area are located around the indoor exhibition hall which serves as a main hall. The main hall can be used as an open space having the area of max.100m x 200m. As the effective height under beam is 15 m and the live load of floor is 1.0 t/m^2, it can exhibit long and heavy items. On the 2nd floor, convention hall (1800m^2) and other meeting rooms are located. The construction was completed on July 1997.
The basic design of BITEC was made by the major Thai designing offices Design 103 (architectural design) and ACS (structural design). For the conceptual design made by Design 103, the three companies, Thai Konoike, NKK Corporation and Tomoe Corporation made the technical proposal, and we have received an order including detailed design and construction. The major points of technical proposal are the application of the designing and construction process which simplifies the details by applying tie rods for the suspending members of large-scale suspension roof and ensures the specified construction accuracy by repeating simple works, and the adoption of "Self-balancing system" to avoid transmitting large lateral force to lower structure, which are columns and foundation made by reinforced concrete.

2. Structural system

The structural system of BITEC consists of reinforced concrete lower structure, steel frame general roof (minor roof truss) and large-scale suspension roof (main roof truss) of exhibition zone.

In Thailand which has tropical monsoon climate and is located on the stable Eurasia continent, the dominant load is not lateral load such as seismic load or wind load but vertical load. Table 2 shows the load conditions for structural design. We considered also the temperature load in addition to own weight, live load, and wind load. The dead load of the large roof, including the heat insulating and sound absorbing insulation board and facilities load, was 180 kg/m^2. Besides, the suspended load (2 t/place) on the 9 m grid was taken into account for the whole large roof surface as additional load.

Figure 3 shows the image of structural system. The lower structure supporting the main roof is made of reinforced concrete. Especially, the RC column under the main column suspending the large roof of indoor exhibition hall has sufficient strength and stiffness. For the part lower than the 1st floor slab, the flat slab based on 9m x 9m grid is used.

For the roof frame of the building, one element (one bay) consists of two main columns facing each other, main truss (3 pieces compose one assembly, and it has 100m span), reaction beam at both ends and suspending member (tie rod). Seven bays are arranged in the beam direction to form the large main roof.

Figure 4 shows reaction mechanism. The vertical load applied to the main truss is suspended from the top of main column as tension of T3 and T4 tie rods. This tensile force is carried by tension of T1 and T2 tie rods and transmitted to the lower structure through the anchorage buried in the block. At this time, the axial force of main column is about 540t, and the drawing force affecting the anchorage is 210t.

In the case where such an external cable suspension structure is adopted, treatment of lateral force which occurs in the peripheral frame is a problem to be solved. The building is designed so that the left and right thrusts are offset to realize the self-balancing system by arranging the reaction beam outside the column and only the drawing force is transmitted to the lower structure.

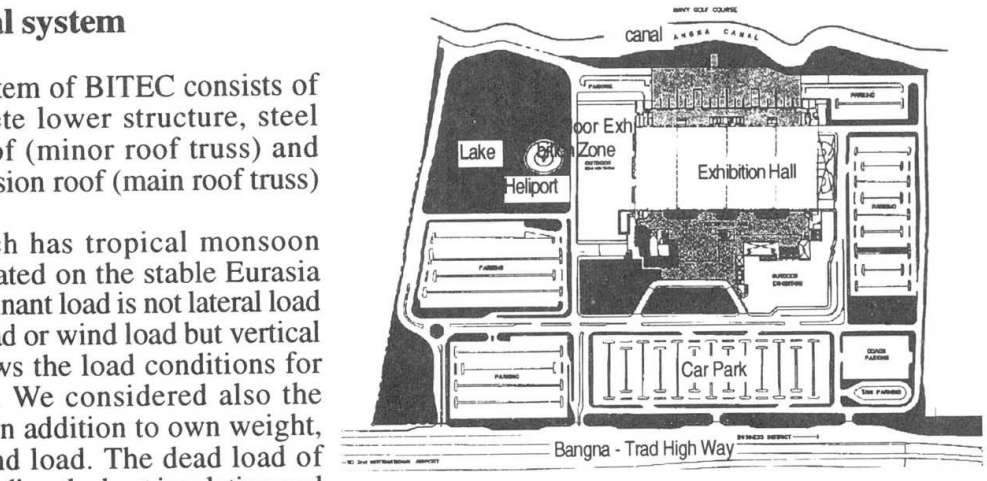

Figure1: Plot plan

Table 1: Outline of the design

Project Name	Bangkok International Trade and Exhibition Center (BITEC)
Building site	Bangna-Trad Highway 1km, Prakanong, Bangkok,Thailand
Client	Parinthorn Co.,Ltd.
Design	Architecture Design 103 Co., Ltd.
	Engineer ACS. Co.,Ltd.
	-Roof Structure
	Thai Konoike Construction,NKK Corporation and TOMOE Corporation
Supervisor	Management 103 Co., Ltd.
Constructor	Thai Konoike Construction Co., Ltd.
Num. of Stories	Under ground 2F and 2F
Building Area	59,788.0m^2
Total Floor Area	126,000.0m^2
Site Area	240,000.0m^2
Const. Period	August, 1995 - July, 1997
Height	Each floor B2F 3.85m, B1F 4.30m, 1F 6.50m
	Max. eaves 23.0m

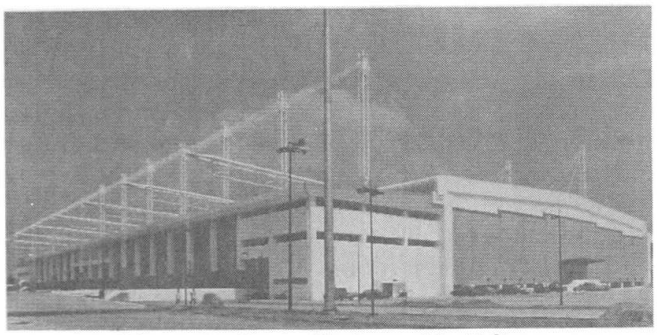

Photo 1: Overall view of building

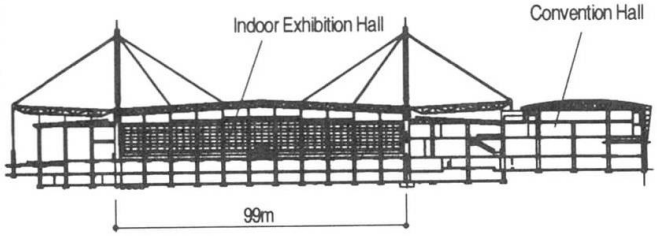

Figure 2: Cross-section of building

Table 2: Outline of load conditions

Dead Load (DL)

Roof Self Weight	
Metal Sheet, Purlin	10kg/m^2
Steel	90kg/m^2
Ceiling (Including Insulation)	30kg/m^2
M & E Equipment	50kg/m^2
Total	180kg/m^2
Owner's Requirement Load, 2t/point x 210 points	
Main Column	700kg/m
Reaction Beam	700kg/m

Wind Load (WL)

120kg/m^2

Thermal Load (TL)

Air Conditioned Case Indoor 25℃ Out door 38℃ (TL1)
No Air Conditioned Case Indoor 38℃ Out goer 38℃ (TL2)
Standard temperature 25℃

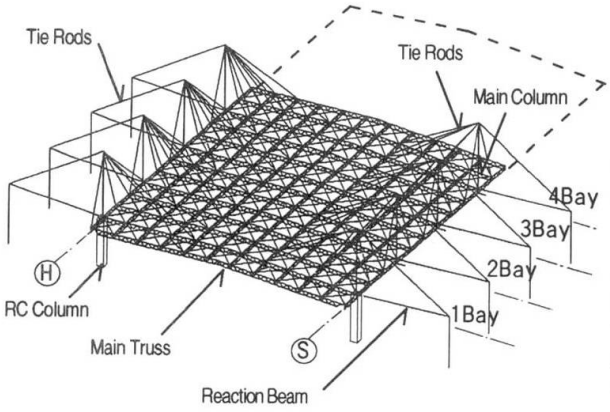

Figure 3: Structural system of main roof

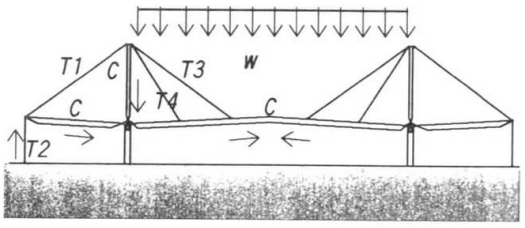

Figure 4: Reaction mechanism

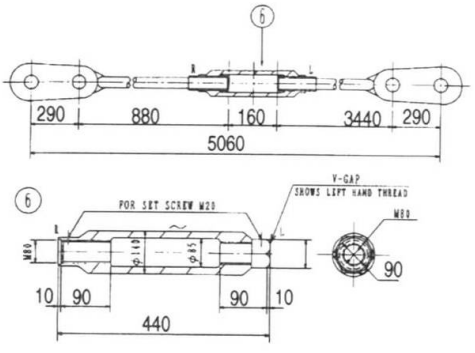

Figure 5: detail of tie rod

3. Structural components

3.1 Tie rod

The suspension structures have conventionally used cables as suspension members. In the case of BITEC, the high strength steel of HT690 class (tensile strength about 690 N/mm^2) is used as suspension member (tie rod). The mechanical properties of tie rod are shown in Table 3. The allowable stress of tie rod is specified as 1/3 of ultimate strength or 1/2 of yield strength, according to the Japanese structural regulations[1),2)]. We selected the tie rod with allowable stress of 220 N/mm^2. The tie rod has threaded end. It is jointed by using the coupler to get the specified length accurately. Figure 5 shows an example of the detail of the joint. Diameter of tie rod used for this building is 90 to 28 mm.

The tie rod has the following advantages compared to the cables.

1) Unlike cables, there is no need to apply pre-tension, so that the detail of joint can be simplified, thereby affording an advantage in cost. Since it has insignificant bending stiffness, it excels also in handling.

2) Unlike cable made by twisting several wires, the tie rod is steel bar characterized by low relaxation which is advantageous for length control.

3) Although the cable has higher strength, the tie rod of HT690 class is applicable to large-scale frames.

3.2 Main column (masts) and reaction beam

Figure 6 shows the joint detail of main column and reaction beam.

The main column is an assembly composed of 4 steel pipes. Tensile force of tie rod is transmitted to the lower structure as compressive force of main column. The length of the column is 36 m, and the size of main member is ϕ 355.6 x 12.7. The pin support is used for the column base. Even when

Table 3: Mechanical properties of tie rod

Name of Material	Code No.	Yield point	Tensile Strength	Elongation	Remark
High tensile Steel	NHT690	≧440N/mm^2	≧690N/mm^2	≧20%	
Rolled steel for welding structure	SM460A	≧315N/mm^2	490 ~610N/mm^2	≧21%	JIS G 3106
Carbon steel for general structure	S35C	≧305N/mm^2	≧510N/mm^2	≧23%	JIS G 4051
Rolled steel for general structure	SS400	≧245N/mm^2	400 ~510N/mm^2	≧21% (Under 5mm) ≧17% (5~16mm)	JIS G 3101
Stainless steel	SUS304	-	560 ~10N/mm^2	≧20%	JIS G 4315

elongation and shrinkage of tie rod occur, secondary stress such as bending does not occur. If the tie rod loses tension, stability is impaired. Accordingly, it is necessary to fix surely the main column with tentative fixing wire when the building is constructed.
The reaction beam is a truss composed of three round pipes. It protrudes at both sides from the left and right column bases. The length of member is 36 m, and size of main member is ϕ 457.2 x 16 and ϕ 216.3 x 12.7.

3.3 Other components

A support, called the embedded column, is embedded at the top of reinforced concrete column where the column, reaction beam and main truss are assembled. All the joints of this embedded column and each member use pin support which is designed so that only the axial force is transmitted. Photo 2 shows the assembled state of embedded column.
The main truss composed of H or L shaped steel is a truss frame having depth 2 m and span 99 m. Adjacent three pieces compose one bay. Two points of a truss are suspended from the left and right columns. Namely, 4 points of a truss are suspended by using tie rods.

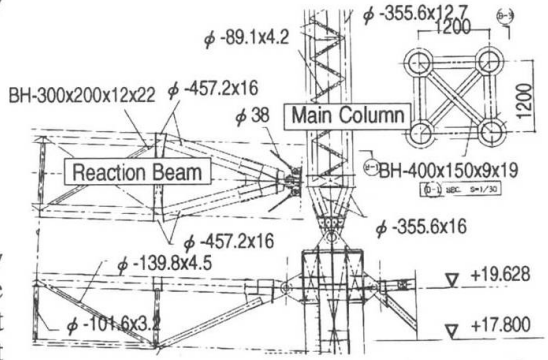

Figure 6: Joint detail of column and reaction beam

4. Construction

4.1 Painting

In view of typical climate of South-East Asia, namely high temperature and high humidity in rainy season, the inorganic zinc paint was used as primer, the epoxy paint was used for second coating, and the polyurethane paint was used for final coating. And epoxy paint was used for corrosion inhibition of indoor steel frame.

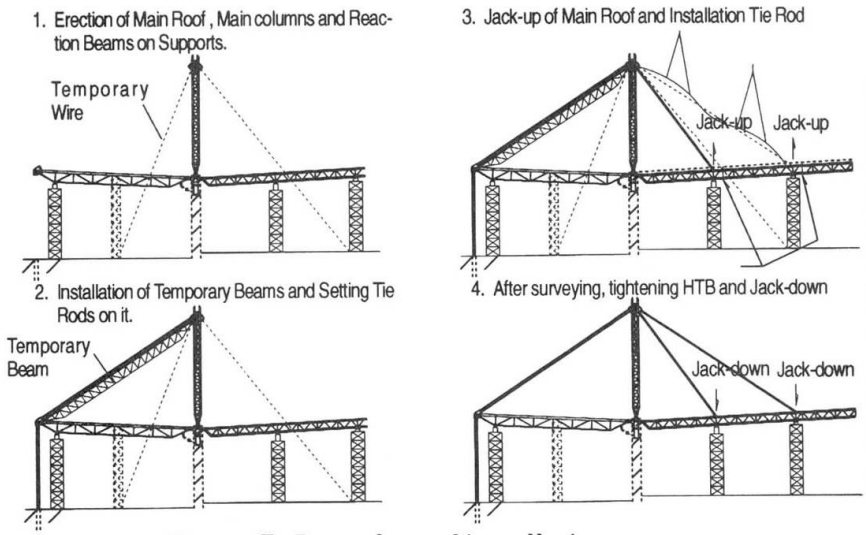

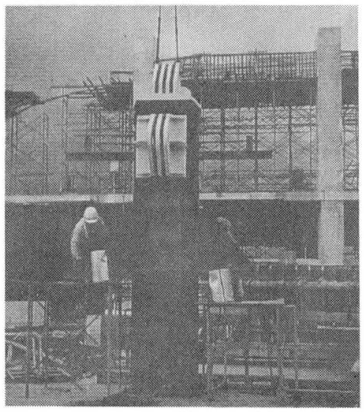

Photo 2: Assembly of embedded column

Figure 7: Procedure of installation

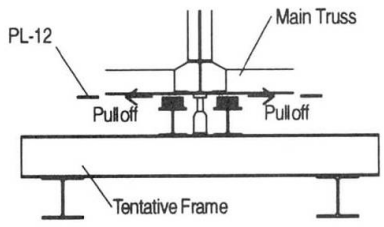

Figure 8: Jack down process

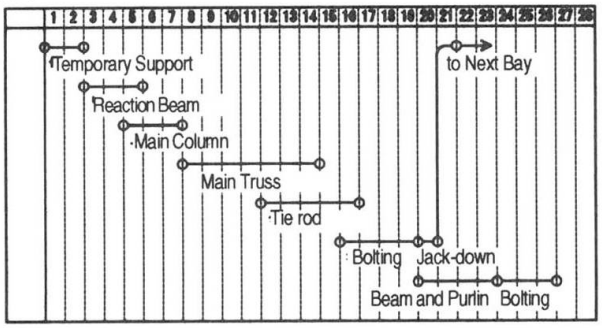

Figure 9: Construction schedule of main roof (for 1bay)

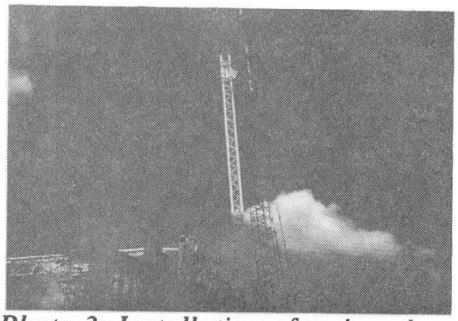

Photo 3: Installation of main column

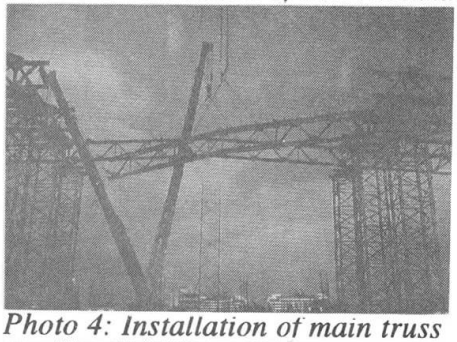

Photo 4: Installation of main truss

Photo 5: Assembly of tie rod

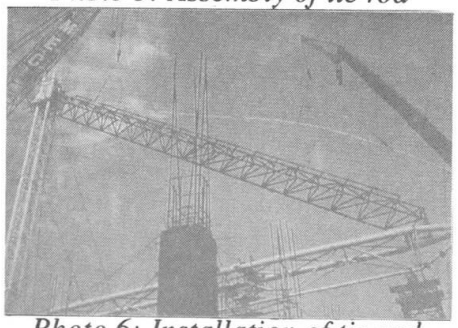

Photo 6: Installation of tie rod

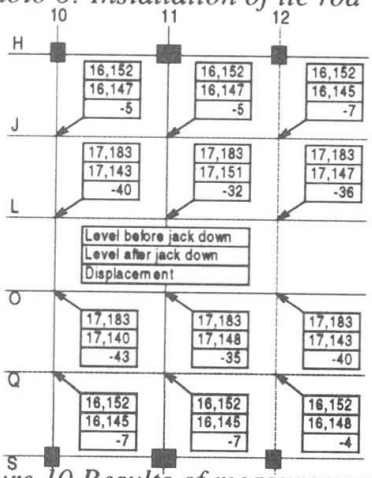

Figure 10 Results of measurement of bay 3

4.2 Construction procedure

The main steel frames of roof were fabricated in Thailand except the tie rods. The fabricator of steel structure has qualification of Class A of Steel Frame Construction Association in Japan and qualification of other main organizations such as API and ASME. The tie rods were made and finished in Japan. After testing and packing they were sent to the construction site.

Figure 7 shows the construction procedure of the roof frames. The roof frame is in unstable state until one bay is assembled. So as to ensure the stability, we adopted the Jack-down process. Namely, the temporary support is used during construction, and after completion of assembling the support is removed. The jack-down was repeated 7 times to complete the construction. To jack down, the filler plate laid on the top of tentative frame, being supported with the hydraulic jack, is withdrawn. The filler plates were drawn out one after another successively, and the jack was lowered. After the whole structure was suspended, jack-down was finished. Figure 8 shows the outline of jack-down process.

While there are several methods to construct suspension structures, we adopted the method based on length control. The deformation of structure was previously calculated, and the position of each member and length of tie rods were adjusted and controlled so that the members were arranged in the specified position after completion of jack-down. For this construction method, it is important to ensure the accuracy of construction. Especially, error of tie rod length decides the stability of the whole structure. Therefore severe check was given to the length control when the members were assembled on the ground. Additionally, we judged some imperfection of length of tie rod and position of steel members cannot be avoided during construction process. So we carried out calculation of roof frame assuming some patterns of imperfection, and checked safety of the whole frames. Table4

Table 4 Patterns of imperfection analysis

Cases	deformation of main truss
Asymmetrical pattern	
Symmetrical patterns (tie rods at center of span are longer)	
Symmetrical patterns (tie rods at center of span are shorter)	

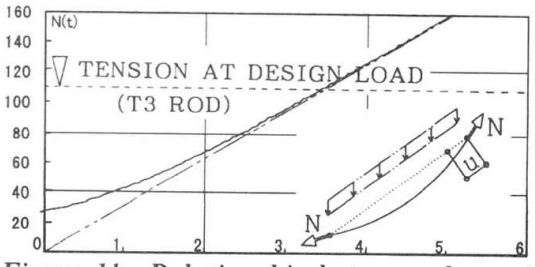

Figure 11: Relationship between elongation and tension

shows examples of assumed pattern of the imperfection. In all cases, we assumed deferences in length of tie rod were 1/1500 of total length of tie rod.
Figure 9 shows the steel frame construction schedule for each bay. It took about 25 days to construct one bay. If the lap period is taken into account, about 120 days are required to construct the whole roof. Photo 3,4 show the installation states.

4.3 Installation of tie rods

Before the tie rod was installed, the temporary support beam was installed between the column top and the front end of reaction beam. The total length of the longest tie rod T3 exceeds 39 m. It was too long to carry to the construction site, so it was divided into some parts and then jointed at the construction site. Therefore, the end of tie rod was threaded, and each end of the tie rod could be jointed with the aid of coupler. Photo 5 shows the assembling state.
After on-ground assembling the length of each tie rod was inspected, because the length cannot be adjusted after construction. To measure the length, the steel tape was used. Measurement error was within 2 mm. After length inspection the members were lifted with two cranes, and the pin was inserted into the end hole of tie rod at its both ends. Photo 6 shows the installation state.

4.4 Installation accuracy of frames

After completion of jack-down, the level of main trusses and inclination of column top were measured. Figure 10 shows the results of measurement of bay 3. Deformation of main truss is almost symmetrical at left and right sides, so that the accuracy control based on length control is proved to be satisfactory. The calculated displacements, based on linear analysis of center part and outer side were 80 mm and 40 mm, respectively, but the actual displacements were 43 mm and 7 mm. The reason why the displacements was so small is that sag of tie rod which was not taken into account in linear-calculation was greater than expected value. In the gravity, the relation between tension and the distance of each end is nonlinear and gravitational tension arises because of the deflection by self weight (Figure 11). At the level of design load, the self weight ratio is 50% in total load and non-linear effect is negligible. However, in the construction stage, the load is only self weight of the roof structure so the tension and the nonlinear effect are to be taken into consideration.

5. Conclusion

In this paper, we have discusses the design and construction of BITEC which has large roof of suspension structure. During structural design and construction, we obtained following important points.
1) Using tie rod as the suspension member makes the structural design clear and makes the accuracy constrol easy by coupler joint in the construction process.
2) The structural design employing "Self-balancing system" cam make the suspension structure stable in the election process.
3) It is indispensable to carry out the structural analysis considering imperfection and geometrical non-linear effect of the structural members - especially tie rods - for the accurate construction.

Acknowledgment

We wish to express our appreciation to Dr. Prasarn of Parinthon Co. who is an active and energetic project owner, to staffs of Design 013 Co., ACS Co. and Management 103 Co. who supported designing and management, as well as to other all persons who took parts in this construction work.

References

1) Architectural Institute of Japan, (1973.5), *Design Standard for Steel Structures*, Maruzen, JPN
2) Japanese society of steel construction, (1983.11), *Recommendation for Design and Construction of Structural Cables in Architecture*, JSSC Vol.19 No.207 , JPN

Large Span Floor Beams with Web Openings

Helmut BODE
Prof. Dr
Univ. of Kaiserslautern
Kaiserslautern, Germany

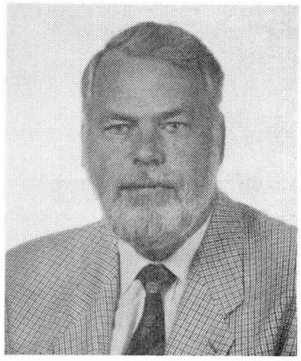

Prof. H. Bode born 1940 in Dresden, received his degree of Doctor of Eng. from Bochum Univ. in 1973. Now Univ.-Professor, holding the chair for steel construction at Kaiserslautern Univ.

Christoph ODENBREIT
Eng.
Univ. of Kaiserslautern
Kaiserslautern, Germany

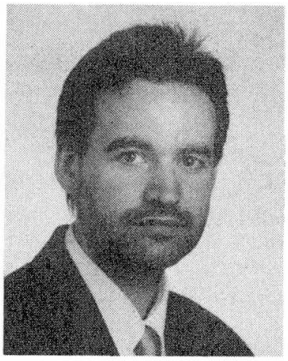

C. Odenbreit, born 1965 in Saarbrücken, received his Civil engineering degree 1993 in Kaiserslautern Univ., worked with Ove Arup and Partners in Berlin. Since 1996 Research Assist. at the Dept for Steel Constr. at Kairserslautern Univ.

Summary

To investigate the behaviour of a long-span floor beam, which is built-in in a high rise building, a full scale test was carried out at the University of Kaiserslautern. Besides other topics, the *different and large web openings* have been the particularity of this beam.

Physically nonlinear calculations show a quite good accordance to the behavior of the test specimen. For calculating the combined bending and shear capacity of the composite beam, a simple engineering model was developed. It is compared with the test results, which have been obtained from two other research projects, conducted at Kaiserslautern University.

In addition the vibrational behaviour of the same beam, which is built-in in a high rise building, is presented. The clear damping effect due to the completion of the building outfit, on the vibrational behaviour can be confirmed and quantified.

1 Introduction

In the past present in Germany buildings have been erected which used more and more the advantages of composite construction. By increasing the span of the composite beams, the number of columns can be reduced and the efficiency and economy of high rise as well as multistorey buildings can be increased. These long-span composite beams have some special aspects, which will be considered in the following:

- Composite beams have their major bending-resistance at midspan, whereas, according to elastic analyses, the largest bending moment firstly appears at the interior column. To yield profit of the bending-resistance at midspan a rotation-capacity of the beam (or the connection) at the interior support is necessary. This rotation-capacity depends on the geometry, the structural system, the construction and the loading
- Plastic analysis leads to an economical solution of the floor-beams. But the activating of the plastic bending moment at midspan and at the interior supports needs a certain rotation capacity of the plastic hinge sections

- Because of the high bending moments and the high resistance, the web openings become more and more critical with regard to deflection and stresses particularly under large transverse shearing forces
- The reduction of the self-weight gets important with increasing span of the composite beam and the number of storeys of the building. A solution could be to use light weight concrete and high strenth material for the steel beams
- The importance of crack-width-control increases by considering these points, especially if the structure is designed plastically

At the University of Kaiserslautern we have made large-scale-testings especially to have a view at these, above-mentioned points. In the following, we have a close look on *one* long span beam test with large web openings:

In January 1995 a *full scale test* of a composite beam containing large web openings was carried out. The composite beam and test setup is shown in Fig. 1 and can be characterized by the following features:

- full scale specimen, very similar to the beams used in the Commerzbank building;
- welded and tapered steel beams made of Fe 510 (= S355; 510 N/mm² tensile strength);
- large rectangular and 2 circular web openings;
- the slab consists of "light" normal concrete LB 35 (C 35/45) with density r = 1.99 kN/m^3 (light weight aggregates "Lipor");
- profiled steel sheeting "Super-Holorib" with embossments, but without any end anchorage means (the ribs were oriented transversely to the beam);

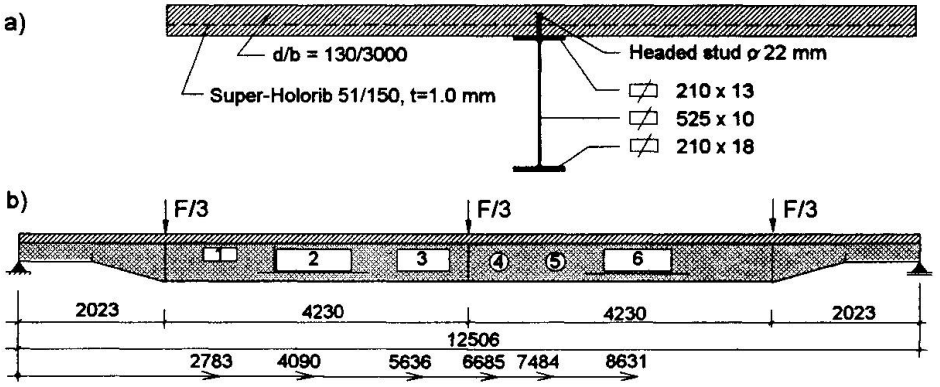

Fig. 1: Test specimen and setup a) cross-section b) elevation

- the sheeting is used in order to serve as shuttering during concreting and as lower reinforcement in the final composite stage, resisting the tensile forces from transverse bending and longitudinal shear;
- shear connection by one headed stud ø 22 mm per rib, as it is the normal practice in Germany. The studs were not throughwelded but welded in the shop. The steel sheets were holed at these points;
- transverse bending was applied using additional jacks independently from the beam cylinder force;
- openings with a minimum number of stiffeners and partly close arranged to each other, thus influencing each other (Vierendeel-action).

Any instability problems, such as local buckling, were not taken into account. But separate calculations have been carried out to ensure that the beams have an adequate margin of safety against buckling, and this is, of course, necessary in any case.

2 Test Performance

Figure 1 shows test specimen and test setup including the test loading by spreader beams under a hydraulic jack.

Measurements were taken by strain gauges on the steel beam, on the reinforcement and on the stud shear connectors. In addition vertical as well as relative displacements at the steel-concrete interface were measured.

The overall behavior can be seen from Fig. 2, where the cylinder load $F = F_{cyl}$ is plotted against deflections at mid span of the composite beam. The behavior can be characterized by a linear elastic relationship from the beginning of loading up to a cylinder load near to the design resistance level (ULS). The loading was further increased step by step, and yielding occurred in the steel beam under the inner web openings, mainly at the unstiffened rectangular opening No. 3. This yielding results in a reduction of stiffness at a cylinder load of $F_{cyl} \cong 550$ kN. The remaining branch indicates yielding with strain hardening, accompanied by large deformations of the composite beam.

- At the end the beam test was stopped at a maximum mid span deflection of $w \cong 350$ mm ($\triangleq$ L/35) without any brittle failure in the concrete slab. Furthermore no instability problems such as local or lateral buckling near the free edges of the openings were observed during this test.
- The slip at the steel-concrete interface was small (< 0.9 mm at ULS), and the shear connection was not decisive for the resistance of the beam tested (full connection).
- The cylinder load $F_{cyl} \cong 226$ kN plus dead weight of the specimen and load spreader beams corresponds to the loading under service conditions (SLS in Fig. 2). In the test the maximum deflection at this load level was $w = 18.7$ mm ($\triangleq$ L/670).
- The natural frequency of the composite beam was measured, and the value of the first natural frequency $f_0 = 6.2$ Hz was indicated.

3 Nonlinear Calculations

In the nonlinear analysis the yield criterion of von Mises, associated with Prandtl-Reuss equations including kinematic strain hardening, has been used for structural steel. The concrete material model predicts the failure of brittle materials. Both cracking and crushing failure modes are accounted for. The concrete is isotropic before cracking, and after cracking a smeared-cracking model is used. It is assumed that concrete becomes orthotropic after first cracking has occurred. The failure surface of concrete is defined according to [7]. The shear connectors are represented by P-δ curves from push out tests, but without transverse bending in the slab.

4 Comparison Between Test-Results and Nonlinear Calculations

Fig. 2 shows the global load-deflection behavior at mid span and contains the comparison between measured and calculated values: the accordance is quite good, but the calculated beam behaves a little bit stiffer than that tested. (The horizontal lines in the diagram mark the load

which can be carried according to the engineering model (see chapter 5.) For the differences the following reasons may apply:

- Residual stresses due to the welding process were not taken into account.

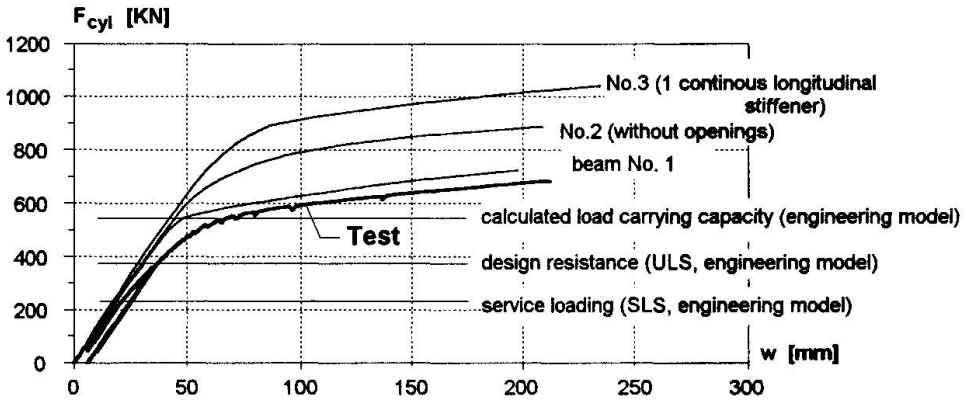

Fig.2 Global load-deflection behaviour

- Because of the absence of a realistic stress-strain relationship for the "light" normal weight concrete, it was approximated.
- The P-δ curve for studs embedded in concrete with light aggregates (LIPOR) and subjected to transverse bending was assessed.
- Creep and shrinkage effects have been neglected. The fact, that the steel beam had to support a certain amount of the dead weight during concreting, was not considered.
- Local as well as lateral buckling and imperfections may have reduced the local stiffness of the beam, though such effects have not been observed in the test at all.
- The composite beam has been modeled by a large number of finite elements, but the mesh should be further condensed, to make allowance for more deformations around the openings.
- The load cycles have not been taken into consideration.

A lot of very interesting results can be achieved by means of ANSYS, so for example slip and connector forces over the whole beam length, see Fig. 3.

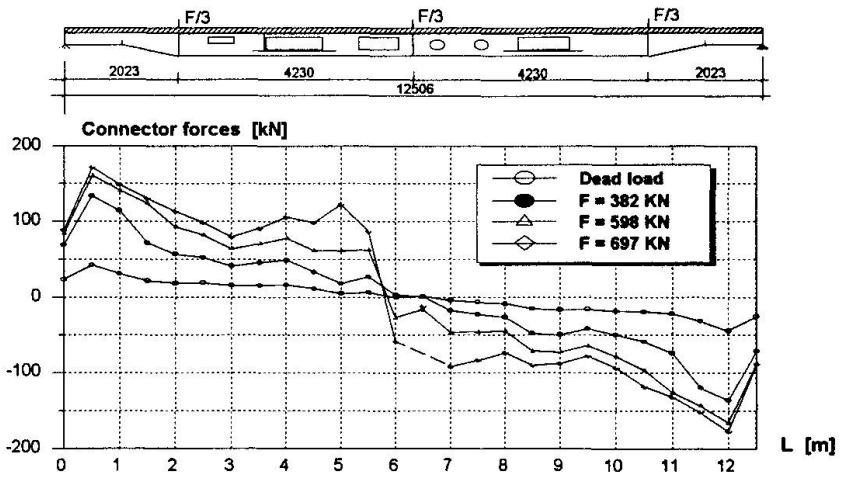

Fig. 3 Connector forces in the composite beam

- It can be seen, that the distribution of the connector forces follows the elastically calculated shear flow, as far as the loading is small.

- In the second, post-yielding phase with strain hardening, the openings as well as the plastic beam deformations near mid span effect the behaviour obviously. But the shear connection is not decisive for the ultimate beam strength, because slip and connector forces are limited to values far below the ultimate values.
- The deflection of beam No. 1 with web openings is only 1.1 mm or 3.5 % larger than that of beam No. 2 without openings. Beam No. 3 with openings and one continuous longitudinal stiffener has about 10 % more stiffness.
- The natural frequencies differ by not more than 1.6 or 4.8 %, respectively.

5 Calculation Model (Engineering Model)

To detail beams with large web openings aimed at a minimum number of stiffeners is a design problem that arises not only in case of composite construction.

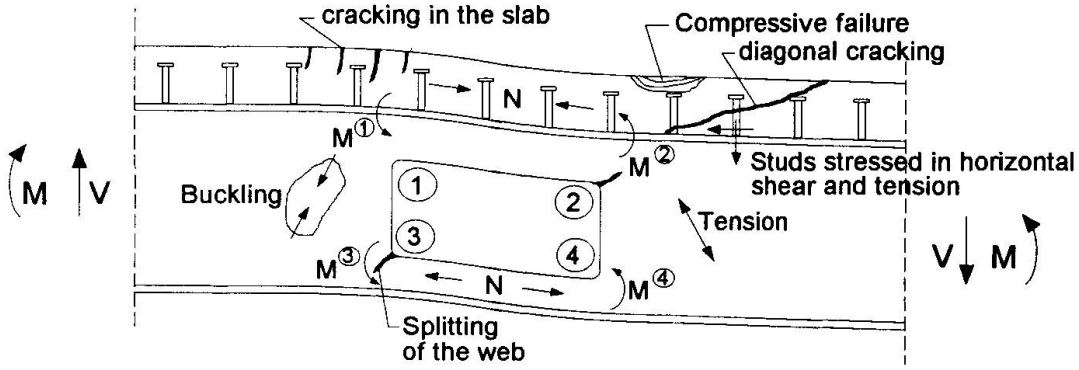

Fig. 4 Deformation at opening No. 3, engineering model

To develop a calculation model for bending and particularly for vertical shearing forces two research projects have been carried out at Kaiserslautern University [4],[5].

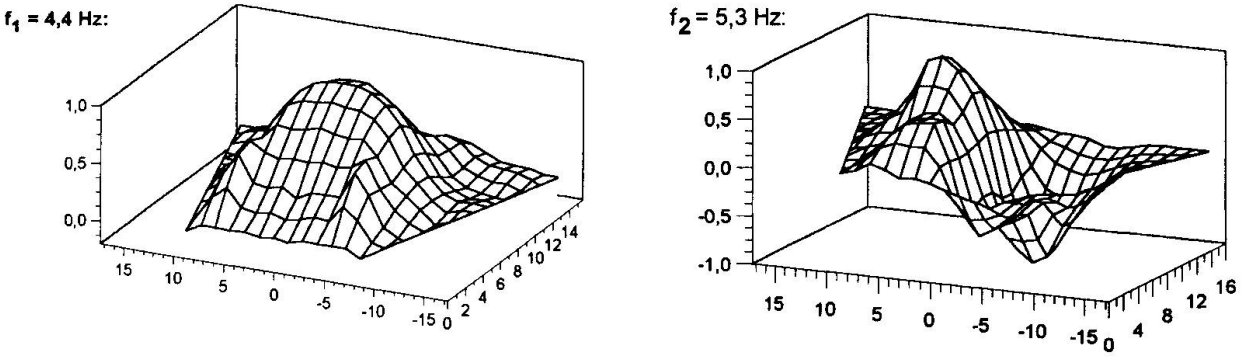

Fig. 5 First two shapes of the maximum acceleration of the slab

To determine the parameters of the engineering model, that is based on the usual beam theory, more than 44 tests from our projects and other researchers were recalculated [4],[5],[6]. The accordance between the test-results and analysed results is quite good (mean value 0.981, standard deviation 0.066).

6 Vibrational Behaviour

The tested beam also is member of a composite floor in a high rise building in Frankfurt/Germany.

Therefore it also was possible to make various measurements of the vibrational behaviour of the beam which is built-in in a real slab construction. To assess the results of the measurement it can be said, that

- the agreement between the calculated and measured natural frequency has been quite good: 4.27 Hz to 4.4 Hz.
- the corresponding shapes (to f = 4.4 Hz and f = 5.3 Hz) are given in Fig. 5.

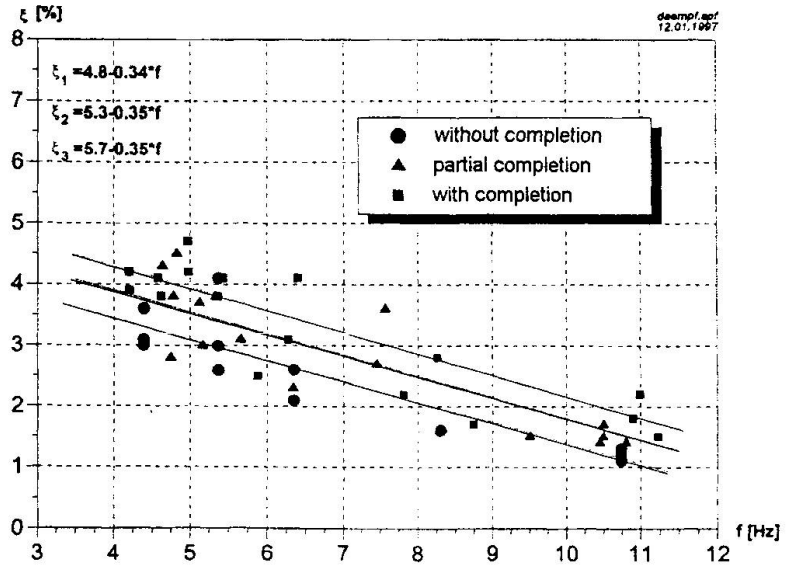

- according to Bachmann [3] the lowest vertical acceleration which can be perceived is 0.034 m/s². The maximum measured acceleration is 0.02 m/s² (with completion of the interior fitting); a reduction of the comfort can surely be excluded.

Fig. 6 Damping effect in relation to the frequency and completion of the interior fitting

- the clear damping effect of the completion of the interior fitting as suspended ceilings and partitions is shown in Fig. 6. The average damping at the frequency of 4.4 Hz is about 4 %.

REFERENCES

[1] Bode, H., Stengel, J., Zhou, D.: "Composite Beam Test for a New High Rise Building in Frankfurt". AISC Conference on Composite Constructions in Steel and Concrete, Irsee/Germany, June 14-19, 1996

[2] Dorka, U.E., Stengel, J.: „Schwingungsmessungen an Verbunddecken". Conference on Composite Constructions, University of Kaiserslautern, July 24-25, 1997

[3] Bachmann, H. et al.: „Vibration Problems in Structures". Birkhäuser Verlag, Basel, Boston, Berlin (1995)

[4] Bode, H., Künzel, R.: „Stahlverbundträger mit großen Stegöffnungen". DFG Research Report Bo 733/6-1, University of Kaiserslautern (1991)

[5] Bode, H., Stengel, J.:"Verstärkte Stahlverbundträger für den Industriebau mit großen Stegöffnungen". AiF Research Report No. 8173, University of Kaiserslautern (7/1993)

[6] Darwin, D., Donahey, R. C.: „Performance and Design of Composite Beams with Web Openings". AISC Research Project 21.82, Structural Engineering and Engineering Materials, SM Report No. 18 (1986)

[7] Willam, K. J., Warnke, E. D.: „Constitutive Model for the Triaxial Behavior of Concrete". Proceedings, International Association for Bridge and Structural Engineering, Vol. 19, ISMES, Bergamo, Italy, p.174 (1975)

New Design of the France-Japan Friendship Monument

Masatoshi MAEDA
Civil Eng.
Assoc.Intercult.Communication
Kobe, Japan

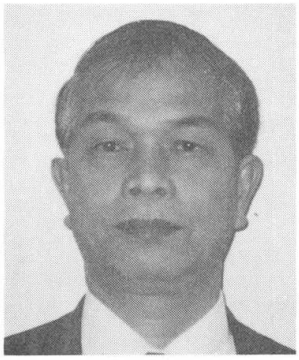

Naoki UCHIDA
Dr Eng.
Nikken Sekkei Ltd
Osaka, Japan

Mikio YOSHIZAWA
Structural Eng.
Nikken Sekkei Ltd
Osaka, Japan

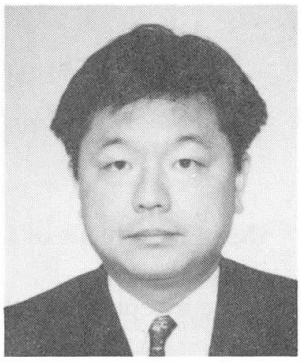

Summary

The construction of the "France-Japan Friendship Monument" introduced at the IABSE Symposium Birmingham 1994, had to be interrupted due to the Great Hanshin-Awaji Earthquake, which occurred on 17 January 1995. In August 1996, a new concept based on the learnings from the Earthquake was proposed from the French side to the Japanese side as "Revised Proposal", and since then the Japanese side has promoted the project by elaborating the basic and detail design based on said "Revised Proposal".

1. Outline of the Monument Project

1.1 Progress of the Design Work

This is a project being promoted jointly by Japan and France to construct a monument symbolizing the friendship between Japan and France under the theme of "friendly exchange and communication".

The concept of the Monument is that its table, covered with bronze and positioned in the north-south direction, is supported by glass-covered pillars located at the both ends.

The "France-Japan Friendship Monument" introduced at the IABSE Symposium Birmingham 1994 represented Plan No. 1 as in Fig. 1, and the construction work was commenced on 12 January 1995 at the north end of the Awaji Island in Hyogo Prefecture, Japan according to this Plan No. 1. However, on 17 January 1995, that is, five (5) days after the work commencement, the Hyogo Prefecture South District Earthquake took place so that the construction work based on Plan No. 1 was interrupted.

In August 1996 a new "Revised Proposal" of the Monument based on the learnings from the

Earthquake as well as the re-recognition of the importance of "communication" and of the coexistence of nature and mankind was presented from the French side to the Japanese side (Plan No. 2 as in Fig. 1).

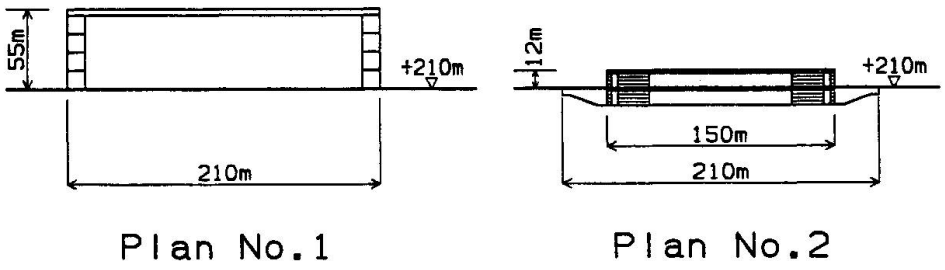

Fig. 1 Transitional change of "France-Japan Friendship Monument" design

1.2 Design Concept of the "Revised Proposal"

The design concept of the "Revised Proposal" for the Monument is as follows:

1) With an emphasis upon horizontality, "communication", which is the theme of the Monument, will be visually expressed.
2) The monument has a basement which will serve exhibition as well as communication promotion functions.
3) Foundations and basement structure, which will be designed to be rigid and very heavy, will be placed in the ground to improve earthquake resisting performance.
4) Steel-and-rubber sheets laminated bearings and dampers will be used at the table bearing portions to reduce seismic loads to act both on the table and on pillars.

The outline diagram in the north-south direction of the Monument as per "Revised Proposal" will be shown in Fig. 2. Ground level of the Monument is 210 m above sea level. The basement is 210 m in longitudinal length. The bronze covered table is 150 m long and 15 m wide, the top level being 222 m above sea level.

2. Outline of the Structural Design

2.1 Structural System

Fig. 3 shows the outline of the structural system of the Monument as per "Revised Proposal". This shows the configurations as of the stage when the basic design has almost been completed.

The depth of the bronze-covered table is 2.2 m, approximately 1/45 of supported span of 100.3 m, and to hold this table truly horizontally is one of the structural features of the Monument design. For this purpose, the structural system of the table is basically made of a steel box-girder within which prestressing tendons are arranged (hereinafter "PS steel girder").

The two (2) inside pillars at each end are planned to support the "PS steel girder" of the table at four (4) bearing points at each ends.

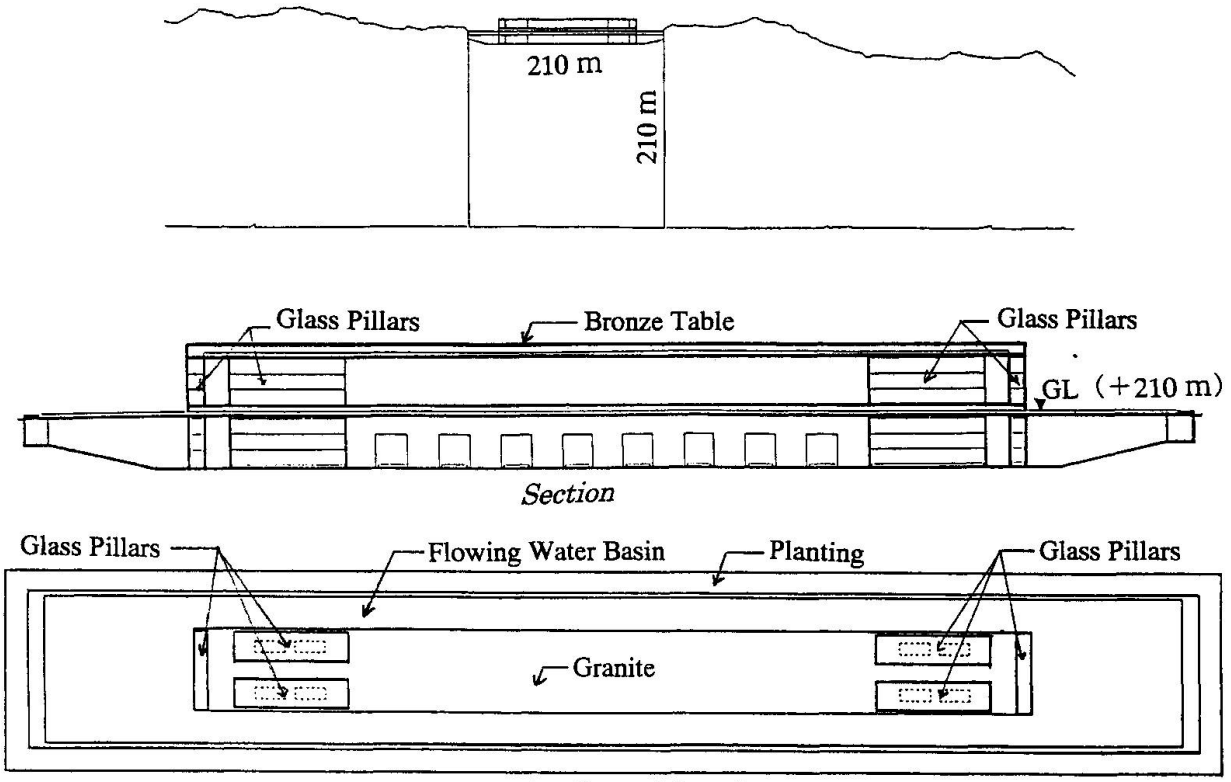

Fig. 2 Outline diagram of New Design

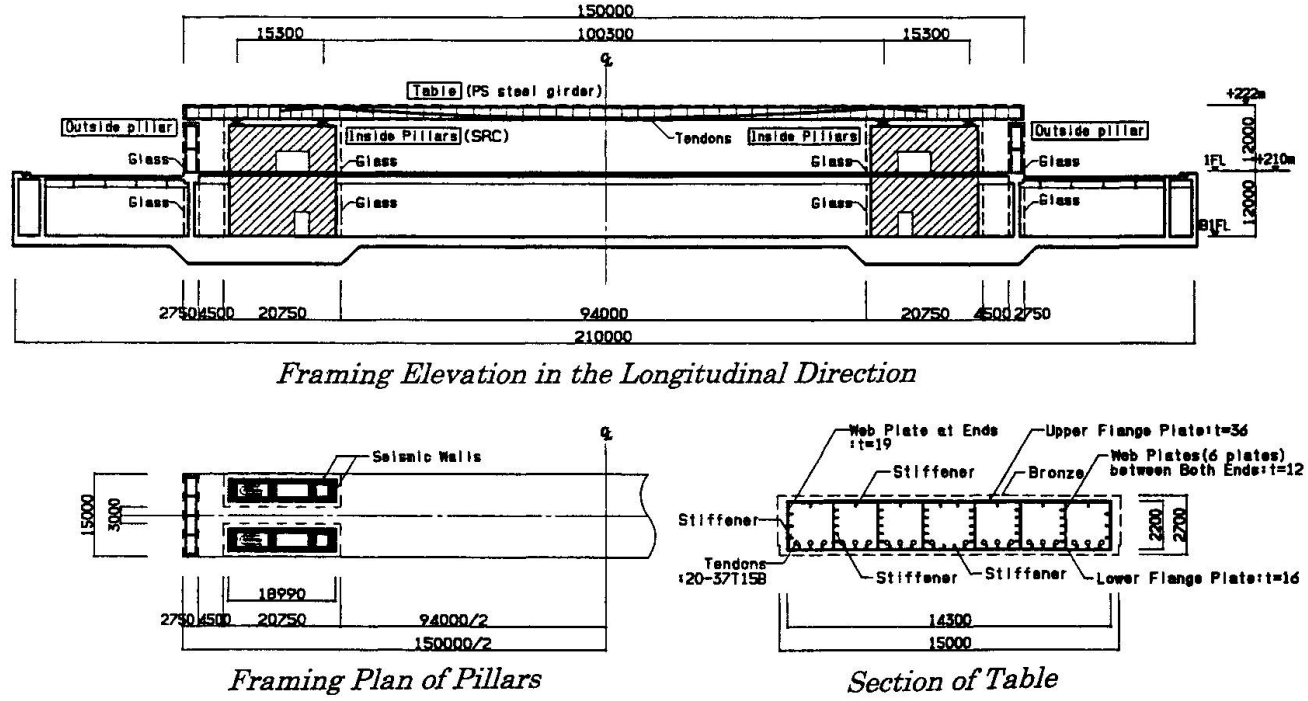

Fig. 3 Outlined structural diagram

2.2 Structure of the Table

Fig. 4 shows the typical diagrams of the structural systems of the "PS steel girder" of the table.

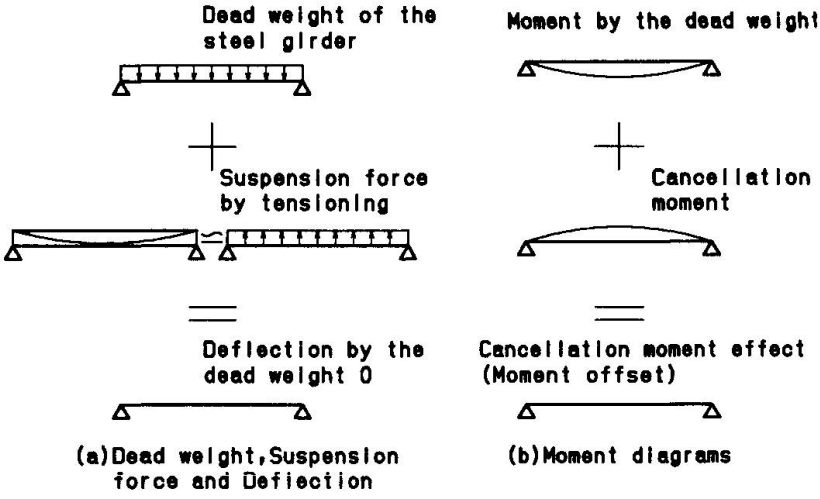

Fig. 4 Structural system of "PS steel girder"

The tensioning force applied to the tendons required for the cancellation moment can be calculated by the following formula:

$$T = \frac{WL^2}{8e}$$

where T : Tensioning force
W : Weight of table per unit length
L : Steel girder bearing span
e : Distance between the centroid of the steel girder and the lowest level of tendon

The tensioning force level is determined to be not more than 60% of the tensile strength considering the fatigue of the tendon material.

2.3 Structure of the Pillar

The two (2) inside pillars at each end are planned as the steel reinforced concrete structure (hereinafter "SRC") to support the table at four (4) bearing points on each end. Seismic walls are distributed to secure sufficient structural strength and rigidity against major earthquakes.

At the present stage, it is planned to use an isolator made by laminating steel plate and rubber sheet, and a damper on each bearing point to distribute the reaction force due to earthquake force or temperature load to the inside pillars of both ends. Further, steel-and-rubber sheets laminated bearings and dampers will be used at the table bearing portions to reduce seismic loads to act not only on the table but also on pillars.

The one (1) outside pillar at each end is planned as the steel structure to support its cladding glass only.

2.4 Structures of the Foundation and the Underground Facilities

The foundations of the Monument and the underground facilities are planned to be directly supported on the rock formation. The foundation of the Monument and the underground facilities are rigid and very heavy so that if they are buried underground, vibration damping by underground dispersion effect can be expected during an earthquake.

2.5 Materials of Structural Members

The major structural materials expected to be employed are as follows:

Structural steel	:	SN490 (tensile strength 490N/mm^2 or over), and SA440 (tensile strength 590N/mm^2 or over)
Prestressing tendon	:	SWPR7B (tensile strength 1865N/mm^{2}or over)

3. Design Load

3.1 Long-term Load

Dead load and live load are mainly considered as the long-term loads that act at all times.

The temperature load and construction work load are also considered as special loads.

The total weight of the table is assumed to be around 27,000kN.

3.2 Seismic Load

The design earthquake load will be determined by the dynamic analysis. The earthquake intensity levels inputted are as follows:

(1) Level 1 Earthquake intensity:
The moderate earthquake intensities that may possibly occur more than once over the life of the Monument, the maximum horizontal ground motion velocity being 25 cm/sec.

(2) Level 2 Earthquake intensity:
The severest earthquake intensity occurred in the past at the site of the Monument or assumed to occur in the future there, the maximum horizontal ground motion velocity being 50 cm/sec.

In the seismic design, the effects by vertical motion is also taken into account.

Further, the seismic safety is to be confirmed by inputting simulation earthquake, reproducing the ground vibration that occurred at the site of the Monument at the time of the Hyogo Prefecture South District Earthquake 1995.

3.3 Wind Load

Design wind load is to be determined based on the assumed design wind velocity and reflecting the result of static and dynamic wind tunnel experiments. The design wind velocity will be calculated considering two return periods.

The return period to be employed will be 150 years for Level 1 and 500 years for Level 2.

The design wind velocities (U_H) for Level 1 (60m/s) and Level 2 (67m/s) will respectively be as follows:

$$U_H = U_O \cdot E_H \cdot R$$

U_O : Basic wind velocity;
E_H : Wind velocity vertical distribution coefficient;
R : Wind velocity return period conversion coefficient;

The design wind load shall take into consideration the average wind load and variable wind loads.

4. Structural Experiment and On-site Observation

One of the features of this project is to perform the structural design reflecting the results of structural experiment as well as the results of observation. Major items are as follows.

- Structural Experiment of PS Steel Girder
  Cancellation moment effects, friction loss, relaxation, strength and deformation property, eigen values, damping ratio
- Wind Tunnel Tests
  Wind force coefficients, dynamic responses of vibration
- On-site Earthquake Observation
- On-site Wind Observation

5. Afterword

The outline of the basic design of the "France-Japan Friendship Monument" was introduced. While proceeding with the design, the details of the table steel girder, pillars and bearings will further be studied for finalization.

Reference

1. Maeda, M. and Uchida, N.: Design of the France-Japan Friendship Monument, IABSE SYMPOSIUM BIRMINGHAM 1994, pp. 97-102

Earthquake Response of Elevated Storage Tanks

Giuseppe DE MARTINO
Prof.
Naples Univ., Federico II
Naples, Italy

Giuseppe De Martino, born 1935, received his hydraulic eng. degree from Naples Univ. in 1962. He is currently Prof. of Hydraulic Constr. at Naples Univ. Federico II.

Maurizio GIUGNI
Assoc. Prof.
Naples Univ., Federico II
Naples, Italy

Maurizio Giugni, born 1953, received his hydraulic eng. degree from Naples Univ. in 1979. He is currently Assoc. Prof of Hydraulic Special Plants at Naples Univ. Federico II.

Summary

With a view to assessing the hydrodynamic effects caused by seismic motions on an elevated storage tank (a vessel fixed to the ground by a single vertical anchorage), we devised a mathematical model representing the tank as an elastic cantilever with a concentrated mass at the head. In our paper, we aim to give a brief outline of this model, corroborating it with additional results obtained from elevated, cylindrical cross-section tanks in concrete.

1. Introduction

Waterworks must always be provided with an earthquake-proof design as they frequently constitute a vital link in a community's lifeline and so must be kept in working order even during emergency situations. A designer engineer must therefore accurately assess:

- design response spectrum and hydrodynamic effects [1] [2] (needless to say, these should be added to inertial loads induced by structural masses);
- structural behaviour and a full analysis of construction details (for example, dampers) to help keep damage to a minimum.

In previous articles, we dealt with the technical problems arising from an assessment of the hydrodynamic effects caused by seismic motion on hydraulic works (e.g. [3]). With particular emphasis on liquid-containing tanks, we initially took a look at ground-supported, flat-bottomed tanks, assumed to follow a rigid pattern [4]. At a later stage, we tried to account for tank wall flexibility (liquid-shell coupling), which is responsible for considerably more dramatic consequences than those in rigid tanks [5] [6].

In this paper, we wish to dwell on the seismic analysis of an elevated storage tank: a vessel fixed to the ground by a single vertical anchorage. To this end, we have come up with a mathematical model representing the tank as an elastic cantilever with distributed mass and a head with a concentrated mass (the value varies according to the extent to which the tank is filled). We based ourselves on the hypothesis that the vessel (assumed rigid) and the liquid in it contained, both absorb energy generated by ground acceleration through the stiffness of the anchorage. As a consequence, the vessel's hydrodynamic response can be assumed comparable to that of a ground-surface tank, provided, however, that the ground acceleration value is replaced by the shell-liquid system acceleration. Our mathematical model therefore covers:

- preliminary structural design (vertical anchorage and vessel itself);
- dynamic component, to assess in the first instance the natural pulsation of the system and in the second the acceleration transmitted to the vessel;
- hydraulic component, to calculate the hydrodynamic effects on the vessel (pressures and

resultant thrust, slosh height).
Once the model has been adequately described, we will then proceed to list the results obtained for cylindrical cross-section, elevated tanks in concrete.

2. The liquid motion in the vessel

A variety of mathematical models (for example, Jacobsen, Housner, Bratu, Veletsos [4]) can be used to assess the hydrodynamic effects caused by an earthquake on a rigid container placed on the ground. Faced with the task of devising a mathematical model to assess the hydrodynamic effect on elevated water tanks, we chose the most broad-based, i.e. the Bratu model [7], which was originally developed for a rectangular water tank stressed by horizontal seismic acceleration acting in any direction relative to the wall. Bratu worked with standard and simplified hypotheses (listed below) which proved to be technically reliable on the whole, as experiments and research bear witness to [8]:

- rigid container and two-dimensional motion;
- homogenous, isotropic and non-viscous liquid;
- non-compressible liquid and negligible surface tension;
- irrotational motion of the elementary particles;
- low wave amplitude of the harmonic sort in the fundamental mode[1].

Using the Laplace equation solution combined with the above hypotheses, Bratu came up with the boundary conditions listed below:

- separation between the storage tank bottom and the liquid;
- water particles sticking to the tank walls as they move;
- lack of horizontal components in the gravitational force.

Bratu discovers the expression for velocity potential function ϕ and introduces into it seismic acceleration. At this stage, Bratu proceeds to write expressions for the contour of the liquid free surface, the hydrodynamic pressure distribution acting on the walls, which turns out to be parabolic in shape, and the resulting thrust. One point Bratu neglects to take into account, however, is the gravitational term gz when applying the linearized motion equation:

$$-\frac{\partial \phi}{\partial t}+\frac{p}{\rho}+g\cdot z=0 \qquad (1)$$

The result of this, as can be gathered from a series of appropriate calculations carried out specially, is an irregularity in the pressure distribution. In fact, the distribution pattern takes on a value not equal to zero at the free surface, whereas, given the boundary conditions a zero value would have been expected. So much is this so that when the seismic period is shorter than that of the liquid sloshing (a frequent occurrence in real life) it takes on a negative value. It continues to be negative to a depth which varies according to the geometric features of the tank and the seismic period.
By applying formula (1) in its complete form, we were able to eliminate this distribution irregularity. We then proceeded to apply the Bratu method to cylindrical section containers (see fig 1): in this case, the radial symmetry of the tank rendered seismic acceleration direction irrelevant, thus simplifying the velocity potential expression [9]. With reference to the liquid fundamental sloshing mode, the following relationships have been obtained to assess the impulsive pressure distribution, p_w, the resulting thrust, S_w, and the peak rise, η, at the walls (see fig 1):

[1] The model actually allows us to account for a number of vibration modes without significantly influencing the results relating to the overall motion [4].

$$p_w(z) = \frac{4}{\pi} \cdot \gamma \cdot C \cdot R \cdot \frac{T_w^2}{T_s^2 - T_w^2} \left[\frac{\cosh \cdot k(z+H)}{\cosh \cdot kH} - 1 \right] \quad (2)$$

$$S_w = \frac{4}{\pi} \cdot \gamma \cdot C \cdot H \cdot R \cdot \frac{T_w^2}{T_s^2 - T_w^2} \cdot \left[\frac{\tanh(kH)}{kH} - 1 \right] \quad (3)$$

$$\eta = -\frac{4}{\pi} \cdot C \cdot R \cdot \left[1 + \frac{T_w^2}{T_s^2 - T_w^2} \right] \quad (4)$$

In the above relationships, the following symbols have been used:

- γ : specific liquid weight;
- C : seismic intensity coefficient (ratio between seismic and gravity acceleration);
- R: tank radius;
- H : water height;
- z : depth (from the liquid surface at rest);
- $k = \frac{\pi}{2R}$
- $T_w = \frac{2\pi}{\sqrt{gk \tanh(kH)}}$: fundamental period of liquid mass sloshing;
- $\frac{T_w^2}{T_S^2 - T_w^2}$:cyclic amplification factor, with T_s being the fundamental period of the earthquake for a tank placed on the ground or that of the structural system for elevated water tanks.

The method above, unlike simpler ones, allows us to take into account the interaction between the T_s period and that of the liquid mass using the amplification factor in the relationships (2), (3) and (4). This way, the different hydrodynamic responses according to the different geometrical tank features and the point to which it is filled can be accurately monitored.

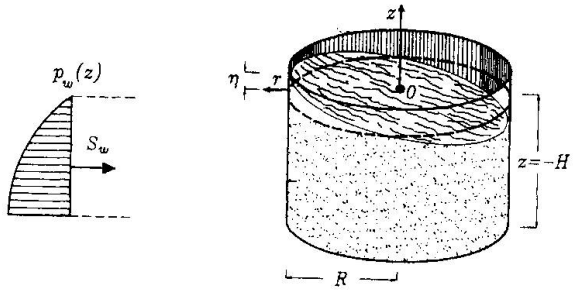

Fig. 1- Cylindrical tank: scheme of reference

3. Elevated water tanks

First of all, it should be pointed out that the column-tank water system can be represented in two ways:

- elastic pattern, accounting for both the elasticity of the column and that of the tank;
- composite pattern, assuming that the column is elastic and the tank is rigid [2].

One must obviously take into account the structural features of the actual column-tank system being looked at: shape, building materials, and size of the various components. At this particular stage of the research project, we chose to look at an elevated water tank in ordinary reinforced concrete with a circular tank and a squared, cone-shaped connection fixed to the column so as to ensure a rigid anchorage (see fig 2). Bearing in mind, the structural features in question, we felt

[2] Only for squat water towers could we talk about a rigid pattern (non-elastic column-tank structure) with a dynamic behaviour similar to that of a monolithic block.

that we could safely overlook the tank elasticity (composite pattern) without significantly changing the outcome.

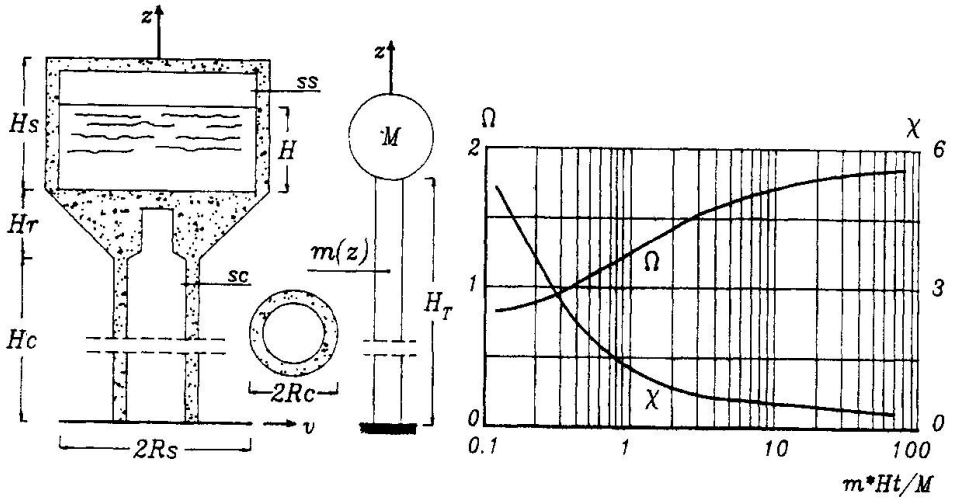

Fig. 2 - Elevated storage tank: system considered

In view of this, it should be noted that whilst a ground-surface tank is subjected to direct stress by seismic acceleration at the base, in an elevated tank the masses involved (support + container + liquid) absorb energy generated by the earthquake and transmitted from the foundation block by means of column elasticity. We can, therefore, assume that the liquid's hydrodynamic response is equivalent to that of a ground-surface tank provided we replace the ground acceleration with elevated storage tank values. In dynamic terms, we take our reference from a theoretical model of an elastic cantilever with distributed mass m(z) and a head with a concentrated mass M (see fig 2). The liquid has a fundamental period of T_w, as if it were resting on the ground. As explained earlier, the T_w expression wholly depends on the tank's geometrical features and on the quantity of liquid contained. The classical differential equation covering the free vibration problem for this sort of constant column system and the frequency equation are expressed in [10]:

$$EI \cdot \frac{d^4 v}{dz^4} - m \cdot \omega_s^2 \cdot v(z) = 0 \tag{5}$$

$$\Omega \cdot \frac{(\sin\Omega \cdot \cosh\Omega - \cos\Omega \cdot \sinh\Omega)}{1 + \cos\Omega \cdot \cosh\Omega} = \frac{m \cdot H_T}{M} \cong \frac{m \cdot (H_c + H_r + 0.5 \cdot H_s)}{M} \tag{6}$$

in which:

- $\Omega = H_T \cdot \sqrt[4]{\frac{\omega_s^2 \cdot m}{EI}}$
- ω_s : structural system frequency;
- M : liquid and tank (including the connecting element) mass;
- m : mass per unit length of the column;
- $H_T \cong H_c + H_r + 0.5 \cdot H_s$ (see fig 2);
- H_c: column height;
- H_r: height of the column-tank connection element;
- H_s: tank height;
- E : Young's elasticity modulus of the material;
- I : moment of inertia of the cross section of the column.

With reference to the fundamental mode, the values of Ω are shown as a function of mH_T/M in the diagram in figure 2; the same applies to the values of the relevant participation factor χ. The

expressions relating to the buckling at the tank centre, $v(H_T)$, and to the corresponding inertial force, $F(H_T)$, have a value of:

$$v(H_T) = \sin\Omega - \sinh\Omega - \frac{\sin\Omega + \sinh\Omega}{\cos\Omega + \cosh\Omega}(\cos\Omega - \cosh\Omega) \quad (7)$$

$$F(H_T) = M \cdot \chi \cdot v(H_T) \cdot S_a \quad (8)$$

in which, S_a represents spectral acceleration, obtained from the design response spectrum and according to the natural period T_s and the damping factor in the structure under examination. As a result, the seismic intensity coefficient C for elevated water tanks to be introduced in equations (2), (3) and (4) is:

$$C_p = C \cdot v(H_T) \cdot \chi \quad (9)$$

which can be defined as the factor of structural amplification.
First of all, we concentrated our efforts on elevated water tanks in reinforced concrete with cylindrical vessels. This preliminary area of investigation put us in a position to analyse the different dynamic response of a range of column features (height, radius and width), different tank features (height and radius) and the extent to which it was filled.
Using the design response spectrum contained in current Italian standards and that of the 6/5/78 Friuli earthquake (the Tolmezzo Station one [11] with peak ground acceleration reaching 0.122 g) and damping factor of the structure equal to 2% or 5%, our calculations gave the following results:
- the vibration period of the structure T_s heavily depends on the column characteristics. More specifically, the less rigid the column, the higher the value of T_s; in other words, when the radius or the column thickness decreases or when the height is greater. T_s likewise increases, albeit to a lesser extent, along with the increase in water volume. An increase in the vibration period within the structure brings about an intensification of the cyclic amplification factor and consequently an increase in the hydrodynamic effects (thrust, water rise);
- for practical applications in this sort of elevated water tank T_s takes on a value ranging between 0.3÷0.5 s and 1.2÷1.5 s: the mathematical model does not cater for earthquake resonance, which is theoretically a possibility, nor does it take into account the subsequent intensification of hydrodynamic effects because of the dissipation effects of the ground-foundation-structure system;
- taking as a reference the Italian standard earthquake spectrum, the K ratio between the hydrodynamic and corresponding hydrostatic thrust takes on values ≤0.2 in practical applications for elevated water tanks of the sort being examined. If, on the other hand, we use the Friuli spectrum, K assumes much higher values, ranging between 0.20 and 0.45. For example, in figure 3 the K value, calculated according to the Friuli spectrum (with a 5% damping factor), is shown for a water tank with a radius of 5m and a height of 6.5m ; both the column height (between 10 to 30 m) and the extent to which it was filled H are varied. In order to provide figures for comparison, the diagram also shows the K value for ground-surface containers of the same size: obviously, as confirmed by other calculations, the hydrodynamic

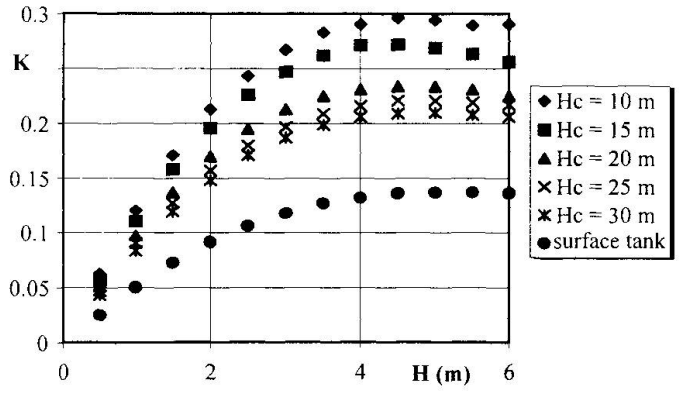

Fig. 3 - K ratio versus H for various Hc values

effects for elevated water tanks in earthquake zones are considerable greater than those for surface or underground tanks. This means that a meticulous assessment must be carried out of these effects;
- the water rise in elevated water tanks, albeit greater than those obtained for ground-surface tanks or underground tanks, is in any case quite small (it does not exceed 0.15÷0.20 m) and therefore, is most certainly contained within the freeboard - not under 0.50 m - generally allowed for in earthquake zones.

4. Conclusions

An analysis of the dynamic response of elevated water tanks using the mathematical model for systems in reinforced concrete and with a cylindrical vessel, will undoubtedly show us that hydrodynamic effects can reach very high levels and that in any case, they exceed those obtained for ground surface tanks of the same size by a long shot: therefore, any calculations must carefully account for them.
Research is currently underway. New materials (such as steel) and new design shapes are being looked at for both for the column and the tank. Moreover, the calculus model is being perfected to account for the dissipation effects of the ground-foundation-structure system. It would be interesting to research further into dissipation systems (e.g. dampers) with an eye to reducing even more the earthquake effects.

References

[1] Chandler, A.M., "Evaluation of site-dipendent spectra for earthquake-resistant design of structures in Europe and North America", The Institution of Civil Engineers, Proceedings, Part I, Vol. 90, 1991
[2] Hashimoto, P.S., Basak A.K., "Seismic Capacity and Failure Modes of Flat-Bottom Vertical Tanks", Journal of Energy Engineering, Vol. 119, No. 2, August, 1993, ASCE
[3] De Martino, G., Giugni, M., De Marinis, G. "Hydrodynamic Pressures on Dams during Earthquakes - Approximate Formulation", Advances in Earthquake Engineering, Vol. 2, Computational Mechanics Publications, 1997
[4] De Martino, G., Giugni, M., "Azioni delle onde sismiche sui contenitori idraulici interrati", Giornale del Genio Civile, Fascicolo 10°-11°-12°, Ottobre-Novembre-Dicembre, 1989
[5] Giugni, M., De Marinis, G., Perillo, G., "L'affidabilità delle strutture idrauliche in zona sismica", Seminario sulla "Affidabilità dei sistemi di adduzione e di distribuzione idrica (nella progettazione, nell'esecuzione e nella gestione)", Fisciano, Univ. degli Studi di Salerno, 1995
[6] Giugni, M., De Marinis, G., Perillo, G., "Sovrappressioni idrodinamiche su contenitori deformabili in zona sismica", 7° Convegno nazionale ANIDIS "L'ingegneria sismica in Italia", Siena, Vol. II, 1995
[7] Bratu, C., "Sul comportamento in regime sismico dei liquidi contenuti in serbatoi rettangolari", IX Convegno di Idraulica e Costruzioni Idrauliche, Trieste, 1965
[8] Cenedese, A., Marchetti, M., Siclari, G., "Analisi sperimentale del moto di un liquido in un serbatoio parallelepipedo oscillante", 17. Convegno di Idraulica e Costruzioni Idrauliche, Palermo, 1980
[9] De Martino, G., Giugni, M., Perillo, G., "Serbatoi circolari in zona sismica. Valutazione delle azioni idrodinamiche", "Giornate di studio in onore di Edoardo Orabona, Bari, 1997
[10] Como, M., Lanni, G., "Elementi di costruzioni antisismiche", A. Cremonese, 1979
[11] Italsider, "Strutture di acciaio per edifici civili in zone sismiche", Quad. tecnico n. 9, 1979

Design and Construction of the World's Largest LNG Underground Tank

Masanobu KURODA
Senior Design Mgr
Shimizu Co.
Tokyo, Japan

Fumiaki SUGINO
Constr. Mgr
Shimizu Corp.
Tokyo, Japan

Masafumi NAKANO
Senior Mgr
Tokyo Gas Co. Ltd
Tokyo, Japan

Yoshinori KAWAMURA
Mgr
Tokyo Gas Co. Ltd
Tokyo, Japan

Summary

The world's largest LNG underground storage tank with the capacity of 200,000 kl will be completed in March 1998. This tank is the first to be buried completely underground, including its roof. This tank has an inner diameter of 72m and a liquid depth of 49.2m. The roof of this tank is a dome shaped structure made of reinforced concrete which supports the soil weight of about 400MN laid on it and dead weight of 150MN. The dome roof is 72.8m in diameter, 7.3m in rise and 1~2.5m in thickness. Rise-diameter ratio is 1/10 which is very small compared to 1/6 of conventional steel roof. The investigation of the buckling characteristics of the domed roof, such as experimental tests and so on, was applied to this tank and both linear and non-linear analyses were performed in order to verify the stability of the dome roof against buckling. The dome roof was constructed above temporary steel truss girders like a huge umbrella.

1. Introduction

A new liquefied natural gas (LNG) receiving terminal has been constructed on Ohgishima Island in Yokohama to meet the burgeoning demand for gas in the greater Tokyo Metropolitan area.[1] This terminal, which will be the most advanced, is scheduled to go into operation from October 1998. The first LNG underground storage tank in the world totally embedded in the ground (including its reinforced concrete roof) will be constructed in March 1998. This tank, capacity of which is 200,000 kl, is one of the biggest LNG tanks in the world. LNG is stored at the temperature of -162°C and this tank itself is like a huge thermos bottle, which has 72m in inner diameter and 49.2m in liquid depth as shown in Fig. 1. It is located in a reclaimed area facing Tokyo Bay and buried underground to achieve greater safety against fire at the adjacent oil terminal and to improve the Bay Area view. In order to build the large underground storage tank, a number of innovative technologies were developed and applied. This paper deals with the technological aspects of this tank, mainly the dome roof, in the design and construction phases.

2. Outline of the tank

Fig. 2 shows the ground condition and the structural configuration of the 200,000 kl LNG underground storage tank. The ground mainly consists of sandy permeable soil with an impermeable silty soft rock layer more than 58m below the surface. For tank construction, deep excavation was carried out by installation of very deep slurry walls into the soft rock as retaining and cut-off walls.

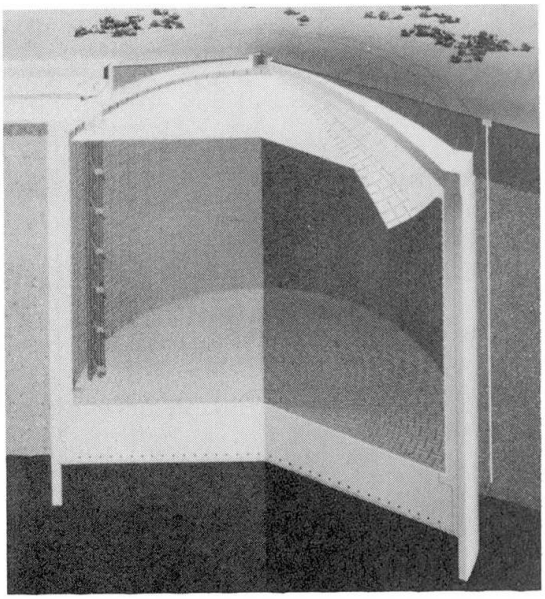

Fig. 1 General view of 200,000 kl LNG underground tank

The side wall is made of reinforced concrete and features a cylindrical configuration because of a structural advantage for inground structures which retain earth and ground water pressure. The thick bottom slab is made of reinforced concrete to withstand high ground water up-lift. The dome roof is also made of reinforced concrete, which supports the weight of soil covering it. Installed inside are insulation made from rigid polyurethane foam panels (PUF), which maintains the cryogenic condition of the tank interior, and a stainless steel membrane with a thickness of 2mm for liquid/gas tightness. Surrounding the side and bottom, a heating system is provided to control ground freezing caused by the LNG's cryogenic temperature. The temperature in the side wall, the bottom slab and the dome roof are average -20~ -30°C.

3. Design [2],[3]

The tank is designed on the bases of both allowable stress design and limit state design for various loads such as dead weight (including covering soil), gas/liquid pressure, earth/water pressure, thermal load produced by LNG's low temperature, seismic load and so on. Two types of design earthquakes are taken into account in the design of the tank; one is a normal design

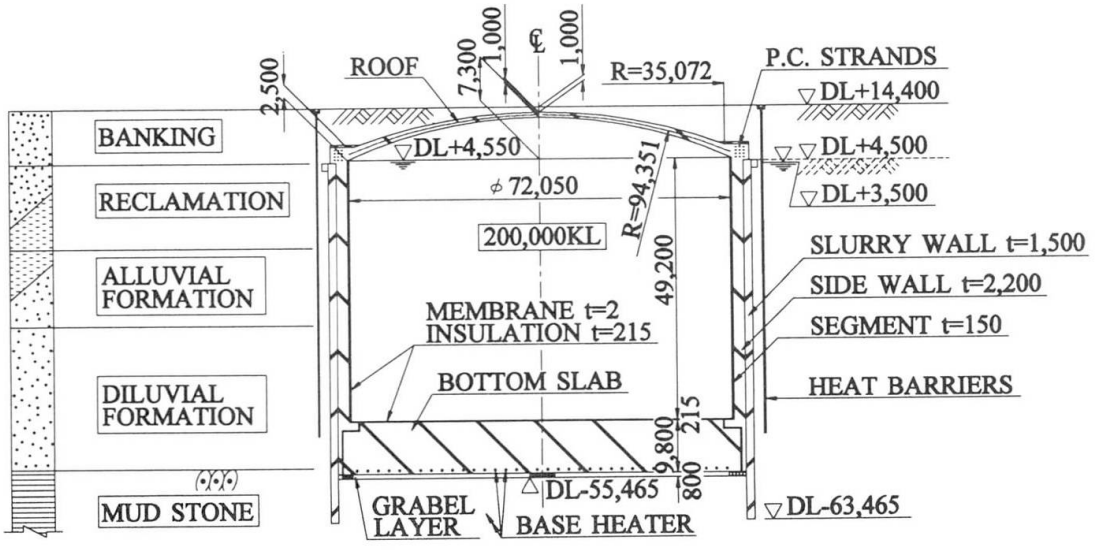

Fig. 2 Section of 200,000 kl LNG underground tank

earthquake which may occur in the life of the structure, and the other is a conceivable greater earthquake like the Great Kobe Earthquake. In the former earthquake the tank should be sound and stable enough to continue operation, while in the latter one, it is required to retain LNG safely.

High strength concrete with a design compressive strength of 59MPa was used for a side wall to reduce thickness from the conventional 4m to 2.2m. The volume of concrete and excavated soil was decreased to a considerable extent and contributed to the economical tank construction. The bottom slab was made of concrete with 24MPa strength and 9.8m thickness to withstand a high ground water pressure of 0.6MPa. A total of 14 layers of reinforcing bars (51mm in diameter) were provided in the bottom slab.

The roof of this tank is a dome shaped structure made of concrete with 29MPa strength to support the soil weight of about 400MN covered on it and dead weight of 150MN. The dome roof has a diameter of 72.8m (D), a rise of 7.3m (H), and the thickness changes from 1m at the center to 2.5m at the circumference. The rise-diameter ratio (H/D) of this tank is 1/10, which is very small compared to 1/6 of conventional steel roof of LNG inground tanks. The less the rise-diameter ratio of the dome roof becomes, the less soil excavated, and economical cost of construction is obtained. However, in the case of low rise-diameter ratio, the dome roof becomes more susceptible to buckling.

In order to clarify the characteristics of the buckling of the flat dome roofs, experimental 1/20 scale model tests, non-linear analysis, and a design study were carried out.[4] The rise-diameter ratio of 1/16 was adopted at these investigations, because 1/16 was considered to the least ratio of the dome roof that could be applied to the underground tanks. Fig. 3 shows the experimental model test. As a result of these investigations,

- Model structures were destroyed without buckling.
- Failure mode and ultimate strength can be estimated with the non-linear analysis of reinforced concrete (including non-linear characteristics of material and geometrical).
- The ultimate strength against buckling can be calculated by "Recommendations for Reinforced Concrete Shells and Folded Plates" by IASS (International Association for Shell and Spatial Structures).[5]

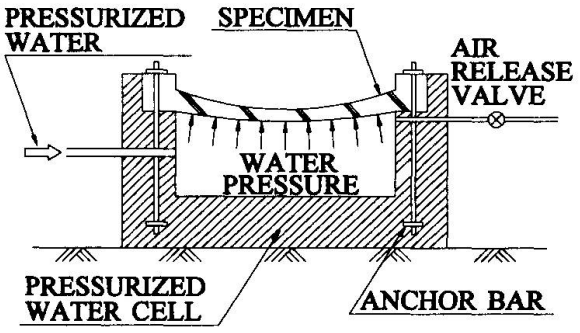

Fig. 3 Experimental model test of dome roof

The dome roof of this tank was designed by both the allowable stress design method and the limit state design method; furthermore, linear and non-linear analyses were performed in order to verify the stability of the dome roof against buckling. Various loads were taken into account, such as dead weight (including covering soil), gas pressure, thermal load, prestressed load, seismic load, loads from the side wall and so on. Concerning the linear analysis, the linear buckling load was computed by the linear finite element analysis for eigenvalue with the program code "NASTRAN". The safety factor (SF) against the buckling was calculated with the method of [IASS], in consideration of cracks and creep of reinforced concrete, and of the initial imperfection of the dome roof. As a result, SF was led to 6.8 and satisfied with SF-req. = 3.5 required on [IASS].

With regard to the non-linear finite element analysis, the non-linear buckling load was computed with the program code "ADINA". Fig. 4 shows the analytical model of the dome roof and the

side wall. Concrete and reinforcing bars were modeled with solid and shell elements, respectively. The dome roof was evaluated with the non-linear characteristics of material and geometrical. Behavior of concrete under biaxial stress and tension stiffening of reinforced concrete were taken into account. After making all design load act on the structure, the load of covered soil, which is the most influential load with respect to buckling of the dome roof, was increased. At the 4.75 times the design load of covered soil, the dome roof was broken without buckling, because the member force became larger than the strength of the cross section of the reinforced concrete in the circumference of the dome roof as shown in Fig. 5, 6. By these analyses, the stability of the dome roof was confirmed.

The top of the side wall is prestressed with 24 cables like a head band to resist large thrust force of the flat dome roof and to prevent cracking of concrete with the compressive stress of 0.7N/mm^2. Though the earthquake produces cracks in concrete, cracks are controlled with the stress of the reinforcing bars within the allowable stress. This cable has the ultimate strength of 10MN and 24 cables give effective compression of 120MN to the top of the side wall. Because the temperature at the top of the side wall is very low, PC system, including PC cable, PC anchorage, reinforced concrete and so on, was confirmed by the experimental tests as shown in Fig. 7. Fig. 8 shows the arrangement of the PC cables and pilasters. 24 cables were divided into 3 groups and pulled between two pillars at an angle of 120 degrees.

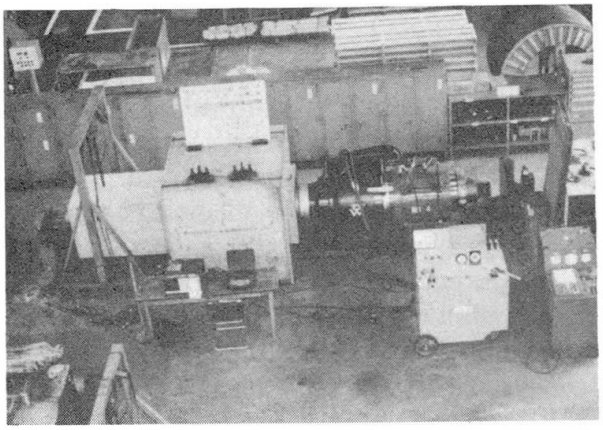

Fig. 7 Experimental test of PC system at usual temperature

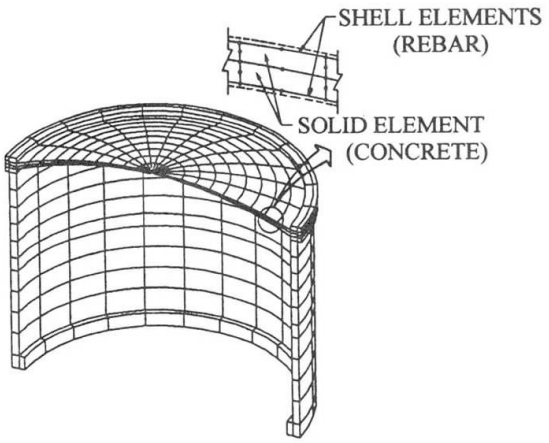

Fig. 4 Non-linear analysis model of underground tank

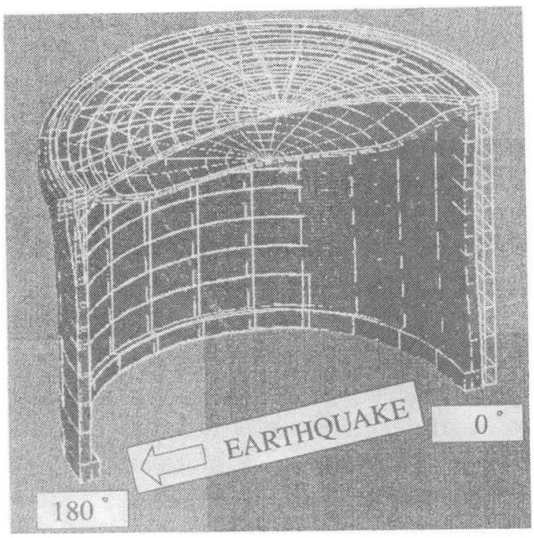

Fig. 5 Result of non-linear analysis (Deflection mode)

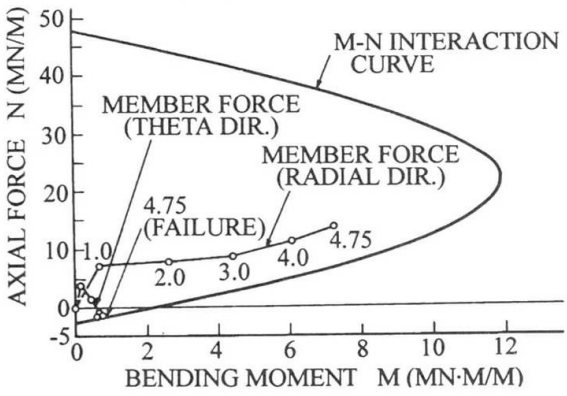

Values 1.0～4.75 show the magnification of the design load of covered soil

Fig. 6 Result of non-linear analysis (Interaction curve)

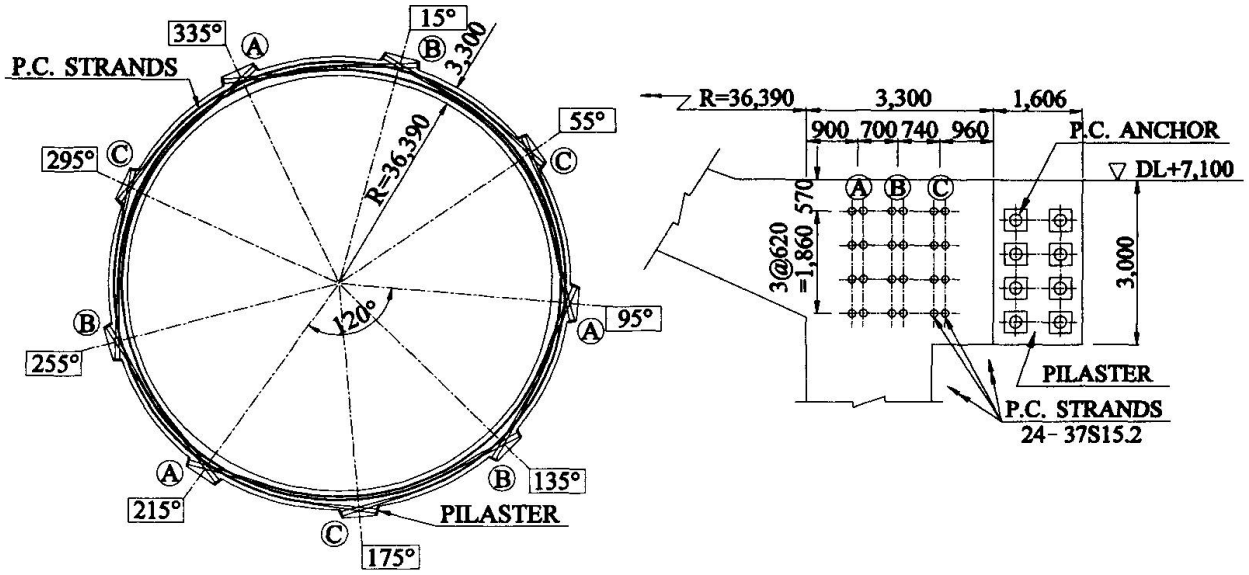

Fig. 8 Arrangement of PC tendons

4. Construction

For the construction of the tank, an accurate deep slurry wall with a high strength of 50MPa was adopted as a ground pressure retaining wall and water cut-off wall. The bottom of the wall is embedded in the impermeable silty soft rock. The depth of the slurry wall is 68m and the accuracy of excavated ditch was within 5cm with respect to absolute verticality. During excavation work, the slurry wall of only 1.5m in thickness supported earth and ground water pressure, so that a large scale underground space of 77m in diameter and 60m in depth was achieved entirely without struts.

Since the slurry wall as well as the side wall is a typical cement rich mass concrete structure, the control of cement hydration was taken into account. In order to obtain concrete strength above 50MPa, the water/cement ratio of concrete needs to be around 30%, which results in low fluidity of the fresh concrete. A water reducing agent was used as an admixture in the mix proportion of concrete to improve the cement dispersion and to ensure high fluidity as shown in Table. 1.

Placement of the bottom slab concrete with a thickness of 9.8m was divided into 2 lots. The first lot was for the lower part of 6.6m height, and the second one was for the upper part of 3.2m where 40MN of main reinforcing bars in weight were densely arranged. 30,000m^3 of the first lot concrete was poured through 70 hours continuously without stopping, and 13,000m^3 of the second lot through 30 hours.

The dome roof was constructed above the temporary steel truss girders, which were combined and made up a three dimensional truss structure like a huge umbrella as shown in Figs. 9 and

Table. 1 Mix proportion of high strength concrete for the side wall

Design strength (MPa)	Max. size coarse agg. (mm)	Slump flow (cm)	Air content (%)	Water-cement ratio (%)	Unit weight of cement (kg/m3)	Sand-aggregate ratio (%)
59	20	60±5	4.5±1	31.0	419	41.1

· Cement: Special Portland blast-furnace cement with added fly-ash for low hydration heat
· Admixture: High-range water reducing agent, Air-entrained water reducing agent, Super plasticizing agent

10. The steel truss structure with a total weight of 20 MN is very rigid in order to satisfy the severe accuracy required for the inner surface of the dome roof, where the insulation and membrane were installed. The truss structure is deflected by the dead weight of fresh concrete of the dome roof. The maximum vertical displacement of the truss structure is 35mm. After the truss structure is jacked down, the dome roof is deflected by the dead weight and creep of it, the soil weight covered on it and others. Therefore, the camber of 0~95mm was taken into consideration in the building of the truss structure. 5,500m^3 of the dome roof concrete was poured from the edge to the top with concentric circle blocks through 28 hours continuously in order to avoid construction joints which might cause harmful gaps for the assembling of the insulation and membrane. Fig. 11 shows the dome roof before being covered with soil.

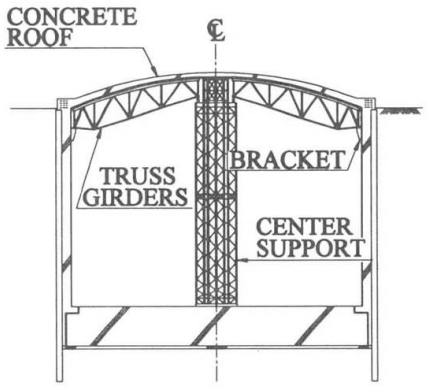

Fig. 9 Section of steel truss structure

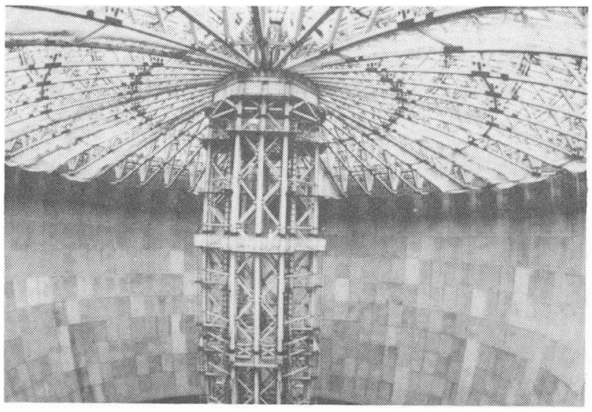

Fig. 10 View of steel truss structure

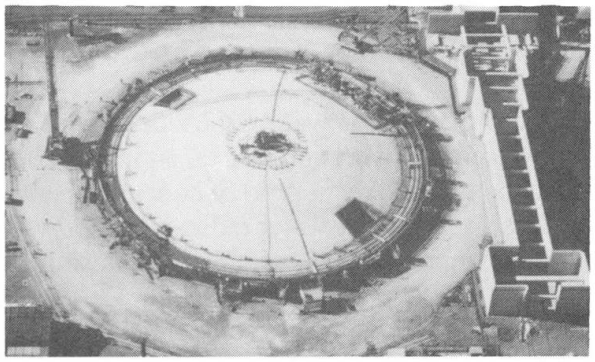

Fig. 11 Over-view of concrete dome roof

5. Conclusion

Construction of the 200,000 kl LNG underground storage tank has been successfully proceeding at the Ohgishima LNG terminal. After completion of the tank, it is totally embedded in the ground and cannot be seen. In the construction of this tank, the newest and most advanced technologies were applied. The Ohgishima LNG terminal starts operation in October 1998, moving rapidly into the 21st century.

References

[1] Umemura J., Goto S., Sakata K. and Nakano M., "Technological Challenges for the Construction of the Ohgishima LNG Terminal ", 12th International Conference on Liquefied Natural Gas, 1998.

[2] Goto S., Nakano M., Nakazawa A. and Kuroda M., "R&D and Construction of the World's First LNG Underground Tank ", Concrete Journal, Vol. 35, No.2, Feb. 1997. (in Japanese)

[3] Nemoto M., Kawamura Y., Sugino F. and Kuroda M., "Design and Construction of the Prestressed Concrete in the World's first LNG Underground Tank ", Prestressed Concrete Journal, Vol.38, No.6, Nov. 1996. (in Japanese)

[4] Okamoto K., Minegishi K, Kuroda M. and Watanabe M., "Structural Stability of Reinforced Concrete Dome Roof " Proceedings of JSCE (under contribution in Japanese)

[5] Dulacska E., "Explanation of the Chapter on Stability of the < Recommendations for Reinforced Concrete Shell and Folded Plates > and a Proposal to its Improvement ", IASS Bulletin, No. 77, 1981, [Translated into Japanese by Hangai. H. et al., Column Journal, No.101, 1986.]

Construction of a Huge Marine Structure in Japan

Naohiro MAEDA
Gen Mgr
NKK Corp.
Yokohama, Japan

Kiminobu NAKAMURA
Chief Eng.
NKK Corp.
Yokohama, Japan

Nahhiro Maeda, born in 1946, received his civil eng. degree from the Hiokkaido Univ. in 1968 and Dr of Eng. in 1996. He was the general Mgr of Akashi Kaikyo Bridge 2P steel caisson fabrication project.

Kiminobu Nakamura, born in 1949, received his civil eng degree from the Kyoto Univ. in 1972 and M.Eng. in 1974 . He was the chief eng. of Akashi Kaikyo Bridge 2 P steel caisson fabrication project.

Abstract

NKK has contributed to society through fabrication of many marine structures, such as jackets and artificial islands, petroleum drilling systems, steel shells for submerged tunnels, hybrid breakwaters, and pontoons and so on. We fabricated the 5P steel caissons for the South Bisan Seto Bridge of the Honshu-Shikoku Bridge, where the "laying-down caisson method" was used for the first time. Among these experiences, the Akashi Kaikyo Bridge 2P Steel Caisson Project was the largest scale and involved a number of technical challenges. This project was a key to the success of the entire Akashi Kaikyo Bridge Project .The new technologies developed through the project will lead new possibilities to construct huge marine structures in Japan. This paper describes the 2P Steel Caisson of Akashi Kaikyo Bridge.

1. Outline of Akashi-Kaikyo Bridge 2P steel caisson

1.1 Structure of Steel Caisson

The Akashi Kaikyo Bridge is the longest suspension bridge in the world. It connects Kobe City to Awaji Island and is 3,910m long with a center span of 1,900m. The 2P steel caisson was a steel form for casting underwater concrete foundation of the Kobe side main bridge tower. Its shape was double cylindrical, with outer diameter of 80m, inner diameter of 56m and a height of 65m. A bottom plate was attached between outer and inner wall, to provide buoyancy . The bouyant zone had 16 bulkheads to improve strength and stability as floating body. This design permitted continuous casting of underwater concrete. Fig.1 shows a general side view image of the Akashi Kaikyo Bridge, and Fig.2 shows general structural diagrams of the 2P steel caisson.

1.2 Construction Method

The 2P main tower foundation was constructed by the "laying-down caisson method." This was a newly-developed method for underwater foundation construction. For the first, it was applied to the 5P caisson of the South Bisan Seto Bridge of the Honshu-Shikoku Bridge, and about 20 foundations had been constructed by this method in the Honshu-Shikoku Bridge. In the "laying-down caisson method," a steel caisson is towed, ballasted and set on a pre-excavated seabed. The underwater concrete is then cast into it to complete the construction of the foundation. Fig.3 shows a flow diagram for construction using the "laying-down" caisson method.

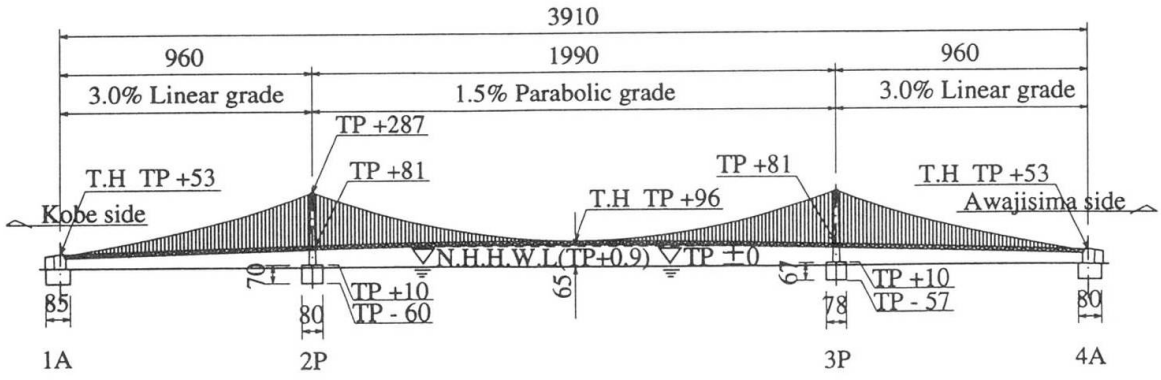

Fig.1 General view of Akashi Kaikyo Bridge

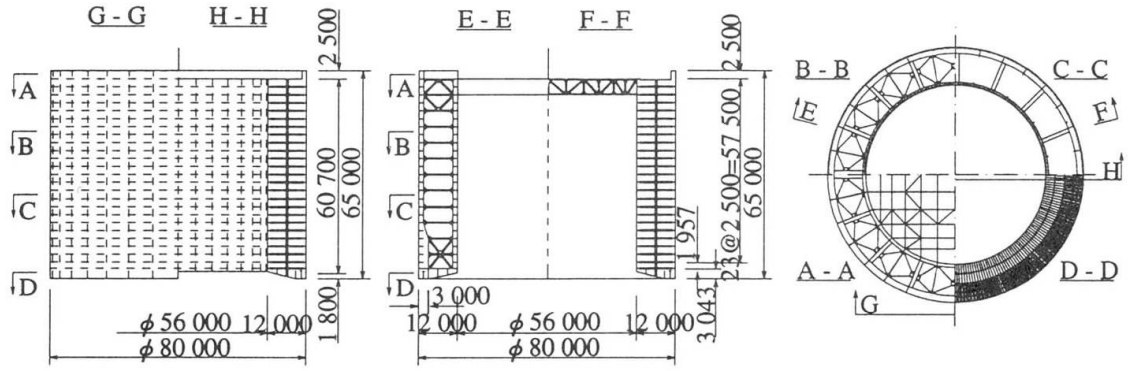

Fig.2 Strucutal Diagrams of 2P steel Caisson

1.3 Design Conditions

In this method, the caisson was used as a form for casting underwater concrete for the main tower foundation. However, it was faced to several different conditions before casting concrete, including launching, towing, mooring and sinking operations. Therefore the caisson had to be safe and functioal under these conditions. Table 1 shows the maximum design tidal current and ocean wave conditions for the caisson, and Table 2 shows the design loads. The combination of loads and safety factors were determined for each construction stage.

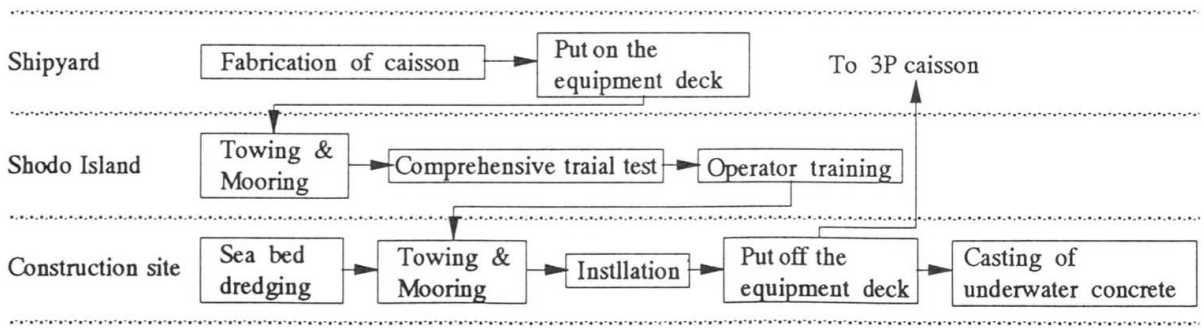

Fig.3 Flow of construction for Akashi Kaikyo Bridge tower foundation

2. Fabrication of Steel Caisson

The steel caisson was divided vertically into 7 stages and circumferentially into 16 sections for a total of 112 blocks. These blocks were fabricated at 6 shipyards in the 4 companies that comprised the consortium. The maximum weight of a single block was 180 tons.
The blocks were then transported to the ocean dock at NKK Tsu Works for final assembly. Assembly work was carried out using three 650-ton and one 450-ton crawler cranes.
In order to achieve the required level of dimensional control for the assembly, datum points were set on the dock floor for the bulkhead and double wall intersections.
Photo 1 shows the caisson being assembled at the NKK Tsu Works ocean dock. To keep the dimensions within the required tolerance, two of the 16 blocks on each stage were adjusted for horizontal dimension, and the 1st and 6th stages were used for vertical dimension adjustments.
Radiographic tests were performed for welded butt joints in the bottom plates, double walls, and bulkheads. The number of radiographs for the block preparation and overall assembly stages was determined using the ABS rules.
Ultrasonic flaw detection tests were performed for complete penetration welds at locations with concentrated loads, such as those for fixing the fairleader, inner core struts, and eyeplates.

Table.1 Maximum Design Tidal Current and Wave Conditions

Item	Condition	Construction Stage
Tidal Current	2.5m/s	Towing,Mooring
	1.75m/s	Install
	3.5m/s	After Install
Effective Wave High	2.4m	Towing,Mooring
	1.0m	Install
	3.4m	After Install

Table.2 Design Loads

Load Name	Contents
Self Weight	Caisson Body 16,500tf
	Equipment 1,000tf
	Scaffolding 400tf
Vertical Load at the top of caisson	Equipment&Deck 2,500tf
	Concrete work load: Inner Core 1.0tf/m² Outer Duble Hull 2.0tf/m²
Concrete Pressure	20tf/m²
Water Pressure	10tf/m²
Wind	Fw=1/2qV²CA※
Tide	Fc=1/2qV²CA※
Wave	Drafting Force: Havelock Equation Wave Pressure: MacCamy-Fuchs Equation
Towing	75tf
Mooring	1,000tf
Ship mooring	100tf
Installing Impact	Pmax=Vo√KW/q※

※: See Reference to 1)

3. Equipment

3.1 Outline of Caisson equipment

The caisson should have two kinds of equipment for installating at the target point and casting underwater concrete. This paper focuses on caisson installation equipment. The caisson installation equipment consisted of systems for mooring, ballasting, monitoring, electrical and other. All these were designed to be mounted on the equipment deck. This special deck could be put on and off the top of the caisson by using a floating crane.
This allowed them to be reused on the 3P caisson after completion of the 2P caisson. However, the water ballast and deballast pumps and sensors were fitted at specified points on each caisson body.
Fig.4 shows a conceptual diagram of the steel caisson equipment.

3.2 Mooring system

The purpose of the mooring system was to hold and adjust the own position against the strong tidal current of the Akashi Strait. The simulation analysis of many different mooring wire layouts was carried out to determine the optimum wire layout and winch capacity. In general, layout of mooring wires parallel and perpendicular to the bridge axis direction is effective. We selected a slightly modified layout (see Fig.5). Accordingly, a holding capacity of 1,000 tons and a winding capacity of 400 tons were determined for the winch. In addition, a high-speed winding and unwinding capacity of 20 tons at 30m / minute was determined to facilitate mooring wire connection and disconnection work. A "linear" type winch was selected. Furthermore, because

the connection of mooring wires on site had to be completed within the short slack tide period, and the mooring wires were too heavy to handle by divers, an automatic "quick joint" device was developed and used for connecting and disconnecting the wires.

3.3 Ballast System

The purpose of the ballast system was to pump water into the caisson after it had been moored for installation at the predetermined seabed location. The draft of the caisson was 8m, and the water depth at the site was 60m, so it was necessary to ballast the caisson 52m. It was also necessary to pump water into the caisson up to the top of the inner core to improve stability against the strong tidal currents after ballasting. The ballast system consisted of (1) a main ballast system, (2) an emergency ballast system and (3) a deballast system. Fig.6 shows the specifications of the ballast systems.

(1) The main ballast system consisted of 32 water pumps (2 pumps for each of the 16 tanks). This system could lower the caisson onto the seabed in a total 6 hours over two consecutive days at a speed of approximately 10m per hour.
(2) The emergency ballast system was a backup system to provide water into any parts of 16 tanks if up to 2 main ballast pumps would fail.
(3) The deballast system allowed the caisson to float off the seabed again for repositioning if the caisson had not been set satisfactorily.

3.4 Monitor system

The monitor system was an information processing system that helped the operation supervisor evaluate, oversee and direct the job of positioning and installing the caisson in a timely and appropriate manner. This system, comprising survey equipment, several types of sensors and a computer, collects measurement data on-line, processes the data into a designated form and displays it on a monitor screen. The system provided integrated control of the position of the caisson, the operation status of equipment, the accuracy of work, and time schedules. All datum were updated every two seconds. Fig.7 shows a diagram of the monitor system hardware. There were 3 patterns of screens image.

CRT-1: horizontal dimensional information
CRT-2: vertical dimensional information
CRT-3: time series information

The screen selection was made using a button box. Photo 2 shows an example of a display screen (CRT-2).

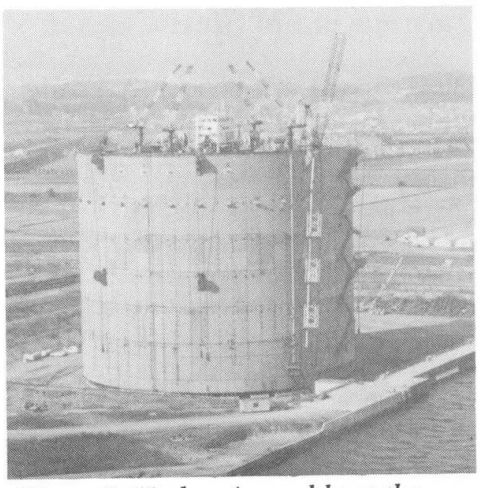

Photo.1 Under Assemble at the NKK Tsu Works ocean dock

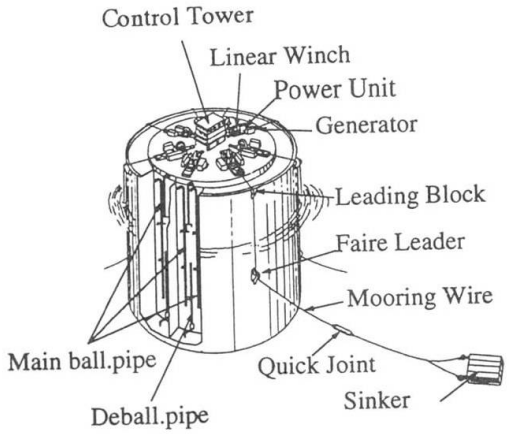

Fig.4 Concept of 2P caisson Equipment

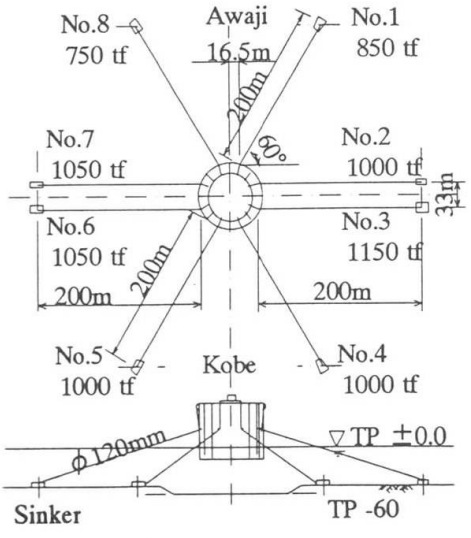

Fig.5 Layout of Mooring Wires

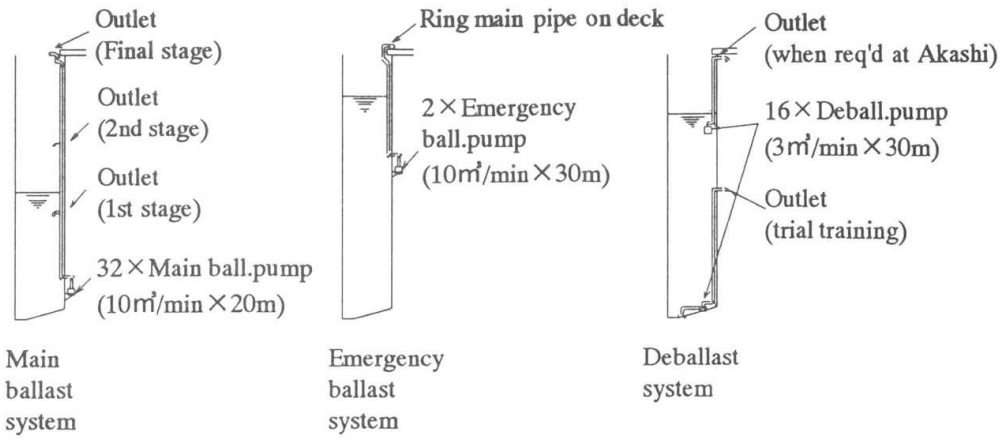

Fig.6 Specificatons of the Ballast systems

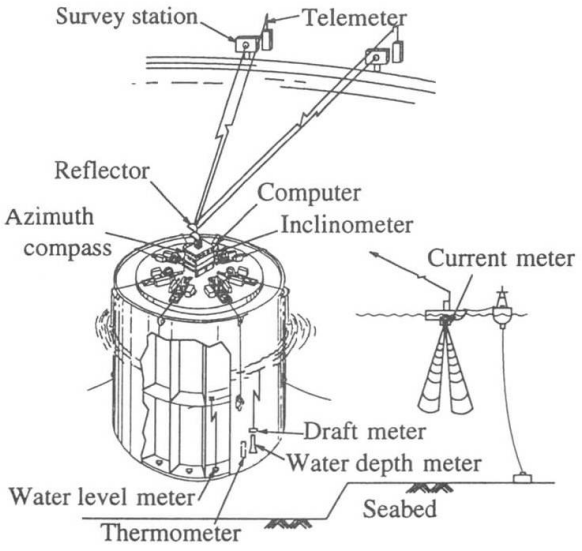

Fig.7 Layout of Monitor System

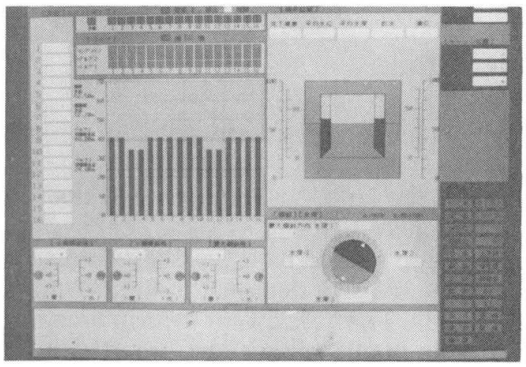

Photo.2 Example of display (CRT-2)

4. Towing

The 2P steel caisson departed from the ocean dock of NKK Tsu Works on January 23, 1989 . It was towed by a group of tugboats and arrived at the location use for comprehensive trial test off the east coast of Shodo Island(Kanagawa Prefecture) on Feb. 1. Fig.8 shows the towing route. The total towing distance was approximately 300 miles. For the section from the Irako Channel to the Tomogashima Channel, a fleet of four oceangoing tugboats (total towing power: 31,600 PS) was used that could easily tow the caisson in the coastal waters of the Pacific Ocean. This was an unprecedented tow in Japan in the sense that the scale of the object towed was huge and the towing distance along the coastal sea was long. Photo 3 shows towing of 2P steel caisson in the Akashi Strait.

5. Comprehensive trial test

A trial test was carried out at Shodo Island during about one month.
This test was simulation and training of prototype. The performance and operability as a total system were checked and confirmed. After the test, the 2P steel caisson was towed and installed on the seabed in the Akashi Strait on March 29, 1989 at 10:20 am. The accuracy of installation was very high, being only a few centimeters off the target position. After the successful installation, casting of underwater concrete was completed in December 1991. And the first important step of the Akashi Kaikyo Bridge Construction Project was completed without any problem.

Fig.9 Towing route of 2P caisson

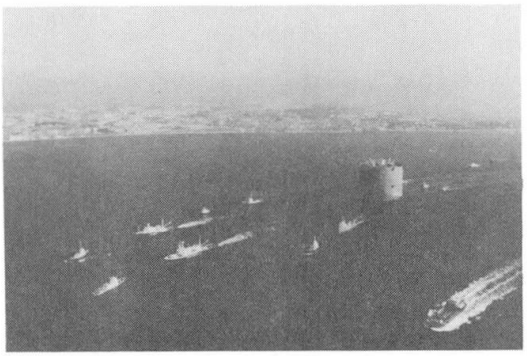

Photo.3 Towing of 2P caisson at Akashi Strait

Conclusions

Two new technologies were developed for the 2P steel caisson of the Akashi Kaikyo Bridge.

The one is the large-scale mooring system. This consists of two basic technologies, namely, a linear winch system and a quick joint system. The linear winch system used in this project was transferred to a large work vessel for reuse after completion of the 2P project. This system is still being actively used, demonstrating its immense potential for large-scale marine structure applications. The quick joint system was further improved after completion of the 2P project and was used in the lifting system for stiffening girders of the Kurushima Kaikyo Bridge. This system is expected to offer great potential for lifting heavy structures and for automatic connection systems in deep water.
The other is the monitoring system. This is a good experience of the utilization of computers for construction. The system demonstrated that computers was used successfully as an effective aid in the construction of large-scale, complicated installations that involve dangerous conditions. We expect that this system will present a leading experience for the use of computers during construction.

References

1) Honshu-Shikoku Bridge Authority, *Design Rule of Substructure* , May 1977
2) A. Senpaku, N. Maeda, at al *Akashi Kaikyo Bridge 2P Steel Caisson* , NKK Technical Report, No131,1990
3) M. Sakamoto, K. Higuti *Fabrication and Installation of Akashi Kaikyo Bridge 2P Steel Caisson* , Kyoryo, September 1989
4) S. Kashima, A. Senpaku, at al *Fabrication of Steel Caisson for Akashi Kaikyo Bridge,* 5th International Welding Symposium, April 1990
5) J. Hirayama , *The Construction method of Underwater Foundation:Experience of Honshu-Shikoku Bridge* , Kisoko, January 1971

Submerged Floating Tubes with Free Spans over 4000 m

Per TVEIT
Dr Eng.
Agder College
Grimstad, Norway

Geir MOE
Prof.
Norwegian Univ. of Science and Techn.
Trondheim, Norway

Per Tveit, born 1930 , received his civil eng. degree from the Norwegian Univ. of Science and Techn. in 1955 and PhD in 1964. He is now Docent Emeritus at Agder College in Grimstad, Norway.

Geir Moe, born 1938, received his civil eng. degree from the Norwegian Univ. of Science and Technology in 1953 and Sc.D. from MIT in 1975. He is now Professor at the Norwegian Univ. of Science and Technology in Trondheim.

The purpose of this poster is to argue that the max. free span of abutment-anchored submerged floating tubes can be more than 4 km. It should contribute to a general acceptance of free spans of up to 2 km. Analysis of these structures will be presented in a handout available at the Congress in Kobe.

The proposed tube is made from concrete with cube strength up to 95 MPa. Elements more than 200 m long can be cast by slipforming. When the elements have been up-ended, they are to be joined together by the usual Dutch method. When the whole tube is assembled it will be installed between the abutments.

During production the buoyancy of the tube can be checked with great precision. When finished, the tube should have a buoyancy equal to about half the max. traffic load. The magnitude of the axial force may be monitored by monitoring the frequency of the horizontal vibrations. Thus little permanent load needs to be considered for the design. Earthquakes have not been considered in this design

Slow changes in dead load, creep and shrinkage will give alterations of the desired shape of the tube. These changes can be counteracted by altering the amount of asphalt or ballast water.

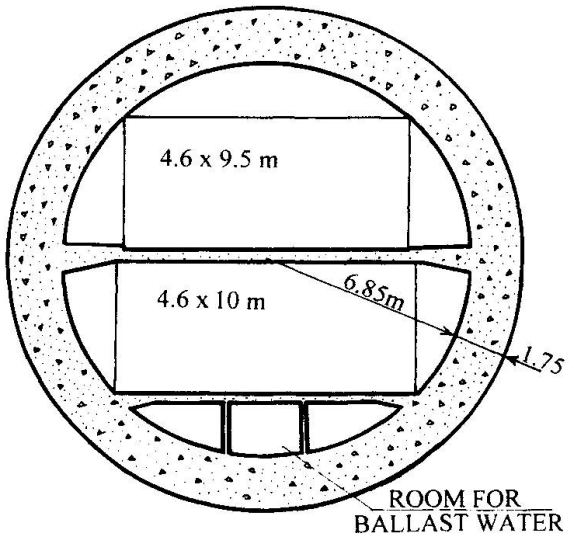

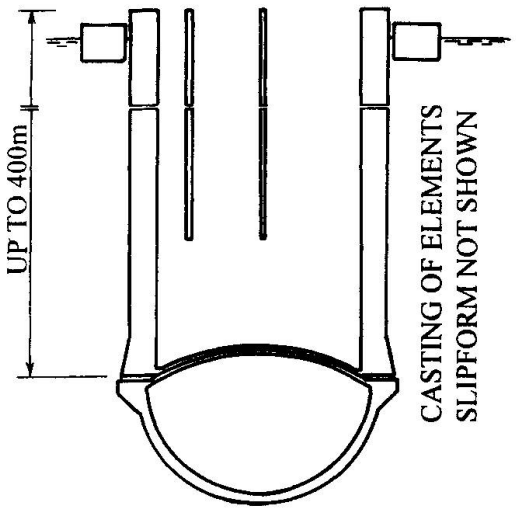

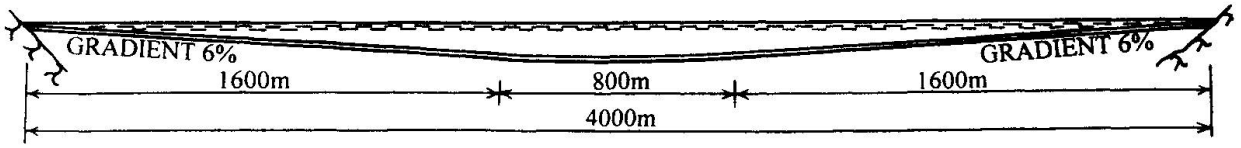

In the serviceability limit state the traffic load is very important. This load is at a maximum when traffic is brought to a standstill. It can be considerably reduced if traffic is not allowed into the tube whenever stoppages lead to undesirable deflections. The corresponding reduction in traffic capacity will be small. The ultimate limit state should be based on max. traffic load.

The tube lies so far below sea level that stresses due to 7 m high waves will be unimportant in the design. The magnitude of thecurrent depends on the site. The current is always strongest at the surface. For this project the average current and the current 50 m under sea level are assumed to be 0.7 $^{m}/_{sec}$. Vertical hydroelastic vibrations will be insignificant for this current.

Deflections due to in-line vibrations never exceed 0.15 times the diameter of the tube. Stresses due to in-line vibrations will be small when there are less than 4 points of inflection along the tube. The moment vector due to in-line vibrations is perpendicular to the moment vector due to vertical loads. Thus moderate stresses due to in-line vibrations have little influence in design. The resulting oscillations will cause accelerations that will not be noticed by the public.

Along the tunnel there is likely to be a great difference between the speeds of currents which last long enough to build up in-line vibrations. More research is needed to decide whether in-line vibrations will be harmful to the suggested tunnel.

At sites where currents and waves cause high stresses the following remedies can be used:

1. Fins attached to the tube can reduce the chance of hydroelastic vibrations. The shape of the fins should be influenced by the fact that the currents are parallel to the surface.

2. Inclined cables to the bottom from points less than 1300 m from the abutments. Cables in the middle of the span would hamper expansion due to temperature.

3. Same as 2, but the cables should be swung over the tube as shown in the drawing. The stays are kept in tension by the weight of a concrete bucket fastened to a pulley that sits on the cables under the tube.

The weight of the bucket can be adjusted by adding or removing sand. Friction between the cables and the tube will dissipate the energy of the vibrations. Stoppers could be fastened to the cable at each side of the pulley to limit horizontal movement of the tube.

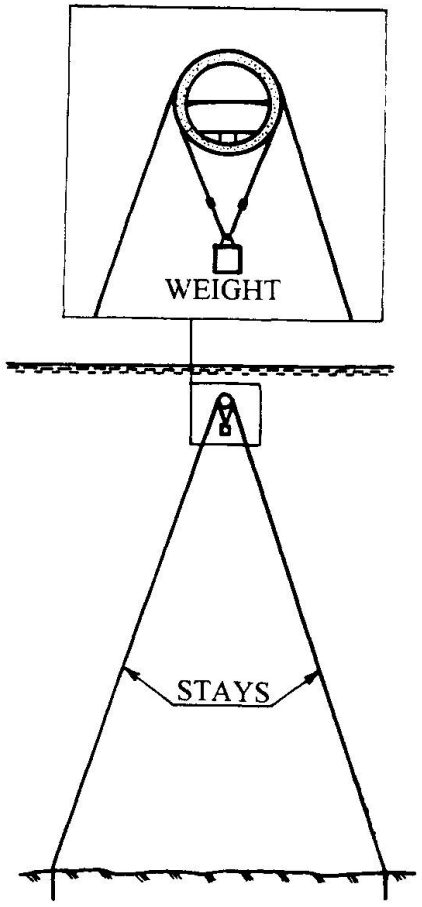

Literature:

Tveit, P. "Design of a submerged floating tube with a free span of 1750m." Proceedings of an International Conference on Submerged Floating Tunnels. Sandnes, Norway 29th to 30th of May, 1996. Norwegian Public Roads Administration. 63 pages.

Tørum, A. & Moe. G. et al. "On Current Induced In-line Oscillations of Pipelines in Free Spans." Proceedings of OMAE-96, June 1996, Florence, Italy. 11 pages.